The role of CCK-interneurons in regulating hippocampal network dynamics

by

Dámaris Ketinó Rangel Guerrero

August, 2019

A thesis presented to the
Graduate School
of the
Institute of Science and Technology Austria, Klosterneuburg, Austria
in partial fulfilment of the requirements
for the degree of
Doctor of Philosophy

The dissertation of Dámaris Ketinó Rangel Guerrero, titled *The role of CCK-interneurons in regulating hippocampal network dynamics*, is approved by:

Supervisor: Prof. Jozsef Csicsvari, IST Austria, Klosterneuburg, Austria

Signature: _____

Committee Member: Prof. Simon Hippenmeyer, IST Austria, Klosterneuburg, Austria

Signature: _____

Committee Member: Prof. Peer Wulff, Kiel University, Kiel, Germany

Signature: _____

Exam Chair: Prof. Maximilian Jösch, IST Austria, Klosterneuburg, Austria

Signature: _____

signed page is on file

IST Austria Thesis, ISSN: 2663-337X
ISBN: 978-3-99078-003-9

I hereby declare that this dissertation is my own work and that it does not contain other people's work without this being so stated; this thesis does not contain my previous work without this being stated, and the bibliography contains all the literature that I used in writing the dissertation.

I declare that this is a true copy of my thesis, including any final revisions, as approved by my thesis committee, and that this thesis has not been submitted for a higher degree to any other university or institution.

I certify that any republication of materials presented in this thesis has been approved by the relevant publishers and co-authors.

Signature: _____

signed page is on file

Dámaris Ketinó Rangel Guerrero

September 9, 2019

Abstract

Brain function is mediated by complex dynamical interactions between excitatory and inhibitory cell types. The Cholecystokinin-expressing inhibitory cells (CCK-interneurons) are one of the least studied types, despite being suspected to play important roles in cognitive processes. We studied the network effects of optogenetic silencing of CCK-interneurons in the CA1 hippocampal area during exploration and sleep states. The cell firing pattern in response to light pulses allowed us to classify the recorded neurons in 5 classes, including disinhibited and non-responsive pyramidal cell and interneurons, and the inhibited interneurons corresponding to the CCK group.

The light application, which inhibited the activity of CCK interneurons triggered wider changes in the firing dynamics of cells. We observed rate changes (i.e. remapping) of pyramidal cells during the exploration session in which the light was applied relative to the previous control session that was not restricted neither in time nor space to the light delivery. Also, the disinhibited pyramidal cells had higher increase in bursting than in single spike firing rate as a result of CCK silencing. In addition, the firing activity patterns during exploratory periods were more weakly reactivated in sleep for those periods in which CCK-interneuron were silenced than in the unaffected periods. Furthermore, light pulses during sleep disrupted the reactivation of recent waking patterns. Hence, silencing CCK neurons during exploration suppressed the reactivation of waking firing patterns in sleep and CCK interneuron activity was also required during sleep for the normal reactivation of waking patterns. These findings demonstrate the involvement of CCK cells in reactivation-related memory consolidation.

An important part of our analysis was to test the relationship of the identified CCK-interneurons to brain oscillations. Our findings showed that these cells exhibited different oscillatory behaviour during anaesthesia and natural waking and sleep conditions. We showed that: 1) Contrary to the past studies performed under anaesthesia, the identified CCK-interneurons fired on the descending portion of the theta phase in waking exploration. 2) CCK-interneuron preferred phases around the trough of gamma oscillations. 3) Contrary to anaesthesia conditions, the average firing rate of the CCK-interneurons increased around the peak activity of the sharp-wave ripple (SWR) events in natural sleep, which is congruent with new reports about their functional connectivity.

We also found that light driven CCK-interneuron silencing altered the dynamics on the CA1 network oscillatory activity: 1) Pyramidal cells negatively shifted their preferred theta phases when the light was applied, while interneurons responses were less consistent. 2) As a population, pyramidal cells negatively shifted their preferred activity during gamma oscillations, albeit we did not find gamma modulation differences related to the light application when pyramidal cells were subdivided into the disinhibited and unaffected groups. 3) During the peak of SWR events, all but the CCK-interneurons had a reduction in their relative firing rate change during the light application as compared to the change observed at SWR initiation.

Finally, regarding to the place field activity of the recorded pyramidal neurons, we showed that the disinhibited pyramidal cells had reduced place field similarity, coherence and spatial information, but only during the light application. The mechanisms behind such observed behaviours might involve eCB signalling and plastic changes in CCK-interneuron synapses.

In conclusion, the observed changes related to the light-mediated silencing of CCK-interneurons have unravelled characteristics of this interneuron subpopulation that might change the understanding not only of their particular network interactions, but also of the current theories about the emergence of certain cognitive processes such as place coding needed for navigation or hippocampus-dependent memory consolidation.

Acknowledgments

For the life and the love that they have given to me, I thank and dedicate this Thesis dissertation to my parents and my sister.

Throughout my life I have also been nourished and supported by a big family and a few close friends to whom I will always be thankful and keep in my heart.

And of course I extend my gratitude to the people that provided me significant professional help:

To my mentor, Jozsef Csicsvari, for his wise guidance, friendly support and his trust.

To my committee members, Peer Wulff and Simon Hippenmeyer for their time, support and valuable input.

To my former mentors, Víctor Ramirez Amaya and Edith Garay Rojas for providing me such an inspiring introduction to neuroscience and molecular biology during my Master studies.

To Jago Wallenschuss for his professional support even beyond technical duties.

To Peter Baracskay for his crucial help for setting the recording techniques.

To Igor Gridchyn for his constant and kind help in software development.

To Philipp Schoenenberger for introducing the optogenetic techniques to the lab.

To Kira Balueva for her dedication in the generating of the viruses used in this work.

To Felipe Fredes for his help in improving techniques and for the fruitful discussions.

To the students that have worked with me during my PhD: Kristóf Klein, Cihan Önal, Sarah Krueckel, Chiara Roth and Uladzislau Barayeu.

To the other current and former members of the Csicsvari group for the friendly atmosphere in the lab and their valuable input, specially to: Michele Nardin, Haibing Xu, Joseph O'Neill, Charlotte Boccara, Federico Stella, Karola Käfer, Karel Blahna, Yosman BapatDhar and Juan Ramirez Villegas.

To the Jonas and Shigemoto groups for the help in eventualities. Especially to their technicians Florian Marr and Elodie Le Monnier.

To the Scientific Service Units (SSUs) at IST Austria: the Bioimaging Facility, the Miba Machine Shop and the Preclinical Facility.

About the author

Throughout the Bachelor in Genomic Sciences at the Universidad Nacional Autónoma de México (UNAM), Dámaris K. Rangel Guerrero forged a predilection for Neuroscience and after graduating with Honours she decided to start the Master in Neurobiology at the UNAM. She worked on a project entitled “Inducible system for tagging neurons activated during the learning of a behavioural task” in the group of Dr. Ramírez Amaya. During that period, she attended the Advanced School on Optical Methods in Physiology Held at the École Normale Supérieure de Paris and presented her work at the 8th IBRO World Congress of Neuroscience in 2011 and at the EMBO Workshop on Single Cell Physiology in 2012. During her PhD studies at the group of Prof. Jozsef Csicsvari she has participated in several projects which have led to two publications and one manuscript in progress.

List of Publications Appearing in the Thesis

1. Rangel-Guerrero et al., 2018. Tetrode Recording from the Hippocampus of Behaving Mice Coupled with Four-Point-Irradiation Closed-Loop Optogenetics: A Technique to Study the Contribution of Hippocampal SWR Events to Learning. eNeuro, 5(4). pii: ENEURO.0087-18.2018.

Table of Contents

List of Figures

List of Abbreviations

Adeno-associated virus (AAV)

Anteroposterior (AP)

Apical dendrite targeting interneurons (ADI)

Archaerhodopsin-T (ArchT)

Calbindin 1 (Calb1)

Cannabinoid receptor 1 (CB1 receptor)

Channelrhodopsin-2 (ChR2)

Chemokine C-X-C motif ligand 14 (Cxcl14)

Cholecystokinin (CCK)

Clozapine-N-oxide (CNO)

Cornu Ammonis (CA)

Cre-Recombinase (Cre)

Depolarization-induced suppression of excitation (DSE)

Depolarization-induced suppression of inhibition (DSI)

Designer receptor exclusively activated by designer drugs (DREADDS)

Diode-pumped solid-state laser (DPSS)

Disinhibited interneurons (DII)

Disinhibited pyramidal cells (DIP)

Dorsoventral (DV)

Endocannabinoids (eCBs)

Flp-Recombinase (Flp)

GABAaR (GABAa receptor)

GABAbR (GABAb receptor)

Gamma-aminobutyric acid (GABA)

Genetically encoded calcium indicators (GCaMPs)

Inhibited interneurons (INI)

Instantaneous firing rate counts (IFRCs)

Local field potential (LFP)

Long term depression (LTD)

Long term potentiation (LTP)

Mediolateral (ML)

Non-responsive interneurons (NRI)

Non-responsive pyramidal cells (NRP)

Parvalbumin (PV)

Perforant path-associated (PPA)

Phosphate-buffered saline (PBS)

Place field similarity (PFS)

Poly-methyl-methacrylate (PMMA)

Rapid eye movement (REM)

Reelin (Reln)

Schaffer collateral-associated (SCA)

Serotonin (5-hydroxytryptamine) receptor 3a (5-HT3)

Sharp wave ripple (SWR)

Somatostatin (SOM)

Standard deviation (SD)

Stratum oriens – stratum oriens (SO-SO)

Tetanus toxin light chain (TeLC)

Vasoactive intestinal polypeptide (VIP)

Vesicular glutamate transporter 3 (Vglut3)

1 Introduction

1.1 Conceptual framework

The brain dynamics can be seen as a multilevel orchestra, where neurons play defined roles performing the symphony that underlies mental processes such as learning and memory formation. Complex molecular signalling networks that give rise to different neuronal characteristics can be analogue to the instruments used to follow the notes in the nucleotide sequences. With synaptic activity being the common language, the basic integration unit can be referred to as the 'state' of a cell, where its activity history determines its dynamics. Cell assemblies originate from such individual correlations, embedded in population-level interactions and brain oscillations. From this, emergent properties can arise, conferring the highest level of complexity that might, for instance, ultimately allow us to appreciate musical compositions.

According to our current understanding memory is encoded in the activity patterns of excitatory (glutamate releasing, i.e. 'Glutamatergic') neurons, whose network activity and synaptic plasticity are meticulously controlled by inhibitory (GABA releasing, i.e. 'GABAergic') neurons. These GABAergic cells actually include several subpopulations which appear to serve specialised functions. The broader classification divides them into long-range projection GABAergic neurons and local inhibitory cells with short axons regulating local circuit excitability, therefore, called 'interneurons' (Freund and Buzsáki, 1996; Maccaferri and Lacaille, 2003; Klausberger and Somogyi, 2008; Pelkey et al., 2017).

Interneurons show a huge variability of afferent and efferent connectivity patterns compared to the relatively homogenous principal (excitatory) neurons, which are primarily pyramidal neurons (Freund and Buzsáki, 1996). Some interneurons target only other GABAergic cells (i.e. interneuron-specific interneurons), but the majority of them target pyramidal cells. Consequently they are usually classified based on the cell-compartment where they target pyramidal cells (e.g. soma-targeting, axo-axonic or dendrite-targeting interneurons), covering all domains of the excitatory neurons and, therefore, raising the idea that interneuron subtypes serve different functions (Pelkey et al., 2017).

Besides these differences in postsynaptic cellular compartments, thanks to a growing amount of descriptive information, interneurons can be further classified based on several criteria: electrophysiological properties (e.g. intrinsic excitability, synaptic conductances, functionality regarding postsynaptic regulation, etc.), morphological features (somatodendritic location and the axonal projections) together with the anatomical location and connectivity patterns, the molecular markers expressed (defined either by immunohistochemistry or by transcriptomics), the afferent connectivity (from recurrent excitatory circuits or from exclusively glutamatergic afferent projections), the oscillatory coupling, their plasticity mechanisms and their developmental origin, among others (Freund, 2003; Maccaferri and Lacaille, 2003; Freund and Katona, 2007; Ascoli et al., 2008; Klausberger and Somogyi, 2008; Chamberland and Topolnik, 2012; Kepecs and Fishell, 2014; Tasic et al., 2016; Lim et al., 2018; Luo et al., 2018).

Although some of these criteria tend to coincide in clustering interneuron types together (e.g. arborisation patterns and gene expression, or morphology and firing patterns), there is a high degree of heterogeneity and overlap (Elowitz, et al., 2002; Kamme,

et al. 2003; Maccaferri and Lacaille, 2003; Rudy et al., 2011; Sohn et al., 2014; Murphey et al., 2014; Tasic et al., 2016; Harris et al., 2018). Early studies already revealed that interneurons are modulated in an activity-dependent fashion and that consequently, some functional properties follow a continuum that cannot be split into different populations (Parra, et al. 1998). Nowadays it is debated whether unique features exist for every cellular identity or if continuous modes of variables should be considered for a complete coverage of interneuronal diversity (Que et al., 2019). While further functional specialisation of each type of interneurons is expected, yet, little is known about the detailed structure of how the known inhibitory interneuron types regulate the overall network activity (Arriaga and Han, 2017).

Given this panorama, I followed a rationale that aimed at grouping neurons into cell types that reflect functional/circuit properties within the widely accepted classes (based on neurochemical expression patterns), by relying on a combination of criteria and approaches, rather than solely focusing on splitting the complex interneuron population. This would allow to continue exploiting the advantage of generated genetic tools (plenty of Cre- mouse lines in combination with adeno-associated viruses –AAVs–). But, at the same time, to be conscious that many functional classes may be comprised. An emphasis on functionality would bring us to a better level of understanding about the brain circuits in which the GABAergic neurons participate.

Following this rationale, the subject of the current study is a neurochemically-defined interneuron subpopulation: the Cholecystokinin (CCK)-expressing inhibitory cells. Due mainly to the lack of a unique genetic marker, these interneurons are one of the least studied cell types, but are suspected to play important roles in higher cognitive processes. Therefore, this work will develop on the study of the different types of cell-responses elicited by their manipulation, as well as the neuronal network effects in freely moving mice.

1.2 The brain circuitry relevant to this work

Due to its relatively simple architecture, a model region in the brain for studying such a complex neuronal population is the hippocampal formation, which includes the Cornu Ammonis (CA) areas, the dentate gyrus and the subicular complex (Lorente de Nó, 1934; Amaral and Witter, 1989). This brain region also happens to be a crucial structure for memory formation (Morris et al., 1982; Sutherland et al., 1982; Good and Honey, 1991). Therefore, the cell types of the hippocampus have been subject to extensive characterisation and evaluation in terms of the roles of particular cell types in mnemonic processes.

The crucial role of the hippocampal formation in spatial memory and navigation, as first suggested by human lesion studies (Scoville and Milner, 1957), was revealed by the discovery that a majority, but not all, of the pyramidal cell activity in the CA areas is related to the location of the animal (O'Keefe and Dostrovsky, 1971). Therefore, hippocampal pyramidal neurons are often referred to as place cells provided that these pyramidal cells exhibit place-related firing. Their maximum firing corresponds to unique parts of the environment (called place fields), which the animal is exploring (O'Keefe, 1976). Both pyramidal cells and interneurons in the hippocampus tend to modulate their firing rate depending on the phase of network oscillations such as 4-10 Hz theta-band

oscillations (Vanderwolf et al., 1969). Furthermore, studies found that pyramidal cell spike timing relative to theta oscillations change so that the cell fires at earlier and earlier theta phases as the animal moves across the place field of the cell, a phenomenon known as phase precession (O'Keefe and Recce, 1993). Up to date, thousands of studies have extended our understanding of the importance of hippocampal cells in processing spatial experiences. It is important to note that an environment is represented not only by where each place cell fires, but also by which cells are active and which are silent there (Epsztein et al., 2011).

For understanding the function of the hippocampal formation in cognitive processes, its anatomical connections are crucial. An important source of olfactory, visual, and auditory information to the hippocampus is coming from the entorhinal cortex, which relays information from other cortical areas to the hippocampus This cortex marks the beginning of what has been coined 'the trisynaptic circuit' (Andersen et al., 1966). Although somehow simplistic, that concept was produced by an integration of early neuroanatomical and electrophysiological studies and has remained as a reference to the mainstream of neuronal communication in the hippocampus. In this view, there are three sequential glutamatergic synapses. First, axons of layer II neurons in the entorhinal cortex project to the dentate gyrus referred to as the 'perforant path'. Then, the axons of the dentate gyrus granule cells, called 'mossy fibres', project to the pyramidal cell proximal dendrites of CA3. Finally, defined axonal projections of CA3 pyramidal cells that target the apical dendrites of CA1 principal cells called 'Schaffer collaterals', (Amaral and Witter, 1989). However nowadays it is known that the flow is not unidirectional (Scharfman, 2007) and that other synapses (i.e. CA2) are crucial (Bartesaghi and Gessi, 2004; Chevaleyre and Siegelbaum, 2010).

An anatomical particularity of the CA hippocampal areas, expected to contribute to the spatial modulation, is the arrangement of the cell bodies of glutamatergic pyramidal neurons into layers or strata (Fig.1-A). The main cell body layer in the CA regions is the stratum pyramidale, where pyramidal cell bodies are found. Also, these pyramidal cells have orthogonal dendrites that span from the stratum oriens where pyramidal basal dendrites are found to the apical dendrites forming the more proximal stratum radiatum and more distal stratum lacunosum moleculare layers. This arrangement allows pyramidal neurons to synapse across well-defined dendritic domains (Pelkey et al., 2017). Such dendritic domains are active compartments capable of integrating their various inputs and undergoing synaptic plasticity (Klausberger, 2009).

Although both CA1 and CA3 areas are the principal pyramidal cell fields in the hippocampus, it has been suggested that they produce differential effects on the encoding and retrieval of contextual memories (Csicsvari et al., 2000; Lee and Kesner 2004; Leutgeb et al. 2005; Daumas et al. 2005). In particular, the CA1 region is considered to convey the output of the hippocampal memory circuit through its widespread extrahippocampal projections. Therefore, it is not surprising that special functions are attributed to CA1, such as contextual memory retrieval, novelty detection, input comparison, and enrichment of hippocampal output (Cenquizca and Swanson, 2007; Ji and Maren, 2008; Soltesz and Losonczy, 2018).

These specific functions of CA1 might correlate with its distinctive non-homogeneity with regard to its pyramidal population. Already from the beginning of hippocampal description, the renowned anatomist Lorente de Nó (1934) noticed a morphological division

along the radial axis, distinguishing between deep and superficial CA1 pyramidal neurons. He observed that the so-called deep cells grouped into several but relatively sparse rows, while the superficial ones into a couple of dense rows. Now, we know that these radial differences are related to their neurogenesis following an inside-out pattern of hippocampal development and with different genetic programs, which result in superficial and deep populations having distinctive molecular, morphological, electrophysiological and connectivity patterns (Slomianka et al., 2011). It has, therefore, been proposed that the two pyramidal subpopulations encode separate features of the environment and differentially contribute to learning (Danielson et al., 2016).

In contrast to pyramidal cells, GABAergic inputs originate from various sources involving different molecular machineries, likely to contribute differentially to dendritic computations (Klausberger, 2009). This is partly due to the fact that in contrast to the organised pyramidal arrangement, the cell bodies of inhibitory neurons are scattered throughout all strata. Another difference is the positioning of their somatodendritic arbors, which allow them to integrate from a more restricted afferent input repertoire than the glutamatergic cells (Pelkey et al., 2017). Consequently, rather than directly contributing to space-specific activity, GABAergic neurons have been considered as time signal generators, providing a temporal context for spatial processing in hippocampal networks (Gloveli, 2010).

Inhibitory cells comprise between 10 to 15% of the total hippocampal neuronal population (Pelkey et al., 2017). Some of these interneurons innervate different subcellular domains of pyramidal cell dendrites and other interneurons, whereas others target only interneurons. GABAergic synaptic terminals on the soma, proximal dendrites and axon initial segment (i.e. perisomatic) control pyramidal cell output and thus synchronise their firing, whereas dendritic-targeting interneurons modulate the efficacy and plasticity of excitatory synaptic inputs (Freund and Buzsáki, 1996). This is of major relevance since CA1 pyramidal cells receive 92% of their GABAergic input onto dendrites (Klausberger, 2009). However, once more, such a broad classification of interneurons (perisomatic and dendritic-targeting) is insufficient to predict their function; depending on the precise identity of the GABA-releasing neuron, adjacent synapses can have completely opposite temporal dynamics *in vivo* (Somogyi et al., 2014).

This brings us back to the cell-classification problem. At least 20 different types of inhibitory interneurons with different properties have been described in the CA1 area, while only 15 of those have been recorded *in vivo* (Somogyi et al., 2014). It is suggested that each type of interneuron participates in different brain states, and regulates the local network in cooperation with other neuronal types. That is how, despite representing a minority within the hippocampus, interneurons may be determinant in regulating pyramidal cells and circuit function (Klausberger and Somogyi, 2008; Pelkey et al., 2017).

1.3 Electrophysiological techniques used to study interneuron activity

Among the plethora of techniques for studying brain activity, there are few that are useful for distinguishing the activity of such complexly defined neuronal types as the interneuron populations. Electrophysiological techniques are one of the most widely used techniques for getting access to the functional relations of the activity of neuronal

populations and single neurons. In general, it is done by inserting electrodes in a target brain region (either *in vitro* or *in vivo*) and recording the electrical signals. The use of electrodes for extracellular recordings allows to measure the local field potential (LFP) and, therefore, to study field oscillations; the signature of the periodical synchronization of the activity of many neurons. The LFP reflects the spatial integration of voltages generated by the flow of extracellular electrical currents along the dendrites of a spatially-restricted group of neurons (Colgin and Moser, 2010).

Glass capillary electrodes can be positioned in 'juxtaposition', very close to the membrane of a neuron in order to record its activity and label it after by iontophoresing tracer molecules into the membrane of the neuron being recorded (Pinault, 2011). This is the so-called juxtacellular recording-labeling technique, having the advantage that the recorded cell can be identified by the tracer and then be subjected to morphological reconstruction, immunostainings or electron microscopy. Therefore, this has been responsible for most of the current knowledge about the activity of interneuron types *in vivo* (McBain and Fisahn, 2001; Klausberger et al., 2003; Roux et al., 2014).

However, the juxtacellular recordings have a limited yield of cells that can be obtained per subject and are impractical for deep target regions. Also, it is so challenging that the most common use has been with urethane-anaesthetized animals and in head-fixed rodent preparations, even though it is possible to extend it to behaving drug-free animals (Lapray et al., 2012). This poses the question of whether the reported characteristics of interneurons under anaesthesia can be extended to the brain activity of freely moving subjects.

Another electrophysiological method are the extracellular recordings that can involve multi-site electrodes such as the so-called tetrodes, which allow to resolve individual units by comparing the signal from the tip of four wires conforming the tetrode (Harris et al., 2000). This methodology overcomes the problems posed by the anaesthesia in the juxtacellular technique, because they can be implanted in a stable preparation lasting up to months (Wilson and McNaughton, 1994; Nicolelis et al., 1997). For studying the particular contributions of each neuronal type, extracellular recordings that allow the simultaneous monitoring of the activity of large numbers of individual neurons in freely moving rodents are an ideal approach because it gives access to the precise timing of their activity and their relationship to brain oscillations and behaviour. However, whereas differentiating the signal from glutamatergic and GABAergic neurons is possible with tetrode recordings in the hippocampus, it is indeed a challenge to distinguishing between their subtypes in population recordings. A pioneer work by Csicsvari and collaborators (1999) proposed a functional classification of interneurons based on the pattern of cell discharge relative to a characteristic sleep pattern in the hippocampus called sharp wave ripple that will be addressed in the following chapter.

A further breakthrough in the field was the combination of optogenetics with extracellular recordings, along with the creation of several mouse lines expressing the Cre recombinase under cell type-specific promoters (Hippenmeyer et al., 2005; Gong et al., 2007; Madisen et al., 2010; Miyoshi et al., 2010; Taniguchi et al., 2011). Optogenetics provides a solution for identifying specific genetically-defined neuronal subtypes in blind extracellular recordings by expressing light-sensitive opsins in a given neuronal population, which is revealed by identifying the light-responsive units (Roux et al., 2014). The most

widely used light activated molecular tools in neuroscience are the cation channel channelrhodopsin-2 (ChR2; Nagel et al., 2003) and the proton pump archaerhodopsin (Arch; Chow et al., 2010). These and other optogenetic molecules allow the activation or silencing of neurons with unprecedented specificity and excellent temporal precision on a millisecond scale (Madisen et al., 2012).

From these optogenetic tools, a variant of Arch will be part of the methodology used in this work. Archaerhodopsins are a family of receptor proteins that respond to light (i.e. opsins) found in Archaea. The first variant described, Arch, is a yellow–green light-sensitive opsin from Halorubrum sodomense that expresses well on the axonal plasma membrane and is commonly used to inhibit neurons in optogenetic experiments (Chow et al., 2010). Another variant, archaerhodopsin T (ArchT), is a more promising approach for acute synaptic silencing due to its increased light sensitivity (Han et al., 2011). These opsins respond to yellow or green light by pumping protons out of cells, thereby producing membrane hyperpolarization (i.e. silencing) the neuron expressing it. However, recent work proposes that neuronal silencing using archaerhodopsins is mediated via changes in pH rather than hyperpolarization (El-Gaby et al., 2016). Apart from the specific mechanisms, archaerhodopsins have been proven to allow fast and reversible synaptic silencing in mammalian neurons.

The optogenetic characterization of molecularly-defined classes is assisting the identification of interneurons on the sole basis of their physiological patterns (Klausberger et al., 2003; Roux et al., 2014). For instance, there are three general interneuron populations that account for 85% of all cortical interneurons described by 3 molecular markers (Xu et al., 2010; Kepecs and Fishell, 2014): parvalbumin (PV), vasoactive intestinal peptide (VIP) and somatostatin (SOM). Generation of mouse lines using these promoters to drive the expression of the Cre recombinase has been a major advance for the study of interneuron function in oscillatory activity and behaviour (Hippenmeyer et al., 2005; Taniguchi et al., 2011, 2014).

However, as mentioned beforehand, for distinguishing between different subpopulations of interneurons, other criteria should be taken into account, such as more specific molecular markers, morphological or electrophysiological features, post-synaptic targets or developmental profiles. In order to provide experimental access to the major classes of cortical inhibitory neurons, Taniguchi and collaborators (2011) described nearly 20 knockin mouse ‘driver lines’ expressing the Cre or the inducible CreER recombinase. They demonstrated that specific subpopulations can be targeted using the intersection of two recombinases (i.e. Cre and Flp) provided by driver lines and by engaging lineage restriction and birth timing mechanisms (Taniguchi et al., 2011).

Another innovative concept emerged from Fenno and colleagues (2014) in order to restrict the transgene expression not only based on molecular markers bur also on connectivity patterns. In principle, this would enable cell-type definition by multiple conditions, such as gene expression and wiring features. Additionally, it would overcome the problem posed by large size of STOP cassettes used normally for conditioning expression upon recombination, because they custom-modified intronic sequences in a system coined as INTRSECT, for 'intronic recombinase sites enabling combinatorial targeting'. This has allowed for the expression of opsins in specified populations of

inhibitory interneurons in mammalian hippocampus and neurons of the ventral tegmental area defined by both genetic and wiring properties (Fenno et al., 2014).

The combinatorial and opto-genetics offer promising approaches for expanding our knowledge of how selective manipulations of functional neuronal ensembles affect various brain function and behaviour. However, there are plenty of creative options for achieving this, as has been shown by Murray and colleagues (2011). This study was the first to combine region-specific and cell type-specific manipulations in the hippocampus during learning and memory. The approach was to block synaptic release of PV-interneurons in CA1 by using an AAV coding for the tetanus toxin light chain (TeLC), which stops vesicle fusion, in a flip-excision cassette that restricted expression to PV-neurons when injected to PV-Cre transgenic mice. After ablation of PV-interneurons selectively in CA1, they found disruption of spatial working memory but not of spatial reference memory (Murray et al., 2011). In this way, this and other experiments highlight the importance of evaluating the role of other classes of CA1 interneurons in memory function.

1.4 Oscillations and memory

During learning, information is encoded and ultimately stored in the brain through experience-dependent cellular and molecular changes in the activated groups of neurons. These neurons form neuronal assemblies by establishing new associations that allow novel information to be transformed into memory through further processing in neuronal circuits (Hebb, 1949). These memory traces are first labile but then stabilize through a process defined as memory consolidation, which has been proposed to occur during post-learning rest or sleep by the reactivation of memory traces (Buzsáki, 1989).

The understanding of the neural basis of spatial memory benefited from the discovery of the already mentioned, spatially-specific firing of the principal hippocampal neurons, therefore, called the 'place cells' (O'Keefe and Dostrovsky, 1971). As these cells encode the current location of the animal, different cell assemblies represent different locations (O'Keefe, 1976; Wilson and McNaughton, 1994). These hippocampal representations develop when the animal is placed into a new environment – a process called remapping – such that neuronal activity reflects a unique internal map of the environment used to solve spatial problems (Muller and Kubie, 1989; Wilson and McNaughton, 1994). Such remapping also occurs in conjunction with spatial learning, even in a familiar environment. Indeed, in the CA1 region, new place maps are established during reward-associated spatial learning, resulting in the formation of new cell assemblies that represent information about the locations of food resources (Dupret et al., 2010, 2013).

For the specific case of spatial memory, it is proposed that the initial encoding of a new environment results from the hippocampus integrating neocortical inputs, facilitated by particular brain oscillations. After behaviour, high recurrent excitation would promote the gradual transfer of information back to the neocortex, leading to a long-term memory storage that could then become independent from the hippocampus (Buzsáki, 1996; Ego-Stengel and Wilson, 2010).

Hippocampal activity is characterized by different frequencies of synchronous activity oscillations, which reflect the rhythmic and highly coordinated firing of neurons. The oscillations often relate to the activity or 'behavioural state' of the animal. There are three most studied oscillatory patterns in rodents: theta, gamma and ripple oscillations (Allen and Monyer, 2015).

The theta rhythm, comprising from 6 to 10 Hz frequency patterns, occurs mostly during periods where the animal is sensing information, such as locomotion in active exploration and voluntary behaviours like whisking, sniffing and some immobility periods (Buzsáki, 2002; Csicsvari et al., 2003; Colgin and Moser, 2010; Hasselmo and Stern, 2013). In addition, there are also theta oscillations during the rapid eye movement (REM) phase of sleep periods (Ruigt et al., 1989). Theta oscillations may serve as a mechanism not only for synchronizing neuronal activity, but also for segmenting, within each theta cycle, samples of stimuli that the animal may be experiencing. This potential makes the theta rhythm to be recognized as a discrete unit for processing sensory information (Colgin and Moser, 2010).

The second brain oscillation, gamma, in the 30 to 100 Hz frequency band, works together with the theta to create a neural code. Gamma oscillations occur in bursts at particular times within the theta cycle in which they 'nest'. Their interactions are expected to serve the function of allowing the representation of multiple items to be organized in a defined order. This proposal was based on the observation that the amplitude of gamma oscillations is modulated at theta frequency. Actually, a revolutionary interpretation of this was that different neuronal ensembles fire at different phases of the theta because the period of theta is slower than the period of gamma (Lisman and Buzsáki, 2008). It has been proposed that different theta cycles and their associated gamma cycles involve the recall of different memories through the sequential activation of ensembles representing sequential positions along different parts of an environment (Johnson and Redish, 2007; Lisman and Jensen, 2013).

The other prominent frequency in rodent hippocampus are the sharp-wave ripples (SWRs). They are triggered by the coincident activity at the CA3 region, which triggers through the synchronous activation of Schaffer collateral synapses large amplitude local field potentials, called 'sharp-waves' in the hippocampal CA1 stratum radiatum. This typically occurs when the animal has minimal interaction with its environment, such as immobility, consummatory behaviours and slow wave sleep (Vanderwolf, 1969; Buzsáki et al., 1983; Suzuki and Smith, 1987). At the same time, sharp-waves induce a local, fast oscillatory event (140–180 Hz) in the pyramidal CA1 layer, seen as the convergent depolarization of neurons known as 'ripple' events. Such events span between 50 to 150 ms, and during this time 10 to 18% of all neurons discharge synchronously in the CA3, CA1, subiculum and entorhinal cortex (O'Keefe and Nadel, 1976; Buzsáki et al., 1983, 1992; Chrobak and Buzsáki, 1996; Csicsvari et al., 1999, 2000).

The canonical function of the SWRs that happen during sleep has been to serve a critical role in memory consolidation. This idea arose from the fact that the cycles of the local field potential ripple oscillation coincide with the sequential activity of place cell sequences observed during previous experience (Buzsáki, 1989; Wilson and McNaughton, 1994; Diba and Buzsáki, 2007; Csicsvari et al., 1999; O'Neill et al., 2006). In support of this hypothesis, selective elimination of SPW-Rs during post-learning sleep results in impairment

of memory performance (Girardeau et al., 2009; Jadhav et al., 2012; Nokia et al., 2012). However SWR can occur during behaviour as well. These awake SWRs also reactivate place cell activity patterns that represent reward locations and occur at locations where decisions are made about where to go next in order to find reward; these include path choice points, the reward location, and brief pauses in locomotion (Karlsson and Frank, 2009; Dupret et al., 2010). The disruption of these waking SWRs at decision points also reduces behavioural performance (Jadhav et al., 2012) in solving complex spatial tasks, suggesting further roles of these waking SWRs in spatial decision making and memory.

Regarding the scope of the current work, it is noteworthy mentioning that all these hippocampal oscillations depend on the interactions between glutamatergic and GABAergic cells. The inhibitory neurons impose the oscillatory context on the pyramidal cells and, therefore, these oscillating inhibitory networks may provide temporal windows that allow individual pyramidal cells to modify their synaptic inputs in a coordinated manner (Freund and Buzsáki , 1996; Csicsvari et al, 1999). A factor contributing to the synchronization of excitatory network activity is the convergence of multiple excitatory inputs onto single inhibitory cells, together with the divergence of each interneuron specific outputs to different glutamatergic and GABAergic cells (Allen and Monyer, 2015). Underlying such notion is the fact that one single stimulated interneuron can synchronize the activity of pyramidal cells, as has been shown *in vitro* (Cobb et al., 1995), together with the observations that millisecond synchronicity occurs *in vitro* among interneurons that appeared to lack electrical connections, presumably through rebound mechanisms (Hu et al., 2011).

Nowadays, it is thought that during a single theta cycle the relative strength of inhibition onto the different pyramidal cell compartments changes systematically from the descending phase to the ascending phase of theta: with maximal inhibition being reached first at the axon initial segment, then at the cell body and the proximal dendrites and finally at the distal dendritic segments (Allen and Monyer, 2015). On the other hand, SWRs seem to be formed by the precise sequential activity of at least four classes of interneurons, resulting in a gradient of inhibition that is maximal in the stratum pyramidale, and decreases towards the oriens and radiatum strata (Cutsuridis and Taxidis, 2013; Allen and Monyer, 2015). Several studies suggest that the occurrence of SWRs is determined by the activity of PV-basket cells (Lapray et al., 2012; Chiovini et al., 2014; Stark et al., 2014; Schlingloff et al., 2014).

In summary, spatial learning reorganizes the connections of CA1 pyramidal cells in a way that the modulation of pyramidal cell spikes and local plasticity of the neuronal network involves the interneurons (Dupret et al., 2013).

1.5 The subject of study: CCK-interneurons

1.5.1 Description and subpopulations

The name of these interneurons derives from their actual release of CCK, as an octapeptide form of the CCK neuropeptide (CCK-8) throughout their somatodendritic and axonal compartments (Harris et al., 1985; Freund et al., 1986; Freund and Buzsáki, 1996; Harris et al., 2018). The main CCK receptors in the brain are the CCK2 receptors (Innis and

Snyder, 1980; Honda et al., 1993), whose activation triggers cell-type specific effects. Presumably through differential coupling to distinct G-protein-mediated signalling pathways, CCK2 receptor activation causes depolarization of PV-interneurons, while it indirectly suppresses GABA transmission from CCK-interneurons to pyramidal cells (Lee et al., 2011). On the other hand, CCK-interneurons GABA release acts via GABAa receptors enriched in α2 subunits that are known to mediate the anxiolytic effects of benzodiazepines (Freund and Katona, 2007).

CCK-interneurons are considered to be a non-overlapping population with the parvalbumin-expressing GABAergic neurons (PV-interneurons), but in rare cases they have been found to express both markers (Gulyás et al., 1991; Acsády et al., 1996; Tricoire et al., 2011; Harris et al., 2018). The predominant exclusivity of these molecular markers is in agreement with the fact that they have different precursors in the basal telencephalon during embryonic development: CCK-interneurons arise from the caudal ganglionic eminence, while PV-interneurons come from the medial ganglionic eminence (Tricoire et al., 2011).

In regard to their abundance in the brain, CCK-interneurons comprise between 20 to 30% of GABAergic neurons in the hippocampus and are present also in other brain regions (Somogyi et al., 1984; Kosaka et al., 1985; Sloviter and Nailer, 1987; Whissell et al., 2015). They are a diverse class with the common characteristic of asynchronous neurotransmitter release (Hefft and Jonas, 2005; Daw et al., 2009). Several CCK interneuron classes have been described, targeting different parts of the soma and dendritic axis of pyramidal cells. In the hippocampus CCK-interneurons contact either the perisomatic region or the dendrites of pyramidal cells (Nunzi et al., 1985; Cope et al., 2002; Klausberger et al., 2005; Whissel et al., 2015). Their spiking phenotype correlates with their synaptic target location, in a way that fast-spiking cells tend to target proximal segments of pyramidal cells and burst-firing or regular spiking phenotypes are more likely to contact pyramidal dendrites (Cope et al., 2002; Pawelzik et al., 2002; Somogyi et al., 2004; Klausberger et al., 2005).

This interneuron population also contacts other inhibitory neurons. Only around 8% of the CCK-basket cell synapses innervate interneurons, which typically are other CCK-expressing interneurons. However, cross-talk between CCK- and PV-basket cells has also been reported (Karson et al., 2009; Klausberger et al., 2005). All dendrite-targeting CCK-interneurons dominantly target pyramidal cells with roughly 6 synapses per connection, but a minority of terminals (roughly 8%) innervate other interneurons (Cope et al., 2002; Klausberger et al., 2005; Bezaire and Soltesz, 2013; Harris et al., 2018).

In the CA1 region of the hippocampus, there have been at least seven classes of CCK-interneurons reported based on their arborisation patterns. The most prominent class is formed by the perisomatic CCK-expressing basket (CCK-basket) cells, having most of their axonal arbours in the pyramidal layer, while their cell bodies have been found in the stratum oriens, pyramidale and radiatum and sometimes at the border between the radiatum and the lacunosum-moleculare layers (Vida et al., 1998; Cope et al., 2002; Pawelzik et al., 2002; Klausberger et al., 2005; Whissel et al., 2015). However, they are more abundant in the stratum radiatum and the stratum pyramidale (Jinno and Kosaka, 2003; Klausberger et al., 2005; Harris et al., 2018).

The dendrite-targeting CCK-interneurons have been classified in several types, here enumerated just for the purpose of clarity. First, are the bistratified CCK-cells having axons

ramifying in the stratum oriens and stratum radiatum (Pawelzik et al., 2002). Second are the CCK-quadrilaminar cells with axons ramifying in the strata oriens, pyramidale, radiatum and lacunosum-moleculare (Pawelzik et al., 2002). Third are the Schaffer collateral-associated (SCA) cells whose axons ramify mainly in the stratum radiatum and primarily target the oblique and basal dendrites of pyramidal cells (Cope et al., 2002; Pawelzik et al., 2002). The fourth are called apical dendrite targeting interneurons (ADI), they are similar to the SCA cells but preferentially innervate the main apical shaft of pyramidal cells avoiding oblique and basal dendrites (Klausberger et al., 2005). Fifth, there is a subtype called 'stratum oriens – stratum oriens' (SO-SO) cells, whose dendritic and axonal arbours are restricted to the stratum oriens. The sixth are the rare 'perforant path-associated' (PPA) cells, having the axonal and dendritic arbours within the distal stratum radiatum and stratum lacunosum-moleculare, targeting the distal apical tufts of CA1, but they also extend axon collaterals across the hippocampal fissure to target the dendrites of granule cells (Hájos et al., 1997; Vida et al., 1998; Pawelzik et al., 2002; Cope et al., 2002; Klausberger et al., 2005).

The best-studied subpopulation is the CCK-basket phenotype because it is the most representative: they comprise 65% of all CCK-interneurons, 9% of all CA1 hippocampal interneurons and 1% of all CA1 neurons (Tricoire et al., 2011; Bezaire and Soltesz, 2013; Chittajallu et al., 2013). As most of the GABAergic cortical cells which do not express PV or somatostatin, they co-express the 5-hydroxytryptamine (serotonin) receptor 3a (5-HT3) (Morales and Bloom 1997; Férézou et al., 2002; Vucurovic et al., 2010; Lee et al., 2010). The majority, but not all of them also express the cannabinoid receptor 1 (CB1 receptor) (Acsády et al., 1996; Marsicano and Lutz, 1999; Katona et al., 1999; Tsou et al., 1999; Klausberger et al., 2005; Glickfeld and Scanziani, 2006). And from all hippocampal interneurons expressing CB1 receptor, 90% express CCK (Marsicano and Lutz, 1999; Jappy et al., 2016). Therefore, CB1 receptor expression is considered a marker for CCK-basket cells, with the same caveats as CCK expression, since pyramidal cells can also express low levels of CB1 receptor (Katona et al., 2006; Kawamura et al., 2006; Robbe et al., 2006).

A population of CCK-basket cells also expresses the vesicular glutamate transporter 3 (Vglut3), which suggests that these cells have the ability to signal with both GABA and glutamate (Somogyi et al., 2004). Some other CCK-interneurons co-expresses the vasoactive intestinal polypeptide (VIP). They have smaller somata than the CCK-basket cells that do not express VIP, and represent 10 to 30% of VIP-interneurons (Kubota and Kawaguchi, 1997; Galarreta et al., 2004).

The genetic characterization of CCK-interneurons has still not reached a consensus allowing a clear correspondence to all the morphologically defined subclasses. As mentioned in the first section of this work, there have been many studies aiming to finely decipher the subclasses of these and other interneurons, facing a continuum of phenotypes that poses a challenge to the classification. For instance, single cell transcriptomics have confirmed that the traditionally called CCK-interneurons indeed strongly express CCK, but many other inhibitory classes, including PV-interneurons, express CCK at lower levels (Tricoire et al., 2011; Harris et al., 2018).

However, transcriptomic analyses have allowed to propose a novel subclass of CCK-interneurons, identified to target pyramidal cells rather than interneurons, expressing both CCK and VIP, which is located at the border of the strata radiatum and lacunosum-moleculare (Harris et al., 2018). Besides, these studies have verified markers related to the

cell localization (e.g. Cxcl14-expressing CCK-interneurons are localized in the stratum radiatum or stratum lacunosum moleculare border) and markers related to either soma-targeting (Vglut3) or dendrite-targeting (Calb1 and Reln) CCK-interneurons (Somogyi et al., 2004; Klausberger et al., 2005; Harris et al., 2018).

1.5.2 Genetic strategies to study CCK-interneurons

Although the immunohistochemical detection of CCK protein is only successful in interneurons (Morozov and Freund, 2003), the CCK mRNA is expressed in both glutamatergic (Morino et al. 1994; Giacobini and Wray 2008) and GABAergic populations in the cortex (Tricoire et al. 2011). Due to this fact, it has been impossible to target them by a simple Cre-driver mouse line. The simplest rationale for addressing this issue seems to be a double transgenic mouse line to condition the expression of the transgene to the promoters identifying the CCK-expression on the one hand, and an interneuron marker on the other. Up to date some approaches have been developed in this regard.

Taniguchi and collaborators crossed CCK-Cre mice with the interneuron specific driver mouse lines Dlx5/6-Flp or VIP-Flp to reveal the corresponding subsets of CCK-interneurons using that intersectional strategy that combines the activities of two recombinases upon dually conditional reporters (Taniguchi et al., 2011, 2014). Their first approach was to combine the CCK-Cre mouse line with the Dlx5/6-Flp, a transgenic line expressing the Flp recombinase in most cortical GABA neurons (Miyoshi et al., 2010). The conditional reporter that they used is a loxP-STOP-loxP-frt-STOP-frt-GFP reporter which expresses GFP only if both Cre and Flp are simultaneously or sequentially expressed in the same cell (Miyoshi et al., 2010). This intersectional strategy has paved the way for identifying interneurons by more than one molecular marker and a specific transgene-carrying vector dependent on both recombinases (Kepecs and Fishell, 2014). A variant of this technique will be the strategy of the present work, relying on the same driver lines but using a different vector design.

Another approach has overcome the need to generate dually conditional reporter lines for each protein of interest by relying on a recombinant AAV that restricts gene expression to GABAergic interneurons based on Dlx5/6 enhancer elements. The AAV can be used in combination with CCK-Cre drivers to selectively introduce transgenes into CCK-interneurons. This allows to introduce exogenous recombinant proteins for activity monitoring (e.g. GCaMPs) or for functional manipulation (e.g. ChR2, DREADDS) selectively into CCK-expressing interneurons (Dimidschstein et al., 2016).

An alternative strategy relied on CCK-Cre mice and a loxP-flanked neuregulin receptor ErbB4, which is thought to mediate the number of excitatory synapses received by PV-basket cells. Given that ErbB4 expression is restricted to a subset of GABAergic interneurons in the cerebral cortex, they found a way to investigate the consequences of disrupting the development of CCK-basket cells (del Pino et al, 2017).

The latest approach aiming to explore the functions of CCK-interneurons in emotion and cognition was made by Whissell and collaborators (2019). They implemented an intersectional approach by generating a triple transgenic mouse model. They combined the CCK-Cre and Dlx5/6-Flpe driver lines with mice that expressed the synthetic excitatory

hM3Dq receptor to perform chemogenetic activation of CCK-interneurons (Whissell et al., 2019).

1.5.3 Plastic properties of CCK-interneurons

The main source of CCK-interneuron plasticity is their endocannabinoid (eCBs) susceptibility. eCB are retrograde lipid messengers fundamental to regulate short- and long-term plasticity at excitatory and inhibitory synapses (Chevaleyre et al., 2006; Kano et al., 2009; Regehr et al., 2009; Castillo et al., 2012). In general, eCBs target presynaptic CB1 receptors, mediate short- and long-term synaptic depression of neurotransmitter release throughout the brain (Katona et al.,1999; Kawamura et al., 2006; De-May and Ali, 2013; Hu and Mackie, 2015; Katona et al., 2006; Kamprath et al., 2009; Younts et al., 2013; Gutiérrez-Rodríguez et al., 2017).

The mechanism behind it begins with the depolarization of the postsynaptic cell, or the activation of metabotropic receptors, both of which can trigger eCB mobilization (Hashimotodani et al., 2007). Once produced, eCBs act presynaptically by engaging CB1 receptors to transiently or persistently depress neurotransmitter release. Short-term eCB-dependent plasticity is usually evoked postsynaptically by depolarization-induced suppression of inhibition (DSI), by depolarization-induced suppression of excitation (DSE), or by brief postsynaptic metabotropic receptor activation (Kreitzer and Regehr, 2001; Ohno-Shosaku et al., 2001, 2003; Wilson and Nicoll, 2001; Maejima et al., 2001; Kim et al., 2002). On the other hand, eCB-mediated long-term depression (eCB-LTD) is usually triggered by synaptic activation of group 1 metabotropic glutamate receptors (Heifets and Castillo, 2009).

In the hippocampus, the expression level of CB1 receptor is higher in inhibitory GABAergic cells synaptic terminals than in glutamatergic neurons, and it seems that CB1 receptors expressed on excitatory terminals have lower sensitivity; therefore, inhibitory inputs are vastly more sensitive to eCB signaling than excitatory inputs (Ohno-Shosaku et al., 2002; Kawamura et al., 2006; Domínguez et al., 2014). This confers a peculiar plasticity to CB1 receptor-expressing CCK-basket cells, involved in the feed-forward inhibition of hippocampal CA1 pyramidal cells (Basu et al., 2013).

Regarding these plastic properties of CCK-interneurons, Younts and collaborators (2013) found that postsynaptic hippocampal CA1 pyramidal cell activity is sufficient to engage presynaptic long-term plasticity via retrograde eCB signaling. They proposed that pyramidal activity depresses somatic and dendritic inhibitory synaptic inputs while sparing excitatory synapses. Therefore, eCB-mediated disinhibition could shift the synaptic balance in favour of excitation and alter information flow through the CA1 circuit (Younts et al., 2013).

In another work, Jappy and collaborators (2016) showed that in vitro theta burst stimulation triggered robust LTD at the synapses between interneurons expressing CB1 receptor (putative CCK-interneurons) and pyramidal neurons in the CA1. The locus of LTD induction was postsynaptic and required activation of GABAb receptors (GABAbR). Also, this LTD involves GABAbR-dependent suppression of adenylyl cyclase and consequent reduction of PKA activity. This makes the CCK-interneuron to pyramidal cell synapses different from

the majority of the other hippocampal inhibitory connections where theta burst stimulation results in long-term potentiation (Jappy et al., 2016).

1.5.4 Proposed functions of CCK-interneurons

The classical view in the field has been that the two main types of perisomatic interneurons have defined distinct functions (Freund and Katona, 2007, Glickfeld and Scanziani, 2006, Klausberger et al., 2005; Harris et al., 2018). Namely, it is believed that since PV-basket cells are efficiently driven by local pyramidal cells, they must operate as 'clockworks' controlling spike timing and the precision of cortical network oscillations. And that since the activity of CCK-interneurons depends on subcortical inputs that carry information about the 'inner world' of the animal, they must be functionally specialized for the regulation of emotional behaviours such as mood, anxiety and fear and in general function as a plastic fine-tuning device (Buzsáki, 1996; Freund, 2003; Freund and Katona, 2007).

This hypothesis has found evidence in the molecular and physiological characteristics of each basket cell population. The PV-basket cells are tight coupling of P/Q-type Ca2+ channels and Ca2+ sensors expressed in the PV-basket terminals allow them to release GABA in a highly synchronized manner (Hefft and Jonas, 2005). In contrast, CCK-basket cells release GABA asynchronously because they express N-type Ca2+ channels, which are loosely coupled to the Ca2+ sensor therefore not do not allow for a precise following of fast signals but favour integration of excitation (Hefft and Jonas, 2005; Glickfeld and Scanziani, 2006; Freund and Katona, 2007). Indeed, as mentioned above, CCK-interneurons express several receptor subtypes involved in controlling emotional behaviour, such as CB1 receptor and 5-HT3 receptors (Morales and Bloom, 1997; Marsicano and Lutz, 1999). Additionally, the postsynaptic targets of CCK-GABA neurons are enriched with α2-containing GABAa receptors (GABAaR), which regulate anxiety behaviours and the effects of anxiolytic drugs (Freund, 2003).

The signalling by CCK-interneurons is complex as it involves both the inhibitory neurotransmitter GABA and the neuropeptide CCK. In the hippocampus, the release of GABA from CCK-interneurons inhibits CA1 pyramidal cells (Basu et al., 2013) whereas the release of CCK excites PV-interneurons (Lee et al., 2011). As PV-interneurons also inhibit CA1 pyramidal cells, these effects may have complex consequences and may lead to an increase in the inhibitory tone within the hippocampus and, therefore, influencing memory processes (Whissell et al., 2013).

Given that CCK-interneurons elicit slow, asynchronous inhibitory events on their targets, they are thought to orchestrate the theta frequency network oscillations associated with cognitive processes (Curley and Lewis, 2012; Nagode et al., 2014). Also, the presynaptic nerve terminals of CCK-interneurons enriched with CB1 receptors have been implicated in cognition and memory as well as the neuronal plasticity linked to them (Katona et al., 1999; Carlson et al., 2002).

In addition to their implication in theta oscillations, CCK-interneurons have been shown to be gamma-modulated. Tukker and collaborators (2007) reported that the CCK-interneurons are gamma-modulated and fire preferentially at an early gamma phase, which is before pyramidal cells fire (Csicsvari et al., 2003). Linking this modulation to their

expression of CB1 receptor (which implies that pyramidal cells can selectively reduce the inhibition from CCK-expressing cells via retrograde CB1 receptor activation), they suggest that CCK-interneurons could contribute to setting dynamic and activity-dependent thresholds for pyramidal cells (Tukker et al., 2007).

Thereafter, it has been proposed that CCK-interneurons are well suited to increase the contrast in the firing of strongly active (disinhibited via CB1 receptors) and weakly active or inactive (still inhibited by CCK interneurons) pyramidal cells, which is expected to aid in the implementation of sparse coding in cell assemblies (Klausberger and Somogyi, 2008).

Regarding to their participation in SWR events, Kohus and collaborators (2016) used slice preparations for characterizing the CA3 network activity and functional connectivity of perisomatic and axo-axonic interneurons. They proposed a description of the interactions between PV-basket cells and pyramidal cells that contribute to SWR generation, involving complex dynamics of CCK-interneuron activity (Kohus et al., 2016). Despite presenting candidate mechanisms for the involvement of CCK-interneurons in the CA1 area, it is worth emphasizing that besides the limited extent to which *in vitro* results can apply for the intact brain, the functional role of the cell types may differ among sub-regions due to the differential network organization and connectivity.

Some manipulations involving CCK-interneurons *in vivo* have shown to have effects in memory expression. For instance, cannabinoids disrupt the temporal coordination of hippocampal neurons and deteriorate theta, gamma and ripple network patterns without substantial changes in the average firing rate of neither pyramidal cells nor interneurons (Robbe et al., 2006). Furthermore, cannabinoids induce memory deficits, and this is proposed to occur due to reduced spike timing coordination and the associated impairment of physiological oscillations (Robbe et al., 2006).

Brown and collaborators (2014) used a transgenic mouse line to inhibit GABA synthesis in CB1 receptor expressing cells, which as before mentioned, are mostly CCK-interneurons. This manipulation enhanced cued fear but did not affect contextual fear learning (Brown et al., 2014). These results contradict another work where inhibiting GABA synthesis in CCK-interneurons disrupted olfaction and locomotion but neither recognition memory nor anxiety (Schmidt et al., 2014).

An additional work linking CCK-interneurons to memory processes has been made by Basu and collaborators (2016), showing that indirect inhibition of CCK-interneurons in the CA1 region altered contextual fear conditioning and object recognition (Basu et al., 2016). Furthermore, del Pino and collaborators (2017) recently found that disruption of CCK-interneuron wiring in the hippocampus diminished the power of theta oscillations during exploration, affected place coding and some instances of spatial memory (del Pino et al., 2017).

Another work emphasizing the relevance of CCK-interneurons in oscillatory activity and memory processes is the one by Whissell and collaborators (2019). They showed that clozapine-N-oxide (CNO)-mediated activation of CCK-interneurons did not alter open field exploration or tail suspension test performance, while it slightly increased anxiety in the elevated plus maze test. However, the chemogenetic activation of CCK-interneurons enhanced cognitive and memory behaviours including social recognition, contextual fear conditioning, contextual discrimination, object recognition, and problem solving in the puzzle box. Therefore, they suggest that the systemic activation of this interneuron

population minimally affects emotion but significantly enhances cognition and memory (Whissell et al., 2019).

For explaining such effects, Whissell and collaborators (2019) propose that by increasing inhibition, CCK-interneurons may reduce 'noise' in the hippocampal network activity, making it possible to encode orthogonal memories that are easily discriminated. This would be in agreement with previous works proposing that they may play a role in signal amplification by enhancing the signal-to-noise ratio at the network level (Bartos and Elgueta, 2012). It is important to note, however, that they did not examine cortical oscillations but rather proposed it as an exciting possibility that may be addressed in future studies (Whissell et al., 2019).

Collectively, these reports emphasize the complex and surprising characteristics of the CCK-interneuron population. Several of the behavioural effects shown here may be explained by the alterations of cortical oscillations and suggest that CCK-interneurons are excellent candidates to regulate cognition and memory.

1.6 Aims of the project

Given the lack of knowledge about the role of the CCK-interneuron population in non-anaesthetised and freely moving animals, we adopted an exploratory approach aiming to:

(1) Specifically identify and manipulate (i.e. optogenetic silencing) the activity of the CCK-interneuron population.

(2) Describe the dynamics of the CCK-interneurons in the 'natural' setting (before the manipulation) in terms of their oscillatory behaviour.

(3) Evaluate the consequences of the silencing CCK-interneurons in the hippocampal network in terms of:

- Firing rate changes in all the recorded cells including differences in single spike and burst firing of pyramidal cells.

- Reactivation of awake firing patterns during sleep periods.

- Oscillatory behaviour of all the recorded cells.

- Place field activity of pyramidal cells.

2 Methods

All procedures involving experimental animals were approved by the IST-Austria ethics committee, carried out in accordance to the IST-Austria Preclinical Facility norms, and complying with the Austrian federal law (1974) under a project license approved by the Federal Science Ministry (license number BMWFW-66.018/0015-WF/V3b/2014).

2.1 Subjects and optogenetic technique

Data from three 3–6 month-old male mice is included in this work. Note that experiments were performed and data analysed a further three animals in which we were not able to detect light responses in any of the recorded cells. These animals will be considered as control experiments in future studies. Moreover, in one additional animal we detected virus expression in one hippocampal hemisphere only. Therefore, data from these animals were not included in this study.

In order to condition the expression of the proton pump Archaerhodopsin (ArchT) to the neurons co-expressing the Cre and Dlx recombinases, we used double transgenic CCK-Cre::Dlx-Flpe mice and AAV1/2 constructs having a STOP cassette flanked with FRT sites and an inverted expression cassette with ArchT-EGFP flanked by a Flex cassette. Both the mice and the virus were kindly provided by Dr. Peer Wulff. We used the opsin ArchT due to its fast kinetics that represented an advantage over the previous version Arch protein (Chow et al., 2010; Han et al., 2011).

For its activation we used a green/yellow laser light provided by a 561-nm diode-pumped solid-state laser (DPSS) laser system (COBOLT Jive 300 mW DPSS) light source equipped with an acousto-optic modulator (Omicron) that enabled the reception of TTL signals from the board and controlling the voltage with an analog controller device. The laser was coupled to a 4.5 m long optic fibre patch cord (Doric Lenses: BFP(2)_200/220/900-0.53_4.5_FCM-2xMF1.25) from where two 200 µm patch cords transmitted the light to the Microdrive fibres. The laser intensity was set to deliver 5 mW total power at the tip of the implanted fibres on the head of the animal.

2.2 Description of surgeries

Surgeries were performed according to standard procedures from the group, in compliance with the applicable laws and guidelines of Austria and of the European Union. In general, surgeries were performed under deep anaesthesia using isofluorane (0.5–3%), oxygen (1–2 l/min) and an initial dose of Metamizol (200 mg/kg). The animals were then placed on the stereotaxic frame properly aligning bregma and lambda. Glucose 5% was administered every hour for ensuring hydration during surgery and Meloxicam (5 mg/kg) was used as a post surgery analgesic. After each surgery, careful examination of the animal was performed for 7 days according to our animal facility guidelines. Virus injection and microdrive implantation surgeries were conducted separately.

Mice were first injected with 500 nl of virus in 2 sites per hemisphere, targeting the dorsal CA1 pyramidal layer. The two sites coordinates (in mm) referenced to bregma are 1) AP -1.7 ML 1.7 DV -1.15 and 2) AP -2.3 ML 1.7 DV -1.3. The craniotomy for the virus injection was set to be already the craniotomy that would be later on needed for

implanting the microdrive. Therefore, the coordinates for the craniotomy encompassed one window (1 mm^2) per hemisphere beginning at ML 1.1 and AP -1.5. In the eventuality of damaging the Dura mater when opening the craniotomy, the brain surface was kept carefully hydrated and surgical wax was secured after the injection to keep the brain protected. At each injection site, a glass capillary delivered 500 nl of undiluted virus at a flow of 100 nl/min. The capillary was let intact for 5 min after the injection and then slowly retracted. After the injections the skin wound was stitched.

Two weeks after the virus injection, animals underwent an additional stereotaxic surgery for implanting the microdrive coupled with two optic fibres. The general procedure for the implant surgery is described in detail in a recent report (Rangel-Guerrero et al., 2018), with the main difference being that the craniotomy was already done during the virus injection surgery.

Briefly, six stainless-steel screws were positioned to anchor a dental acrylic wall that would hold the microdrive to the mouse skull, two of such screws were placed above the cerebellum to serve as a ground. Then the microdrive was loaded centred at the dorsal hippocampus (AP -1.9 ML 1.7) and the optic fibres were placed in the stratum oriens (DV -1 mm) to ensure the light spreading to the CA1 pyramidal layer when the mouse would be plugged to an optic fibre connecting with the laser source, in order to control the activity of CCK-expressing inhibitory neurons. The placing of the optic fibres to that depth ensured as well that the tetrodes were positioned in the cortex. Next, the tetrodes were paraffin wax coated and the whole microdrive was attached with dental acrylic to the screws fixed on the skull. Finally a black coating of carbon-painted acrylic was applied to prevent light scattering when the laser light would be delivered.

The mouse was then surveyed while resting on a heating pad until waking up from the anaesthesia and carefully monitored during the seven days of recovery. After the surgery and before the beginning of the recording sessions mice were individually housed with *ad libitum* access to food and water.

Data acquisition began between 2 to 3 weeks after the implant surgery, also allowing for sufficient AAV expression levels. After completion of the experiments, the mice were deeply anesthetized and perfused through the heart, first with 0.9% saline solution followed by a 4% buffered formalin phosphate solution for further histological processing.

2.3 Immunohistochemistry

The perfused brain was sliced to generate 40 µm sections in a microtome, collected in free-floating mode. Immunostainings for CCK were performed using the proCCK primary antibody 1:1000 (rabbit, L424) kindly provided by Dr. Andrea Varro, and a secondary anti-Rabbit 1:1000 conjugated Alexa-594 fluorophore (donkey, Life Tech: A21207). For enhancing the viral EGFP signal we used a conjugated antibody GFP-FITC 1:500 (goat, ABcam ab6662). Briefly: The primary antibody was applied for 36 hr in permeabilization buffer (PBS containing 1% BSA, 0.3% Triton X-100). After washing, the secondary antibody was applied for 1 h in PBS. After extensive washing, the tissue was mounted on glass slides and stored at 4 °C until imaging.

2.4 Description of the optogenetic microdrive

With the purpose of increasing the number of independently movable tetrodes, we improved the microdrive preparation described in the previous report (Rangel-Guerrero et al., 2018). Therefore, we used a different microdrive body designed together with Jim Donnett (Axona Ltd, Saint Albans, UK). It allowed to hold 12 independently movable tetrodes together with two fixed optic fibres at 45° from the lateral walls of the microdrive body, that protruded from the bottom of the microdrive, in the middle of the tetrode bundles. The two optic ferrules coupled to high numerical aperture poly-methyl-methacrylate (PMMA) optic fibres (Doric Lenses MFC_240/250-0.63_16.5mm_MF1.25(GR)_C45) had a groove etched into the ferrule to correspond to a locking system implemented in the microdrive lid in order to prevent its movement during the continuous plugging and unplugging events when recording.

The tetrodes were constructed from four tungsten wires (H-Formvar insulation with Butyral bond coat, California Fine Wire, Grover Beach, CA, USA) 10 µm in diameter twisted and then heated up to bind them into a single bundle. The tetrode tips were plated with gold to reduce their impedance to 200-300 kΩ. Since the tetrodes were inserted into a shuttle which was mounted onto a screw, we could independently lower the tetrodes by turning the screws (250 µm per full turn).

2.5 Description of the data acquisition process

We used an INTAN data acquisition system (RHD2000-Series Amplifier Evaluation System, Intan Technologies, CA, US, analog bandwidth 0.09–7603.77 Hz) via a lightweight cable and the signal was sampled at 20 kHz. We used the Ktan Software developed by Kevin Allen (https://github.com/kevin-allen/ktan/wiki). Two LEDs mounted on the headstage, with a distance of 5 cm between their centers, were used to track the trajectory of the mouse. A video camera (RICOH FL-HC0614-2M, 6mm F/1.4 2MEGA) was mounted on the ceiling above the recording environment and connected the Positrack software developed by Kevin Allen (https://github.com/kevin-allen/positrack/). The tracking signal was recorded together with the electrophysiological data on the same data file and read offline to match the tracking timestamps to the electrophysiological samples.

Given that the target recording area was the pyramidal CA1 layer and the tetrodes were implanted in the deep cortex, the screws had to be slowly turned while monitoring the electrophysiological signal in order to bring them to the layer. The standard procedure for verifying the position of the tetrodes in the layer, is the abundance of spikes, increased amplitude of theta oscillations with respect to the cortical signal, and specially, the presence of high frequency events termed as sharp wave ripples (150-250Hz), which can be observed clearly only during slow wave sleep stages. This process depended on the mouse getting accustomed to sleep after the tetrodes were moved, a process that could be very time consuming for some mice. Therefore, the animals were first manipulated and familiarized with an open box (12 x 12 x 26 cm) containing their nesting material on the floor, which would be designated as their ‘sleeping box’. Together with the process of positioning the tetrodes, the mice were also familiarized with the behavioural tasks.

2.6 Description of the behavioural paradigms

Previous to the beginning of recording, the mice were habituated to the environments and the tasks for 20 minutes per day during 4-6 days. Each mouse performed several behavioural paradigms, two of which will be the subject of the current work: the familiar environment exploration and the linear track running. For both of them, the animal was subjected to a food restriction protocol to keep it at 85% of the initial weight in order to increase the motivation to perform the tasks.

The familiar open field environment exploration consisted of a square arena (56 x 56 x 30 cm) where the animal was encouraged to be foraging. The floor of the environment was spread with pellet pieces at random. The order of recording sessions was as follows: 1) The previous sleep was a 25 min sleep session (sP). 2) The first exploration (e1) was a 25 min session where the animal was free to look for food in the arena. 3) The following 25 min sleep session (s1) served as a control for reactivation in the intact brain (without light application). 4) The second exploration 25 min session (e2) had a randomly selected half of the environment designated as the 'light-sector'. When the mouse was moving inside this sector, the laser was triggered for as long as the animal was not immobile for more than 2 s. Therefore, the neuronal silencing was conditioned to the position of the animal and the active movement during this session, which from now on will be termed 'the light session'. 5) The subsequent 25 min sleeping session had no light application. 6) The third exploration 25 min session (e3) of the familiar environment was used to test the effect of the previous optogenetic manipulation on the stability of place cell firing. 7) The following 25 min sleep session (s3) had no light application. 8) An additional 40 min sleep session (sL) with trains of 100 ms long light pulses (1 s intervals) that were used for the offline identification of the light-responsive cells.

The linear track running was performed on a long, rectangular environment with high dark walls (110 x 7 x 26 cm) where the animal was habituated to be running for gathering a reward at both ends of the track. The reward provided was 2 µl of a sweet liquid reward (30% sucrose condensed milk) provided by the experimenter with a pipette at a food plate on each side. The floor of the environment was rough in order to help the mouse movement. The order of recording sessions was as follows: 1) The previous sleep was a 25 min sleep session (sP). 2) The first exploration (e1) was a 25 min session where the animal was running back and forth collecting the rewards at the ends of the track. 3) The following 25 min sleep session (s1) served as a control for reactivation in the intact brain (without light application). 4) The second exploration 25 min session (e2) had a randomly selected half of the environment designated as the 'light-sector' as previously explained. 5) The subsequent 25 min sleeping session had no light application. 6) The third exploration 25 min session (e3) of the familiar environment was used to test the effect of the previous optogenetic manipulation on the stability of place cell firing. 7) In contrast to the open field exploration protocol, this sleep session (s3) was 50 min long. During this time we administered trains of 15 sec long light pulses interleaved with 20 sec of periods where the light was turned off. Such long pulses were planned to let us evaluate the effect of the CCK-interneuron silencing upon the sleep activity patterns. 8) An additional 40 min sleep session (sL) with trains of 100 ms long light pulses (1 s intervals) that were used for the off-line identification of the light-responsive cells.

2.7 Offline data processing

The offline data processing began by extracting the spikes (action potentials) from the raw 20 kHz sampled recordings from the high-pass filtered signal (800–5000 Hz). First, spike features were extracted using custom software for principal components analysis. Then, the spikes were segregated using automatic clustering software (http://klustakwik.sourceforge.net/) in order to assign them to putative individual neurons corresponding to the identity of each cluster. Those clusters were then manually refined by a graphical cluster cutting program (Csicsvari et al.,1998).

Autocorrelation and cross-correlation histograms reflect discharge probabilities. For constructing them, the correlation functions were calculated and the histograms were normalized by dividing each bin by the number of reference events. Only units with clear refractory periods (<2 ms) in their autocorrelation and well-defined cluster boundaries were considered for further analysis. The sessions of waking spatial exploration and sleep were clustered together. Stability of the cells was verified visually by plotting spike features over time and by plotting two-dimensional unit cluster plots in different sessions. In addition, an isolation distance (based on Mahalanobis distance) was calculated to ensure that the spike clusters did not overlap during the course of the recordings. CA1 pyramidal cells and interneurons were discriminated by their autocorrelations, firing rate and waveforms as previously described (Csicsvari et al., 1999; Henze et al., 2000).

2.8 Analysis of the processed data

To identify periods of theta activity, we used the ratio of theta (5–10 Hz) and delta (2–4 Hz) frequency band in 1600 ms segments (800 ms steps between measurement windows), using Thomson's multitaper method (Thomson, 1982; Mitra and Pesaran, 1999). Exploratory epochs included periods of locomotion and the presence of theta oscillations, which were revealed by the theta/delta ratio, so that no more than two consecutive windows of transient immobility were included. Waking immobility sessions were selected when both the speed and theta/delta ratio dropped below an established threshold (speed, 5 cm/s; theta/delta ratio, 2) for at least 2.4 s. Sleep sessions were recorded separately and identified by occasional occurrence of rapid eye movement (REM)-theta periods and the presence of slow-wave oscillations.

In order to classify the light response of individual neurons, we considered their firing during application of laser pulses during the 'phototagging' sleep. During the 40 min of this session, 100 ms light pulses were applied at 1 Hz while the animal rested in the sleep box. In this way, we classified the neurons as 'inhibited' or 'silenced' if they exhibited a firing rate reduction >10% during the light application. The threshold was set considering the high and stable baseline firing rate of interneurons, however the majority of the cells classified as inhibited actually displayed a higher reduction in firing rate. The neurons that displayed an increase of firing rate >30% were classified as 'disinhibited' as described previously (Schoenenberger et al., 2016). The rest of the cells not passing these criteria were assigned to the 'non-responsive' class.

For the detection of theta-oscillatory waves, the local field potential was filtered (5–28 Hz) and the large amplitude negative peaks of individual theta waves that occurred in theta band intervals (4-12 Hz) were detected. For gamma oscillations, local field potentials

were bandpass filtered (30–80 Hz) and the power (root mean square) of the filtered signal was calculated for each electrode (Csicsvari et al., 2003). Gamma epochs began when gamma power exceeded 2 SD above the mean for the recording session, and ended when gamma power dropped below 1 SD, and had to include detection of individual gamma cycle peaks and troughs (2 SD) (Senior et al., 2008). For the detection of SWRs, local field potentials were band-pass filtered (150–250 Hz), and a reference signal (i.e. a channel without ripple oscillations) was subtracted to eliminate noise (e.g. muscle artefacts). The power (root mean square) of the filtered signal was calculated for each electrode and summed across electrodes designated as being in the CA1 pyramidal cell layer. The threshold for SWR detection was set to 7 standard deviations (SD) above the background mean. The SWR detection threshold was always set in the first available sleep session but kept for the rest of them.

For calculating the phase relationship between single unit activity and theta or gamma oscillations, each spike was assigned to a given phase (20-30° bin size) of the normalized field cycle. From here, a phase histogram was calculated by summing unit discharges that occurred at different phases. The phase histograms were then normalized by dividing each bin by the number of cycles. And then we calculated the probability of unit discharge at each phase. For determining whether individual units were significantly phase locked to the waves, we applied the Rayleigh test to the unit-discharge field phases. The average angles were calculated as the circular means.

The place rate maps were calculated by dividing the environment area into 1.5 cm × 1.5 cm bins. For each bin, spikes were counted and divided by the animal's occupancy time in that bin. Raw rate maps were smoothed using a two-dimensional Gaussian kernel (SD, 3 cm). To compare place maps between exploration sessions, firing rates of all bins visited in both sessions were correlated bin-by-bin (Using Pearson correlation coefficient) to calculate PFS. Therefore, a high PFS indicates high stability of the place maps between the two sessions. To compare the place representations inside or outside the light zone between two exploration sessions, place maps were generated for these zones separately and smoothing was limited to within a given zone to prevent zone-specific effects from spuriously spreading into the neighbouring zone as a result of smoothing. Cumulative rate maps were constructed by adding up the firing rates of all individual pyramidal cells or interneurons, respectively, for each bin.

The spatial tuning of cells was calculated with Skaggs spatial information measure (Skaggs et al., 1993). In the analysis we only included CA1 place cells with place-field sparcity <0.3 (Skaggs et al, 1996), coherence >0.4 (Muller et al., 1989) during the reference exploration sessions. The bursting events were identified as the identified spikes occurring within <10 ms interspike intervals.

To compare firing rates between two sessions, we calculated a firing rate score by dividing the signed difference between the mean firing rates by the sum of the mean rates (that is, $c=(r2-r1)/(r2+r1)$, where r1 and r2 denote the mean firing rates in the two sessions that are compared). This score is always between −1 and 1, and the extreme values −1 and 1 mean that a neuron is firing exclusively in one of the two sessions.

The reactivation during sleep SWRs was measured by testing whether the tendency of cell pairs to fire together during SWRs was similar to the tendency during the previous exploration session. In order to measure the strength of their joint firing tendency we

calculated the cofiring values. For that we established the instantaneous firing rate counts (IFRCs) for each cell in 100-ms windows during theta activity in the exploration session. And the same for sleep SWR periods. The correlation coefficient between the IFRCs for each pair was then calculated separately for exploration and sleep sessions. The similarity of cell pairs' cofiring tendency across exploration and sleep/rest sessions was then assessed by calculating the correlation coefficient between exploration and sleep/rest period cofiring.

2.9 Statistical analyses

Statistical analyses were performed using custom software and the R Statistical Software (Foundation for Statistical Computing, Vienna, Austria). The means are plotted with the standard error of the mean (SE). All tests reported were done two-sided. Given that our data tended to not be normally distributed, we used non-parametric tests. The p-values and statistical tests for all experiments are reported in the respective figure legends. Holm–Bonferroni method was used when several pair-wise comparisons were done. Unless explicitly stated in the main text, all analysis included data from both recording paradigms (familiar environment exploration and linear track running) pooled together.

3 Results

3.1 Evoked light responses

3.1.1 Conditional silencing of CCK-interneurons

As mentioned in the introduction, there is no single molecular marker known up to date that unequivocally identifies the CCK-interneurons. This led us to rely on combinatorial genetics in order to manipulate the activity of this specific interneuron subpopulation. With the aim to silence these interneurons when green laser light (561 nm) was applied, we used an AAV expressing the light-driven outward proton pump archaerhodopsin (ArchT). The viral vector is designed to condition the expression of two recombinases (Cre and Flp) to the neurons expressing CCK (pyramidal and GABAergic cells) and Dlx (GABAergic cells) respectively. Transgenic CCK-Cre::Dlx-Flp mice were first virus injected and two weeks later they were implanted with a recording microdrive coupled with optic fibres to deliver light into the brain as indicated in the Methods section. With this approach, the co-expression of CCK and Dlx restricted ArchT expression - and therefore the silencing - to CCK-interneurons (Fig. 1).

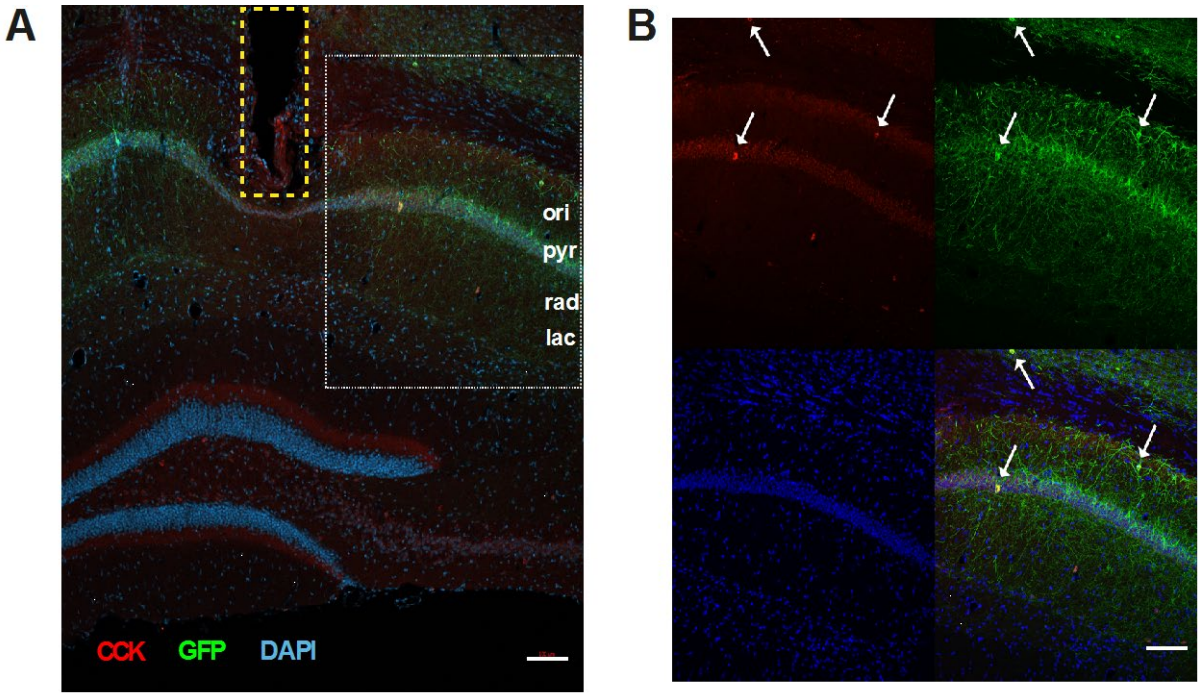

Fig. 1 *Confocal microscopy images of the hippocampal region of a mouse injected with our conditional ArchT-GFP viral vector targeting CCK-interneurons, and implanted with a microdrive coupled with optic fibres.* ***A)*** *One hemisphere of dorsal hippocampus illustrates the result of the stereotaxic viral injection and optic fibre implantation site (yellow dashed lines). A selected CA1 region (white dashed lines) indicates the strata: oriens (ori), pyramidale (pyr), radiatum (rad), lacunosum-moleculare (lac) is shown. DAPI staining indicates the nuclei (blue). Immunohistochemestry against GFP (GFP) and against CCK (CCK) revealed the interneurons expressing the transgenes and all neurons expressing CCK, respectively.* ***B)*** *Display of the CA1 selected region in separate channels. White arrows indicate co-localization of ArchT-GFP (green) with CCK immuno-staining (red). It suggests the specific viral expression in CCK-interneurons. White scale bar indicates 100 µm.*

This allowed us to record from dorsal CA1 pyramidal cells and interneurons, with or without manipulating the activity of the target interneurons. For this, two experimental protocols are the subject of the current work: the familiar open field environment exploration (referred to later as familiar exploration paradigm) and a familiar linear track running (referred to later as linear track paradigm). As explained in detail in the Methods section, the main behavioural difference between them is that the former is an open field foraging with food rewards randomly dropped to different locations while in the second, the location of food rewards only at the end of the linear track encouraged the mouse to run towards them following a one dimensional path. Both protocols consisted on 3 exploration sessions interleaved with sleeping sessions (Fig. 2).

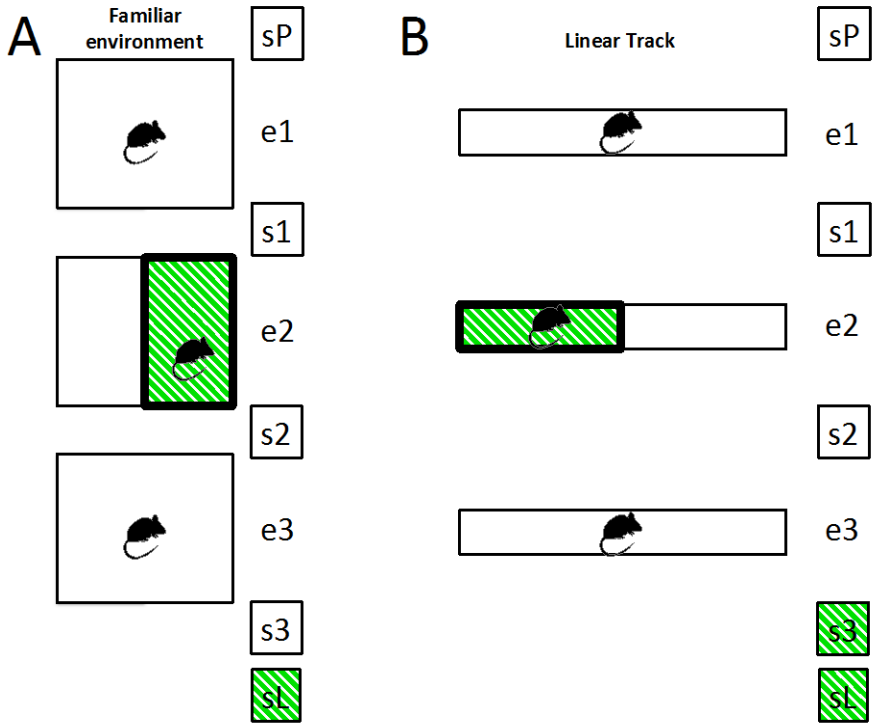

Fig. 2 *Illustration of the experimental protocols performed.* ***A)*** *Familiar exploration protocol: The first session was a pre-sleep (sP). The first exploration session (e1) and the following sleep session (s1) served as a control. For the second exploration session (e2), a random half of the environment was designated as the 'light-sector'. When the mouse was moving inside this sector, the laser was triggered. The third exploration session (e3) intended to evaluate possible light effects. The following sleep session (s3) had no light application. An additional sleep session (sL) with trains of short light pulses was used for the off-line identification of the light-responsive cells.* ***B)*** *Linear track running protocol: the sessions are the same as in A, except that during the s3 we administered trains of 15 sec long light pulses.*

The first recorded session was a sleep (sP) followed by an exploration session (e1) and the following sleep session (s1). For the second exploration session (e2), a randomly selected sector covering half of the environment was designated as the 'light-sector'. When the mouse was moving inside this sector, the laser was triggered. Therefore, the neuronal silencing was conditioned to the position of the animal during this session, which from now on will be termed 'the light session'. The subsequent sleeping session (s2) had no light application. The next exploration session (e3) of the same environment was used to test the effect of the previous optogenetic manipulation on the stability of place cell firing. The

following sleep session (s3) varied depending on the protocol used: it had no light application for the familiar exploration, while for the linear track we administered trains of 15 sec long light pulses interleaved with 20 sec of periods where the light was turned off. Such long pulses were planned to let us evaluate the effect of the CCK-interneuron silencing upon the sleep activity patterns. Finally, in both protocols, an additional sleep session (sL) with trains of short light pulses was used for the off-line identification of the light-responsive cells ('phototagging'). Unless indicated, in the subsequent analysis data from both protocols will be analysed together.

3.1.2 Identification and classification of light responses

For each animal recorded, we needed to validate that the optogenetic manipulation had been successful. This began by verifying the viral expression in histological samples (Fig. 1) and was followed by an off-line analysis of the electrophysiological signal based on the phototagging sleep session. We first looked if we could observe gross changes in the field activity as the ones happening when other interneuron populations have been silenced (Royer et al., 2012; Schoenenberger et al., 2016).

When averaging the traces around the light pulses, we found that indeed, there was a marked field deflection aligned with the laser light onset. The magnitude of such deflections would in principle depend on the relation between the power of light reaching each of the optic fibres in the brain, the layer where they were implanted and the position of the recording tetrode and the number of CCK interneurons that were impacted by light application. Therefore, we observed a variety of field responses across animals and recording days (since we reposition the tetrodes every day). However, this approach served as an initial validation of the experimental success from a technical perspective.

The final experimental validation came with the individual identification of light-mediated silencing of recorded neurons. This stage could only be reached after processing the data into clusters of spikes assigned to individual identifiers corresponding to different recorded cells (see Methods). Note that in two animals we observed field responses but the recorded cells did not exhibit any light responses. We excluded these animals from further analysis. After such a 'clustering' procedure, we identified 36 cells that were supressed during the whole length of the light pulses. Given that only the CCK-interneurons are expected to be inhibited by the light in our experiments, we conclude that we recorded the activity of 36 CCK-interneurons. To our knowledge, this is the first time that reliably identified CCK-interneurons are recorded during behavioural tasks in freely moving rodents. Therefore, their specific activity will be the subject of a following chapter in the current report.

Besides identifying the light-inhibited neurons, we also observed an increase of firing probabilities in response to light by other neurons (Fig. 3). In order to study all the recorded cells, as a standard procedure, we first classified them into putative pyramidal cells or interneurons based on a combination of criteria: their autocorrelogram (the probability that a cell fires an action potential at different times relative to the previous spike) and their firing frequency (Ranck et al., 1973; Fox and Ranck, 1981; Csicsvari et al., 1999). Next step was to refine the classification based on their light responses. We considered a cell to be 'disinhibited' when, during illumination, it increased its firing above a threshold (see

Methods). While we also observed 'non-responsive' cells whose activity did not change (i.e. its rate change did not exceed the rate increase or decrease thresholds) as a result of the light application. This left us with five main neuronal classes: disinhibited pyramidal cells (DIP, n = 380), non-responsive pyramidal cells (NRP, n = 95), disinhibited interneurons (DII, n = 39), non-responsive interneurons (NRI, n = 46) and inhibited interneurons (INI, equivalent to CCK-interneurons, n = 36). As expected none of the recorded putative pyramidal cells showed an inhibitory light response.

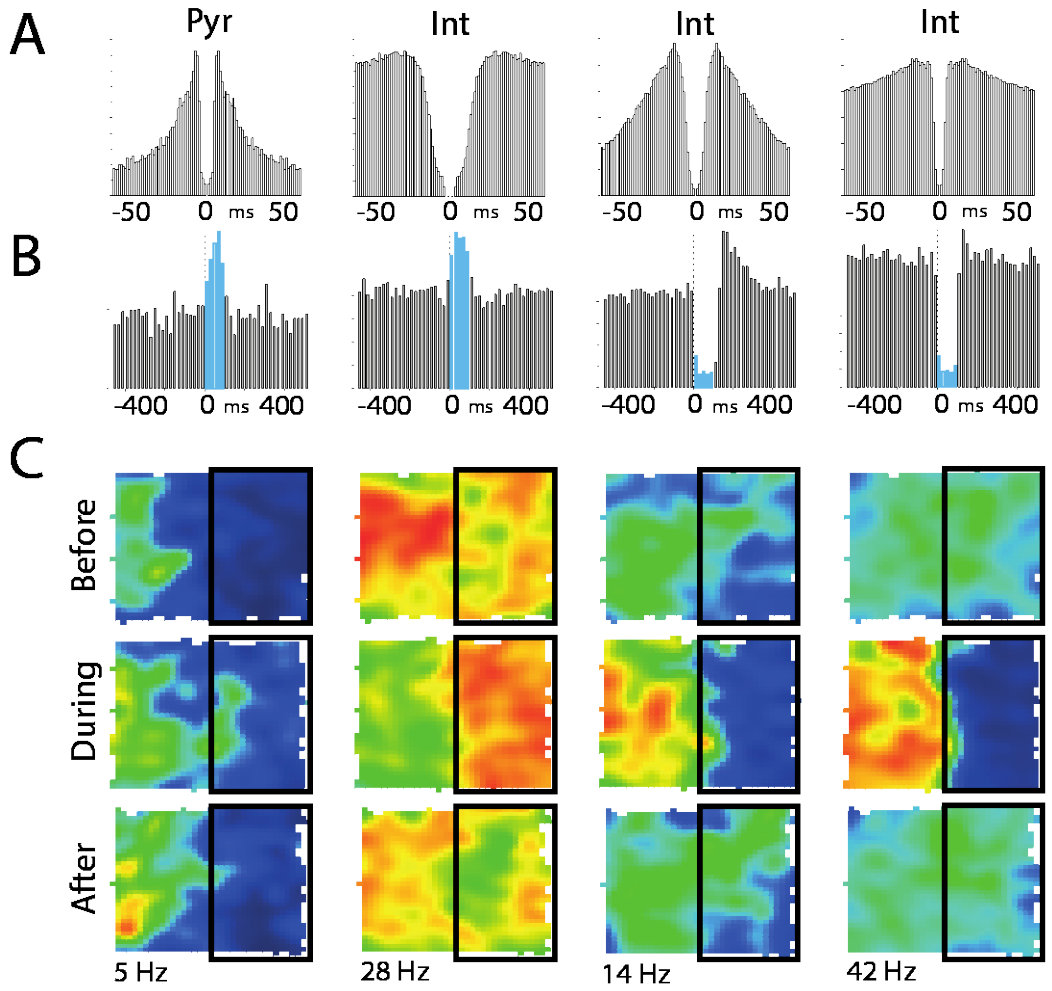

Fig. 3 *Examples of identified cells from the familiar environment exploration protocol.* ***A.*** *Autocorrelograms of example neurons: pyramidal (Pyr), interneurons (Int).* ***B.*** *Firing probabilities of the same cells during a 100 ms photo-tagging laser pulses. Note the laser-triggered cell disinhibition of the Pyr and one Int, while the other two Int show inhibition, therefore expected to be CCK+ cells.* ***C.*** *Rate maps of the indicated cells in three explorations sessions: before, during and after the laser was triggered when the animal entered to the indicated sector of the environment (black rectangle). Maximum firing rates (Hz) indicated at the bottom.*

3.2 Evaluating the light effects in the firing of cell populations

For the purpose of evaluating the effect of the light-mediated silencing of the CCK-interneuron population in the network activity of the recorded hippocampal region, we assessed the modulation of the firing rate (i.e. rate remapping) related to different

conditions. Since we identified pyramidal cells and interneurons, we calculated the rate remapping of all the cell classes in this work. To quantify rate remapping, a firing rate score (see Methods) was calculated which represented the normalized firing rate differences between different sessions (Leutgeb et al., 2005). This measure was positive (maximum value 1) if the relative firing rate increased and was negative (minimum -1) when a firing rate decrease was detected. This way we compared the exploration 1 (e1, before the laser session) and either exploration 2 (e2, the laser session) or exploration 3 (e3, after the laser session). While doing such calculations, we considered the activity in the light sector (IN) separated from the sector without light triggering (OUT) for their comparison.

At first, we evaluated the rate remapping of pyramidal neurons. Significantly larger than zero rate remapping scores were detected in every category (e1/e2, e1/e3) and condition (IN, OUT) for disinhibited pyramidal cells (Fig. 4-A). This indicates that the light application triggered an upregulation of firing rates both inside and outside the light zone relative to e1, even when light was turned off in e2 and this rate upregulation was maintained even in e3. However, for both the DIP and NRP classes, a stronger rate remapping was observed for the IN sector compared to the OUT but only for the e1/e2 comparison. While between e1/e3, the rate remapping was similar in the IN and OUT sectors (Fig. 4 A-B).

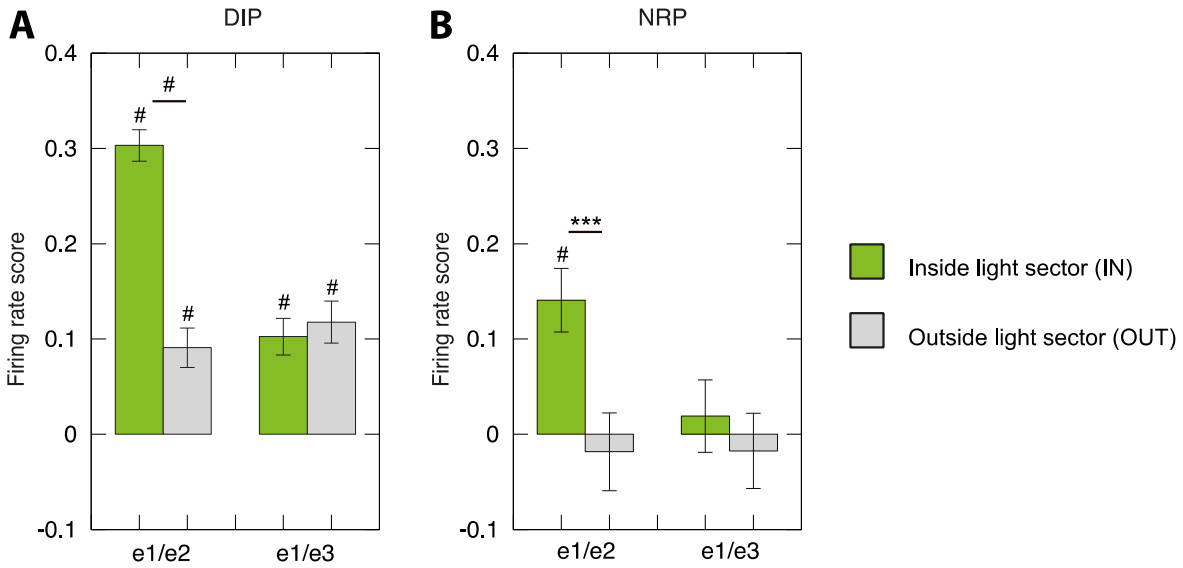

Fig. 4 *Rate remapping for the pyramidal cell classes, calculated between the exploration 1 (e1, before the laser session) and either exploration 2 (e2, the laser session) or exploration 3 (e3, after the laser session.* ***A)*** *Rate remapping for the disinhibited pyramidal cells (DIP) showed to be significantly larger than zero in all cases indicating that light application triggered an upregulation of firing rates both inside (IN) and outside (OUT) the light sector relative to e1, even in e3 when the light was no longer applied (Wilcoxon Rank Test, IN[e1/e2] p = 2.085621e-40; OUT[e1/e2] p =. 3.247098e-06; IN[e1/e3] p = 6.782809e-07; OUT[e1/e3] p = 5.990011e-08). When comparing the sector IN versus the OUT, only the e1/e2 rate remapping score showed a stronger rate remapping for the IN sector. While between e1/e3 rate remapping was similar in the IN and OUT sectors (Mann-Whitney U Test, e1/e2 p = 5.799485e-14; e1/e3 p = 0.3061093).* ***B)*** *Firing rate ratios for the non-responsive pyramidal cells (NRP). Identified significant rate remapping was specific for the e1/e2 ratio at the IN sector (Wilcoxon Rank Test, IN[e1/e2] p = 0.0001501594; OUT[e1/e2] p = 0.4665390286; IN[e1/e3] p = 0.5509357829; OUT[e1/e3] p = 0.5933764255). When comparing IN versus OUT sectors, significant rate remapping differences were detected for the e1/e2 ratio only (Mann-Whitney U Test, e1/e2 p = 0.001177024; e1/e3 p = 0.455333110). P-values *p ≤ 0.05, **p ≤ 0.01, ***p ≤ 0.005, #p ≤ 0.0005, indicate significance level.*

Therefore, rate remapping was seen in this case not only during the light application but lasted even after the cessation of the light application. It was surprising to observe that the non-responsive pyramidal neurons also changed their firing rates, although in this case the change was specific for the IN sector and only for e1/e2 rate remapping (Fig. 4-B), likely reflecting rather a network effect than direct disinhibition.

We next ran the same analysis on the three interneuron classes (Fig. 5). We only found significant changes in the e1/e2 category. A positive change in the firing rate was seen for the remapping in the IN sector compared to the OUT sector in the case of the DII, while the INI showed a significantly negative change in the IN sector compared to the OUT one.

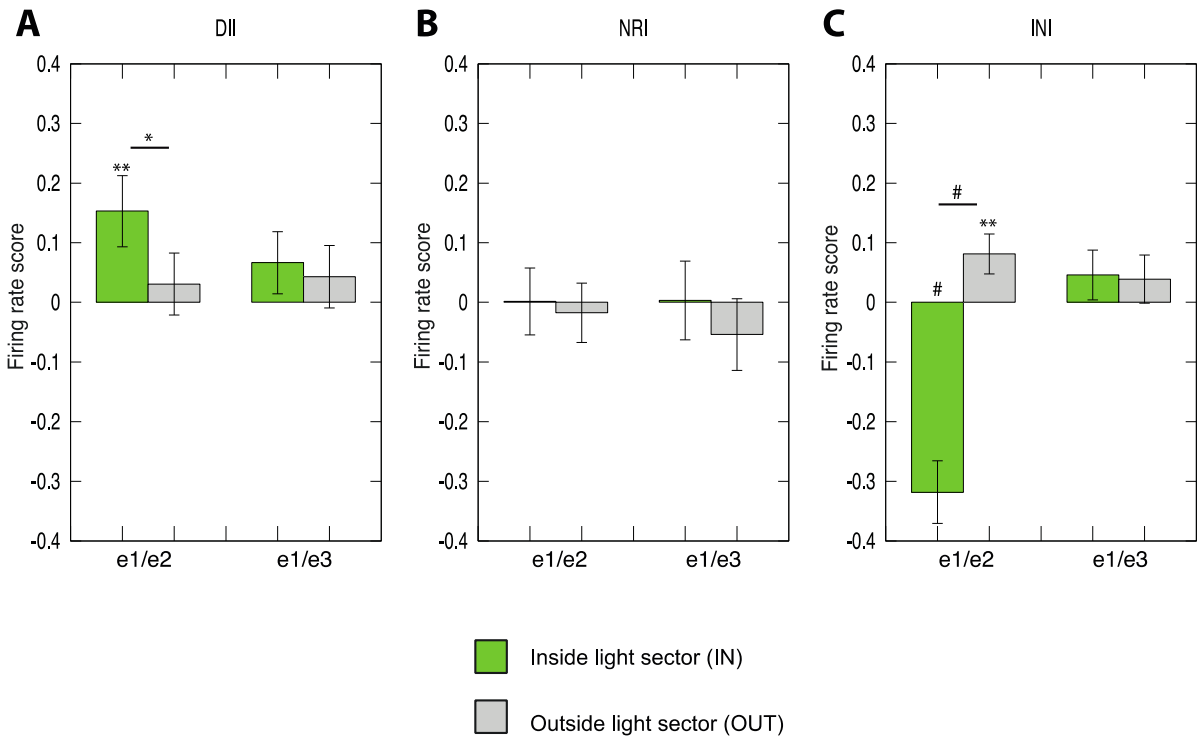

Fig. 5 *Rate remapping for the interneuron cell classes, calculated between the exploration 1 (e1, before the laser session) and either exploration 2 (e2, the laser session) or exploration 3 (e3, after the laser session.* ***A)*** *Rate remapping for disinhibited interneurons (DII) showed to be significant (larger than zero) between e1/e2 inside the light sector (Wilcoxon Rank Test, IN[e1/e2] p = 0.00560315; OUT[e1/e2] p = 0.79656226; IN[e1/e3] p = 0.33856552; OUT[e1/e3] p = 0.71136640). When comparing rate remapping in the light sector (IN) versus without light triggering (OUT) only the e1/e2 case rate remapping was stronger in the IN than in the OUT sectors (Mann-Whitney U Test, e1/e2 p = 0.04067285; e1/e3 p = 0.70237259).* ***B)*** *The rate remapping of the non-responsive interneurons (NRI) were not significant in any case (Wilcoxon Rank Test, IN[e1/e2] p = 0.9944966; OUT[e1/e2] p = 0.6240097; IN[e1/e3] p = 0.6737286; OUT[e1/e3] p = 0.3359775). When comparing IN versus OUT sectors, no significant differences appeared (Mann-Whitney U Test, e1/e2 p = 0.8424800; e1/e3 p = 0.5574891).* ***C)*** *The inhibited interneurons significantly rate remapped in the e1/e2 cases but was not significant between e1/e3 (Wilcoxon Rank Test, IN[e1/e2] p = 4.003756e-06; OUT[e1/e2] p = 0.009736925; IN[e1/e3] p = 0.4327209; OUT[e1/e3] p = 0.4327209). When comparing IN versus OUT sector rate remapping, significant differences were evident for the e1/e2 instance only (Mann-Whitney U Test, e1/e2 p = 3.749048e-08; e1/e3 p = 0.8668047). P-values *p ≤ 0.05, **p ≤ 0.01, ***p ≤ 0.005, #p ≤ 0.0005, indicate significance level.*

The later decrease in firing rate remapping was expected, reassuring that the classified INI are reliably silenced and indeed CCK-interneurons. Interestingly INI showed a positive rate remapping between e1/e2 in the OUT sector suggesting that once the cell was released from the light mediated inhibition, it triggered a rebound excitation in its activity. The rate changes of the non-responsive interneurons were not significant in any case. The fact that no significant differences were found in in the e1/e3 category suggests that the light-driven rate remapping did not alter the subsequent network activity in the exploration of the same environment after the light session.

As a second approach, we aimed to further study the effects of our manipulation not only in the waking activity but also during the sleep period and compare whether light application triggered stronger network changes during waking or sleep periods (Fig. 6). We compared the rate changes between the e2 session in the OUT and IN sectors, to the rate change inside and outside 100 ms light pulses at the last sleep session where laser test pulses were applied (sL).

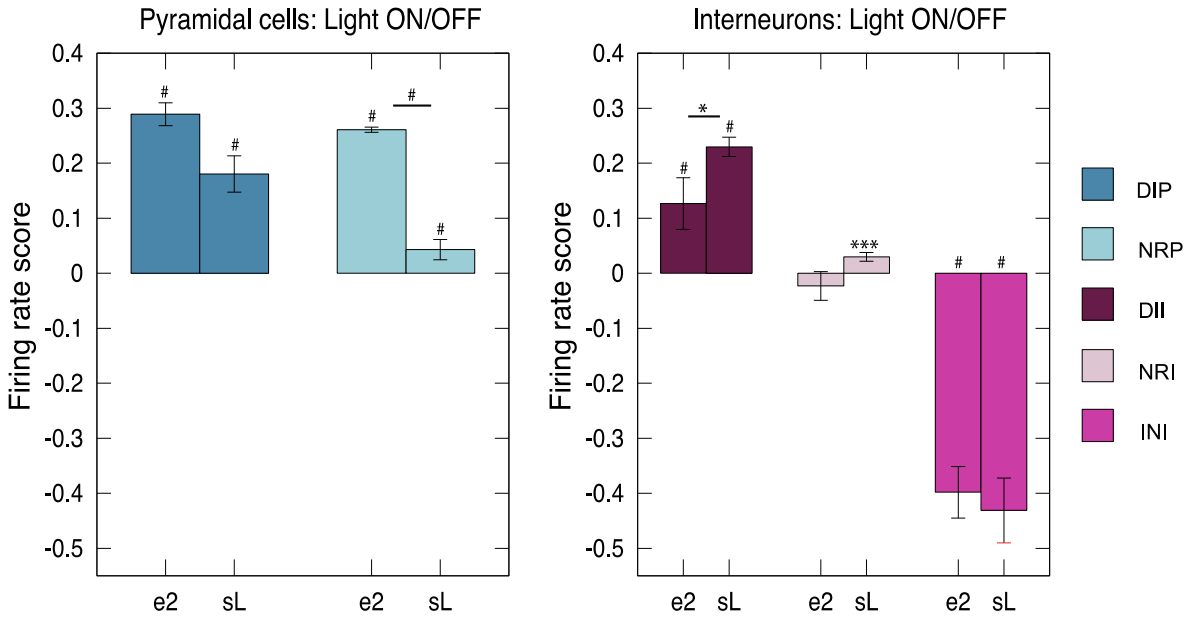

Fig. 6 *Normalized firing rate differences between the laser ON and OFF epochs either during the exploration 2 (e2) in the IN and OUT sectors or during the last sleep where regular laser pulses were applied (sL).* ***A)*** *Pyramidal cells showed a significant relative rate differences between the IN (i.e. ON) and OUT (i.e., OFF) sectors during e2 (Wilcoxon Rank Test, DIP p = 2.129253e-30; NRP p = 5.951165e-07). Both pyramidal classes exhibited significant differences in the relative rates between the ON and OFF periods during the sleep light application session (Wilcoxon Rank Test, DIP p = 1.058033e-54; NRP p = 1.117393e-03). There were also significant differences between the normalized rate differences of the ON and OFF periods when these were compared in exploration and sleep but only for the pyramidal cells classified as nonresponsive (Wilcoxon Rank Test, DIP p = 0.1071052; NRP p = 2.986291e-05).* ***B)*** *The disinhibited and inhibited interneuron classes showed a significant relative ON/OFF rate differences during e2 (Wilcoxon Rank Test, DII p = 8.859716e-03; NRI p = 0.402687910; INI p = 2.793968e-09). All interneuron classes exhibited significant differences in the relative rates between the ON and OFF periods during the sleep light application session (Wilcoxon Rank Test, DII p = 7.450581e-09; NRI p = 0.001468203; INI p = 4.004687e-08). There were also significant differences between the normalized rate differences of the ON and OFF periods when these were compared in exploration and sleep, specifically but only for the DII (Wilcoxon Rank Test, DII p = 0.03170907; NRI p = 0.06824152; INI p = 0.4327209). P-values *p ≤ 0.05, **p ≤ 0.01, ***p ≤ 0.005, #p ≤ 0.0005, indicate significance level.*

All but the NRI cell class showed significant relative rate differences between the ON (i.e. IN) and OFF (i.e. OUT) sectors during e2, and all neuron classes exhibited significant differences in the rates between the ON and OFF periods during sL. There were also significant differences between the normalized rate differences of the ON and OFF periods when these were compared between exploration and sleep, but only for the pyramidal cells classified as nonresponsive and the disinhibited interneurons.

This revealed that the DIP are recruited as efficiently by the light in awake than in sleep periods, whereas the NRP are not recruited during sleep as much as in the waking condition. Finally the DII are more disinhibited in the sleep than during the waking period but the strength of rate suppression was similar in waking and sleep for the INI.

3.3 Alterations in single cell activity during waking and sleep

3.3.1 Effect of CCK-interneuron silencing on pyramidal firing modes

It is known that the pyramidal neurons can discharge spikes or bursts while the animal is in their place field (Ranck, 1973). Previous works have shown that both discharge modes are specifically regulated by GABAergic activity (Royer et al., 2012; Schoenenberger et al., 2016). We therefore considered crucial to study if the manipulation inflicted any difference in the bursting and the single spiking rate.

We considered action potentials as part of a burst if another action potential preceded or followed it within 10 ms. Single spikes and bursts were identified during the exploration 1 (e1) and the exploration 2 (e2) in order to calculate their relative rate change (Fig. 7). Similar to the previous firing rate analysis, there was a significant increase of the relative change of burst and single spikes happening when the animal entered the light sector (IN) during the exploration 2 for both DIP and NRP (Wilcoxon Rank Test, DIP-1spike p = 2.916614e-38; DIP-burst p = 3.827620e-30; NRP-1spike p = 0.001090689; NRP-burst p = 0.002449093). And the same happened outside of the light sector (OUT) for the DIP but not for the NRP, for which a not-significant decrease of the relative change of bursts between e1/e2 was observed (Wilcoxon Rank Test, DIP-1spike p = 1.179544e-04; DIP-burst p = 8.653797e-04; NRP-1spike p = 0.978936037; NRP-burst p = 0.270935585).

Despite the increase in both, there seemed to be a stronger relative change of bursting than of single spikes occurring during the light triggering. To evaluate this possibility, we compared whether the relative rate change of bursts to the one of single spikes (Fig. 7). This revealed that indeed, there was significantly more relative change in the number of burst events due to the light application for both the IN and OUT sectors for the DIP but not for the NRP (Wilcoxon Rank Test, DIP-IN p = 2.319374e-11; DIP-OUT p = 0.003471646; NRP-IN p = 0.09056622; NRP-OUT p = 0.224381393).

Next, we compared the relative rate changes (e1/e2) of bursts and single spikes occurring at the IN versus the OUT sector (Fig. 7). In this case, both the DIP and NRP values were stronger in the IN sector than in the OUT for both the single spiking and the bursting activity (Mann-Whitney U Test, DIP-1spike p = 2.720434e-15; DIP-burst p = 6.555795e-09; NRP-1spike p = 0.013530799; NRP-burst p = 0.005643157).

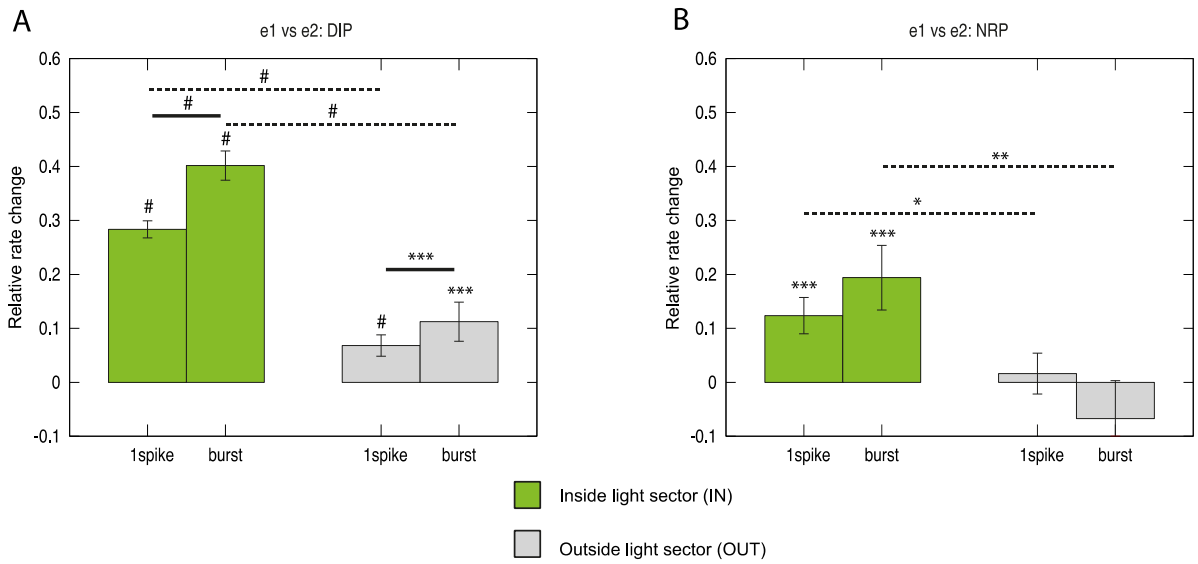

Fig. 7 *Relative rate change of the incidence of single spikes and burst events between exploration 1 (e1, before the laser session) and exploration 2 (e2, the laser session).* ***A)*** *Disinhibited pyramidal neurons (DIP) had a significant rate change when the animal entered the light sector (IN) (Wilcoxon Rank Test, DIP-1spike p = 2.916614e-38; DIP-burst p = 3.827620e-30) and outside (OUT) of it (Wilcoxon Rank Test, DIP-1spike p = 1.179544e-04; DIP-burst p = 8.653797e-04). Comparing the rate changes of bursts to the one of single spikes revealed between e1 and e2 there was higher relative change in the firing rate of burst spiking than those of singles spikes for both the IN and OUT sectors (Wilcoxon Rank Test, DIP-IN p = 2.319374e-11; DIP-OUT p = 0.003471646). Comparing the rate change of bursts and single spikes occurring at the IN versus the OUT sector (dashed lines) showed significant changes for both (Mann-Whitney U Test, DIP-1spike p = 2.720434e-15; DIP-burst p = 6.555795e-09).* ***B)*** *Non-responsive pyramidal neurons (NRP) have a significant e1/e2 rate change for both single spikes and burst when the animal inside the IN sector (Wilcoxon Rank Test, NRP-1spike p = 0.001090689; NRP-burst p = 0.002449093), but not for the OUT (Wilcoxon Rank Test, NRP-1spike p = 0.978936037; NRP-burst p = 0.270935585). There were no significant differences in the e1/e2 rate changes between single spikes and bursts for both the IN and OUT sectors (Wilcoxon Rank Test, NRP-IN p = 0.09056622; NRP-OUT p = 0.224381393. Comparing the e1/e2 rate changes of bursts and single spikes occurring at the IN versus the OUT sector (dashed lines) showed significant changes for both (Mann-Whitney U Test, NRP-1spike p = 0.013530799; NRP-burst p = 0.005643157). P-values *p ≤ 0.05, **p ≤ 0.01, ***p ≤ 0.005, #p ≤ 0.0005, indicate significance level.*

While the results above suggests that there is overall more change in the burst activity of pyramidal neurons than in the single spike firing as a consequence of disinhibition when the mouse is in the IN sector, there is still the question of whether the CCK-interneuron silencing leads to changes during the sleep of the animal.

The same rationale of analysis was then applied for comparing the relative rate changes of single spikes and bursts as for the overall firing rates, laser ON and OFF rate changes were compared, either during the exploration session 2 (e2) with the position of the animal conditioning the light application, or during the last sleep (sL) when trains of light pulses were applied (Fig. 8).

For both pyramidal classes, there was a significant increase of the ON versus OFF relative change of burst and single spike rates either during waking (Wilcoxon Rank Test, DIP-1spike p = 1.944998e-30; DIP-burst p = 1.624515e-19; NRP-1spike p = 3.080470e-06; NRP-burst p = 4.204560e-05) or during the sleep period, except for the NRP burst (Wilcoxon Rank Test, DIP-1spike p = 1.541819e-54; DIP-burst p = 2.877747e-41; NRP-1spike p =

1.978208e-04; NRP-burst p = 0.783931). There were also higher changes in burst than single spike rates during wake regarding the DIP but not the NRP (Wilcoxon Rank Test, DIP p = 0.01437366; NRP p = 0.0937427) while during sleep also only for the DIP but not for the NRP showed such a change (Wilcoxon Rank Test, DIP p = 0.0002481588; NRP p = 0.2229991).

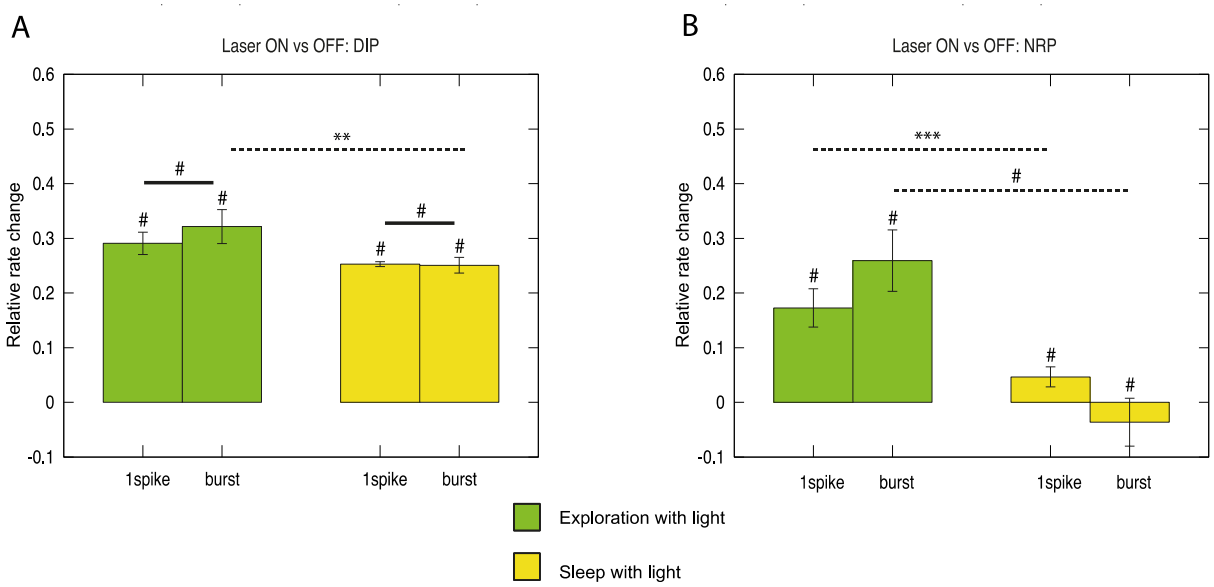

Fig. 8 *Relative rate changes of single spikes and bursts comparing the laser ON and OFF periods, either during the exploration session 2 (e2) or during the last sleep (sL).* ***A)*** *Disinhibited pyramidal neurons (DIP) show a significant increase of the relative change of burst and single spikes happening when the light was triggered in the ON periods compared to OFF either during waking (Wilcoxon Rank Test, DIP-1spike p = 1.944998e-30; DIP-burst p = 1.624515e-19) or during the sleep period (Wilcoxon Rank Test, DIP-1spike p = 1.541819e-54; DIP-burst p = 2.877747e-41). There were higher changes in burst than single spikes during wake (Wilcoxon Rank Test, DIP p = 0.01437366) and during sleep (Wilcoxon Rank Test, DIP p = 0.0002481588). Comparison of the rate change (ON vs OFF) of bursts and single spikes occurring at the waking versus the sleep periods (dashed lines) revealed a significant change for the bursting condition only (Mann-Whitney U Test, DIP-1spike p = 0.113401527; DIP-burst p = 0.0076838053).* ***B)*** *Non-responsive pyramidal neurons (NRP) show a significant increase of the relative e1/e2 rate change of burst and single spikes happening when the light was triggered during waking (Wilcoxon Rank Test, NRP-1spike p = 3.080470e-06; NRP-burst p = 4.204560e-05), while during the sleep period only for the single spike ratio exhibited significant changes (Wilcoxon Rank Test, NRP-1spike p = 1.978208e-04; NRP-burst p = 0.783931). There were no significant differences in the e1/2 rate change of bursting vs single spiking neither during wake (Wilcoxon Rank Test, NRP p = 0.0937427), nor during sleep (Wilcoxon Rank Test, NRP p = 0.2229991). Comparison of the e1/e2 rate changes between ON and OFF of bursts and single spikes occurring at the waking versus the sleep periods (dashed lines) revealed significant changes (Mann-Whitney U Test, NRP-1spike p = 0.0015664789; NRP-burst p = 0.0001192264). P-values *p ≤ 0.05, **p ≤ 0.01, ***p ≤ 0.005, #p ≤ 0.0005, indicate significance level.*

Finally, we independently compared the change (ON versus OFF) of bursts and single spikes occurring at the waking versus the sleep periods. From such analysis we observed that the DIP change was only significant for the bursting condition (significant stronger ON versus OFF rate change in the waking condition than in sleep), while the NRP values significantly changed for both the single spiking and the bursting activity and showing larger values in waking periods than in sleep (Mann-Whitney U Test, DIP-1spike p = 0.113401527; DIP-burst p = 0.0076838053; NRP-1spike p = 0.0015664789; NRP-burst p = 0.0001192264).

3.3.2 Effect of CCK-interneuron silencing on the reactivation of waking firing patterns in sleep

Cofiring is the correlation of the instantaneous firing rates (i.e. spike counts) of pyramidal cell pairs measured in 100 ms consecutive time windows. The similarity of cell-pair cofiring was measured by the correlation coefficient of corresponding cofiring of cell pairs during exploration and subsequent sleep to quantify the strength by which waking firing patterns of place cells are reactivated in sleep (Wilson & McNaughton, 1994). Given that this form of reactivation is likely to contribute to the stabilization of cell assemblies and relevant for memory (O'Neill et al., 2008; van de Ven et al., 2016), we assessed whether and how it was affected by the optogenetic silencing of CCK-interneurons. For that, we calculated the cell-pair cofiring correlations for the three sessions (e1, e2, e3) reactivated in the subsequent sleep periods. For the case of the e3 comparison we considered only the data from the linear track running protocol, since the subsequent sleep had the laser pulses applied. Our results show first the reactivation of the exploration 1 during the following sleep session, representing a reference without the silencing of CCK-interneurons (Fig. 9).

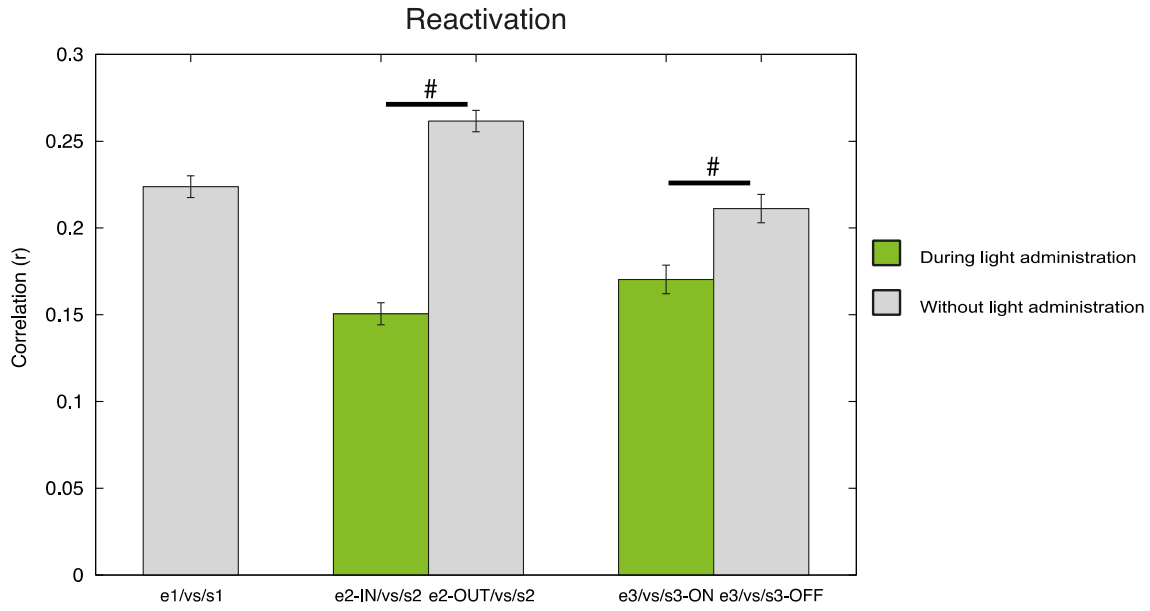

Fig. 9 *Correlation of cell-pairs cofiring at different exploration sessions and their respective sleep session that immediately followed the exploration. From left to right: Reactivation of the exploration 1 (e1, before the laser session). Reactivation of exploration 2 (e2, the laser session): activity split into the laser sector (IN) the outside of it (OUT) during exploration and cofiring was calculated separately and related to the subsequent sleep cofiring, showing that activity correlates better in the OUT sector (Z-test, p < 0.0005). Reactivation of exploration 3 (e3) cofiring was related to cofiring measured in the subsequent sleep separately for occurring during (ON) and outside (OFF) the laser pulses taken during sleep only in the linear track running protocol. Waking activity correlated better with undisrupted laser OFF periods (Z-test, p = 0.000178). P-values *p ≤ 0.05, **p ≤ 0.01, ***p ≤ 0.005, #p ≤ 0.0005, indicate significance level.*

When comparing the correlations of the waking patterns during the light session, we found that the IN sector cofiring patterns were less reactivated than the OUT sector ones (Z-test, p < 0.0005). The OUT sector of e2 was reactivated stronger in the subsequent sleep

than the level of reactivation was of e1 in the following sleep. Moreover, the reactivation e3 linear track cofiring patterns showed weaker reactivation in sleep periods where CCK interneuron activity was disrupted (Z-test, p = 0.000178). From this we conclude that the silencing of CCK interneurons during sleep disrupted the reactivation of recent waking patterns. Besides, firing activity patterns of exploratory periods in which CCK interneurons were disrupted were reactivated weaker than those in which CCK interneuron activity was not affected.

3.4 Activity of CCK-interneurons in freely moving mice

Since the reports on modulation of CCK-interneurons mostly come from anaesthetized animals (Klausberger et al., 2005; Tukker et al., 2007), it was important to evaluate how the light-inhibited cells classified as belonging to this interneuron subpopulation behaved during the three characteristic hippocampal rhythms (theta, gamma, SWR) in our freely moving animals during the first exploration (e1) before performing the light-mediated silencing.

In the first place, we evaluated how they participated during theta oscillations in our freely moving animals during the first exploration. The presence of theta modulation is evident in our results (Fig. 10). Our results show that CCK-interneurons (n = 35) were theta-modulated and preferred theta-phases grouped near the trough, beginning to raise at -120°, they peaked at -30° and had a pronounced decrease up to 90° after the trough. Therefore, the distribution of the CCK-interneuron preferred phases was skewed towards the descending portion of the cycle.

Next, we evaluated the CCK-interneuron behaviour during gamma oscillations (Fig. 11) during the exploration before the light session. We observed that cell activity of CCK-interneurons (n = 28) had some degree of gamma modulation. However, the firing probability remained rather constant across the gamma cycle, with the only marked change being a reduction aligned with the trough of the oscillation.

The last question we addressed was whether the optogenetically discerned CCK-interneurons are active during the SWR events identified during the sleep session 1 (s1) before the light session, therefore without any laser exposure. Our results showed that the average firing rate of the CCK-interneurons (n = 36) increased around the peak activity (centred at zero) of the SWR events (Fig. 12-A). The distribution of the average firing rates was highly asymmetric around the SWR peak. The average firing of CCK-interneurons increased in a time window of -50 ms, reached its maximum before the SWR peak, and returned to the baseline activity within 50 ms.

In addition, comparing the baseline to peak activity (Fig. 12-B) showed a widespread distribution of points, revealing that CCK-interneurons display a high variability in firing phenotypes during SWR. On the one hand, a group of cells that had a low firing rate (less than 10 Hz) in the baseline showed a minor increase in the peak rate. On the other hand, cells that had higher firing rates tend to show higher increases during the peak times.

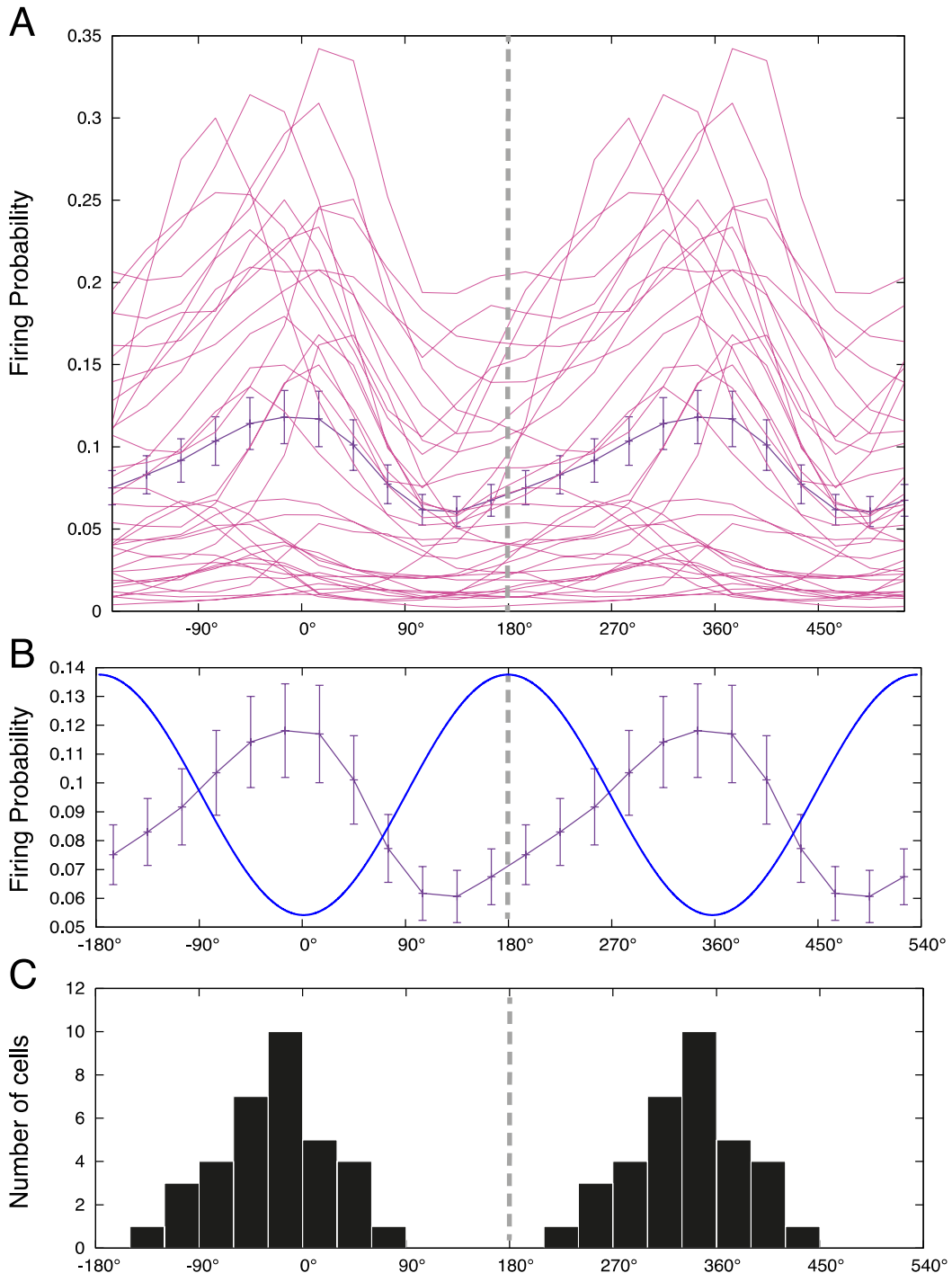

Fig. 10 *CCK-interneurons activity during identified theta oscillations during the exploration before the light session. Zero refers to the theta trough.* ***A****) Individual cell activity (pink traces) overlaid to their population activity represented as mean and the SEM (purple traces) showing the firing probability of cells at different phases of the theta oscillations.* ***B****) The same population firing represented as mean and the SEM (purple traces) of the average population firing probability at different phases of the theta oscillation overlaid with a representative theta oscillation along two cycles (blue trace). The presence of theta modulation is evident, with a skewed distribution towards the descending portion of the theta wave.* ***C****) Histogram of the preferred theta phases for all identified CCK-interneurons (bin size = 30), showing consistency with the average activity.*

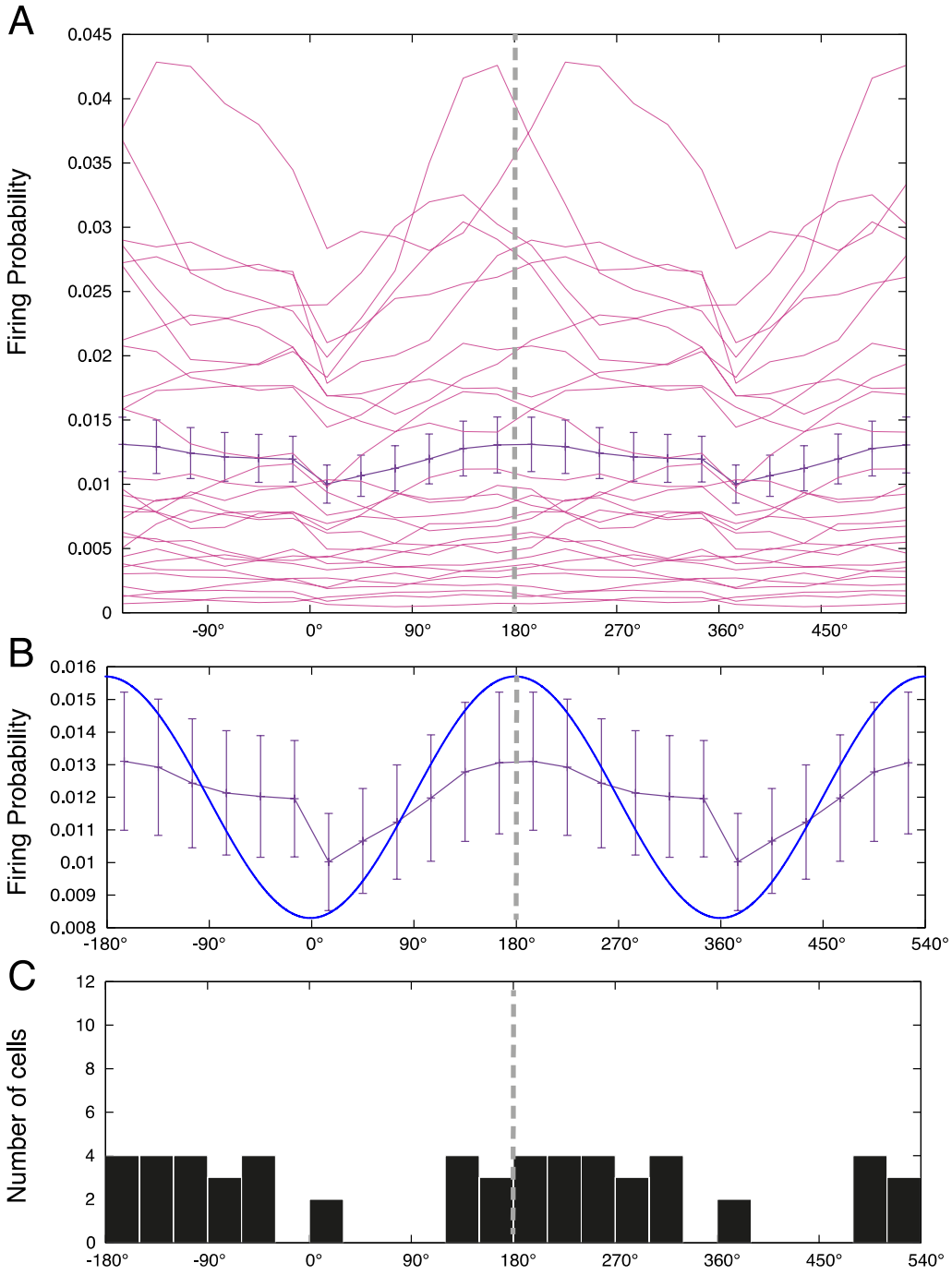

Fig. 11 *CCK-interneurons activity during identified gamma oscillations during the exploration before the light session. Zero refers to the gamma trough.* ***A****) Individual cell activity (pink traces) overlaid to their population activity represented as mean and the SEM (purple traces) showing the firing probability of cells at different phases of the theta oscillations.* ***B****) The same population firing represented as mean and the SEM (purple traces) of the average population firing probability at different phases of the gamma oscillation overlaid with a representative gamma oscillation along two cycles (blue trace). There is some degree of gamma modulation.* ***C****) Histogram of the preferred gamma phases for all identified CCK-interneurons (bin size = 30), showing consistency with the average activity.*

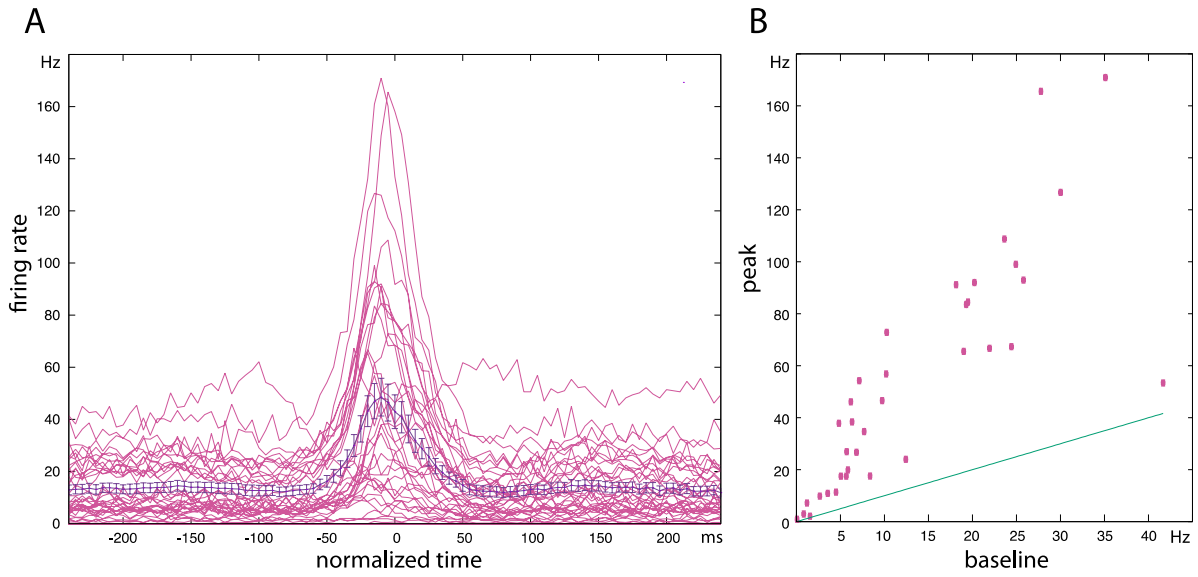

Fig. 12 A) *Average firing rate (±SEM) of CCK-interneurons (purple traces) and individual cell activity (pink traces) during sharp-wave ripple (SWR) events in the sleep session 1 (s1) without laser triggering before the light session. This shows that CCK-interneurons fired during SWR events. The CCK-interneurons' firing rate increased in a time window of -50 ms, reached its maximum before the SWR peak, and returned to baseline within 50 ms.* ***B)*** *Scatterplot of the baseline (x-axis) versus peak (y-axis) average firing rate of CCK-interneurons during SWR in the s1 session. The green diagonal indicated the x=y line to compare the firing rates at each condition. A widespread distribution of points revealed that CCK-interneurons display a high variability in firing phenotypes during SWR.*

3.5 Activity of all interneuron classes in freely moving mice

3.5.1 Evaluating preferred firing in theta oscillations before the light session

In order to verify how our light classification relates to the current knowledge of preferred phases for different physiologically and anatomically defined cell classes, we first looked at the modulation histograms of our recorded cells during the exploration session 1. The theta rhythm was the first brain oscillation that we studied, finding that the pyramidal and interneuron populations clearly differed as a population, as well as the subdivision of pyramidal cells (Fig. 13).

The first observation is that the preferred theta phase of the interneurons (n = 108) grouped around -30°, while the pyramidal cells as a population (n = 258) had a wider distribution of preferred phases, rising from -90° and abruptly dropped after 30°. The further split of the pyramidal population into the light responsive (DIP, n = 202) and the rest of the pyramidal cells (NRP, n = 56) revealed that the gross population phases were dominated by the DIP class. While the DIP phase distribution histograms of cells with significant theta phase modulation matched the one seen for the pyramidal cells in general, the NRP class had a peak in the preferred phases around the trough of the theta cycle, around -30° and 30°. This suggests that the classification based on the light-responsiveness yields a hint to some intrinsic differences within the recorded pyramidal cells, which is independent from the light manipulation.

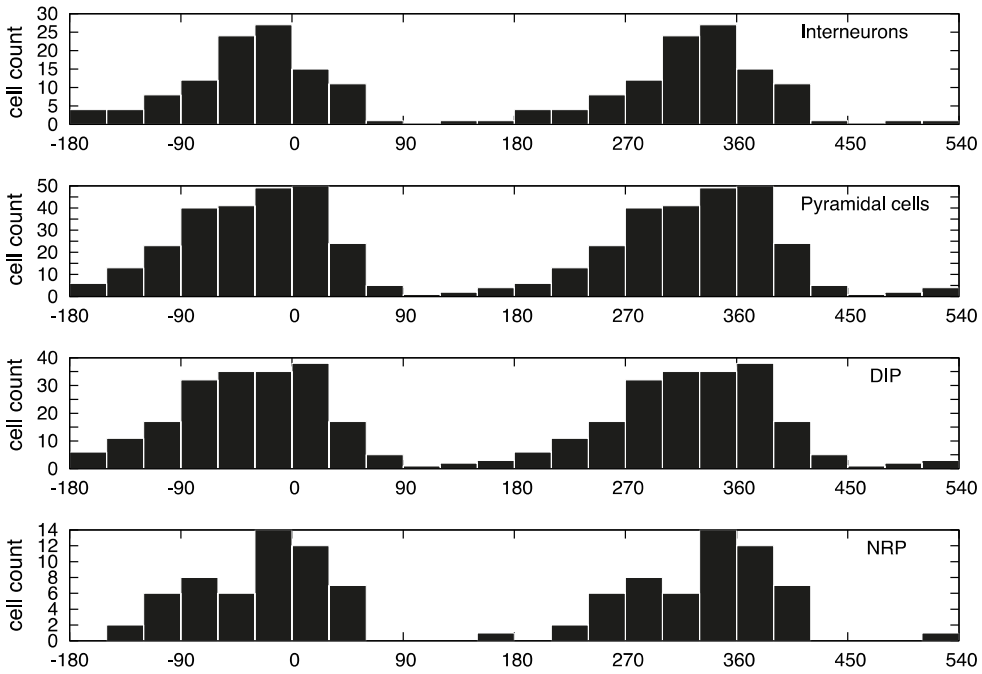

Fig. 13 *Theta phase histograms at the first exploration session (e1). Preferred phases for pyramidal cells interneurons and pyramidal cells as a population (top) and for each of the pyramidal cell subclasses (bottom): disinhibited pyramidal cells (DIP), non-responsive pyramidal cells (NRP). It was clear that each population and subpopulation differed in the phase distribution histograms of neurons with significant theta phase modulation. For displaying periodicity the theta cycles were doubled. Zero refers to the theta trough.*

When assessing the distribution of interneuron classes regarding their theta phase modulation (Fig. 14), it was evident that they were indeed three different cell types.

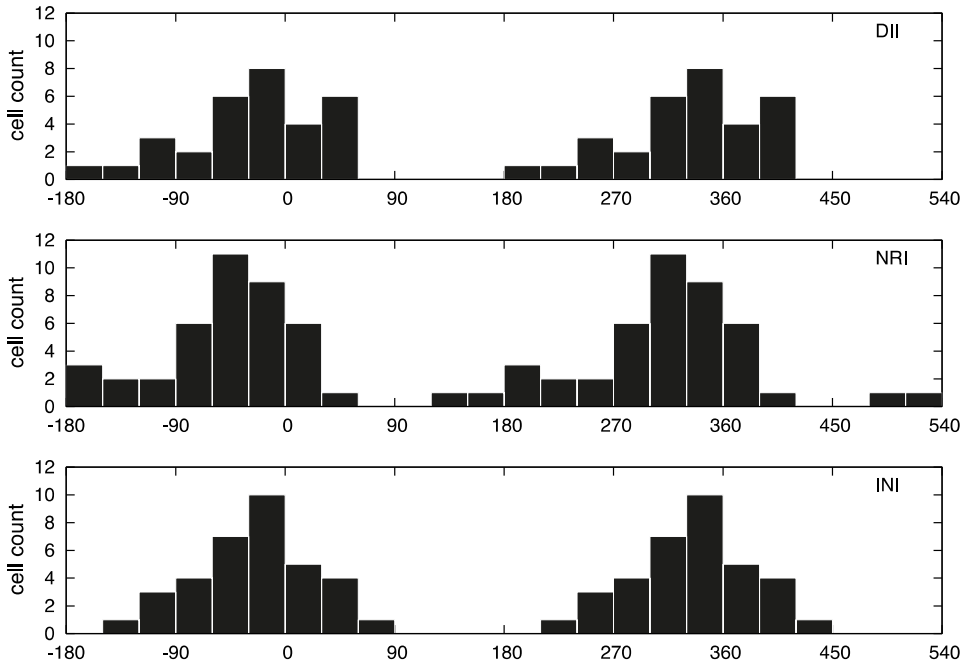

Fig. 14 *Theta phase histograms at the first exploration session (e1). Preferred phases for disinhibited interneurons (DII), non-responsive interneurons (NRI) and inhibited interneurons (INI). It was clear that each population and subpopulation differed in the phase distribution histograms of neurons with significant theta phase modulation. For displaying periodicity the theta cycles were doubled. Zero refers to the theta trough.*

The DII (n = 31) preferred phases grouped between -60° and 60°. The NRI (n = 42) distribution on the other hand, began a sudden raise at -90°, peaked at -60° and decreased at 30° from the trough of the theta cycle. As seen in the previous section, the CCK-interneurons (INI, n = 35) had preferred theta-phases grouped near the trough, beginning to rise at -120°, they slowly peaked at -30° and had a pronounced decrease up to 60° after the trough of the theta cycle. Therefore, once more our classification of cells based on the light responses led to a splitting of the population that corresponds to different properties reflected in the differential timing of the average cell discharges with respect to the theta phase.

3.6 Evoked changes related to brain oscillations

3.6.1 Evaluating preferred firing in theta oscillations during the light session

Given that the CCK-interneurons have been reported to be involved in theta oscillations in urethane-anaesthetized animals (Klausberger et al., 2005), we tested whether there was any modification on the preferred phases of the recorded cells that correlated to the presence of the light. We therefore compared the preferred phase for each cell at the IN or OUT sectors during the light session (e2).

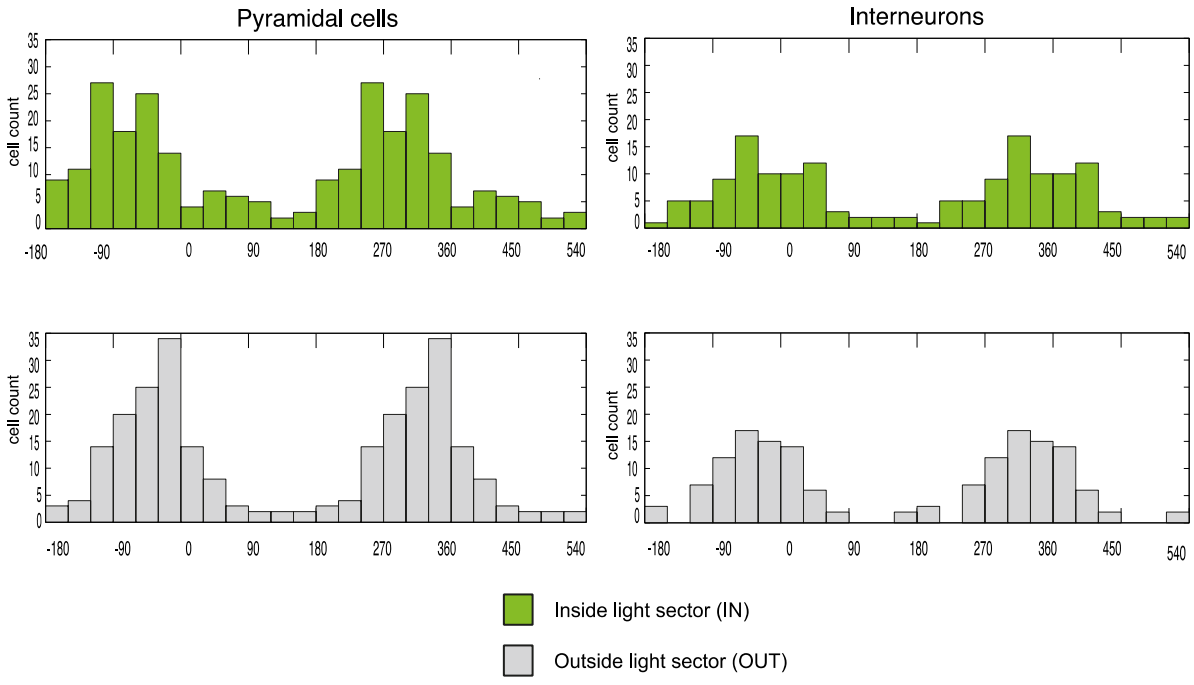

Fig. 15 *Theta phase histograms of preferred phases for pyramidal cells (left) and interneurons (right) at the IN or OUT sectors. The pyramidal cells, but not the interneurons, shifted their preferred theta phase (Wilcoxon Rank Test, pyramidal cells p = 0.002292; interneurons p = 0.312). For displaying periodicity the theta cycles were doubled.*

The first approach was a quantification testing whether there was a consistent shift in the preferred phases of the pyramidal and interneuron populations (Fig. 15). To do so we tested the phase difference of each cell between IN and OUT and tested whether this

consistently showed positive (i.e. forward) or negative (i.e. backward) shift when all cells of the population were taken. This analysis showed that the pyramidal cells (n = 131; backward shift), but not the interneurons (n = 78), shifted (Wilcoxon Rank Test, pyramidal cells p = 0.002292; interneurons p = 0.312). Then, when looking at subpopulations based on the light response classification (Fig. 16-18), we observed that DIP (n = 100) and NRP (n = 31) pyramidal cells had a significant (backward) shift, and only INI interneurons (n = 29) exhibited a significant (forward) shift (Wilcoxon Rank Test, DIP p = 0.02646; NRP 0.0221; DII p = 0.4749; NRI p = 0.2053; INI p = 0.03863).

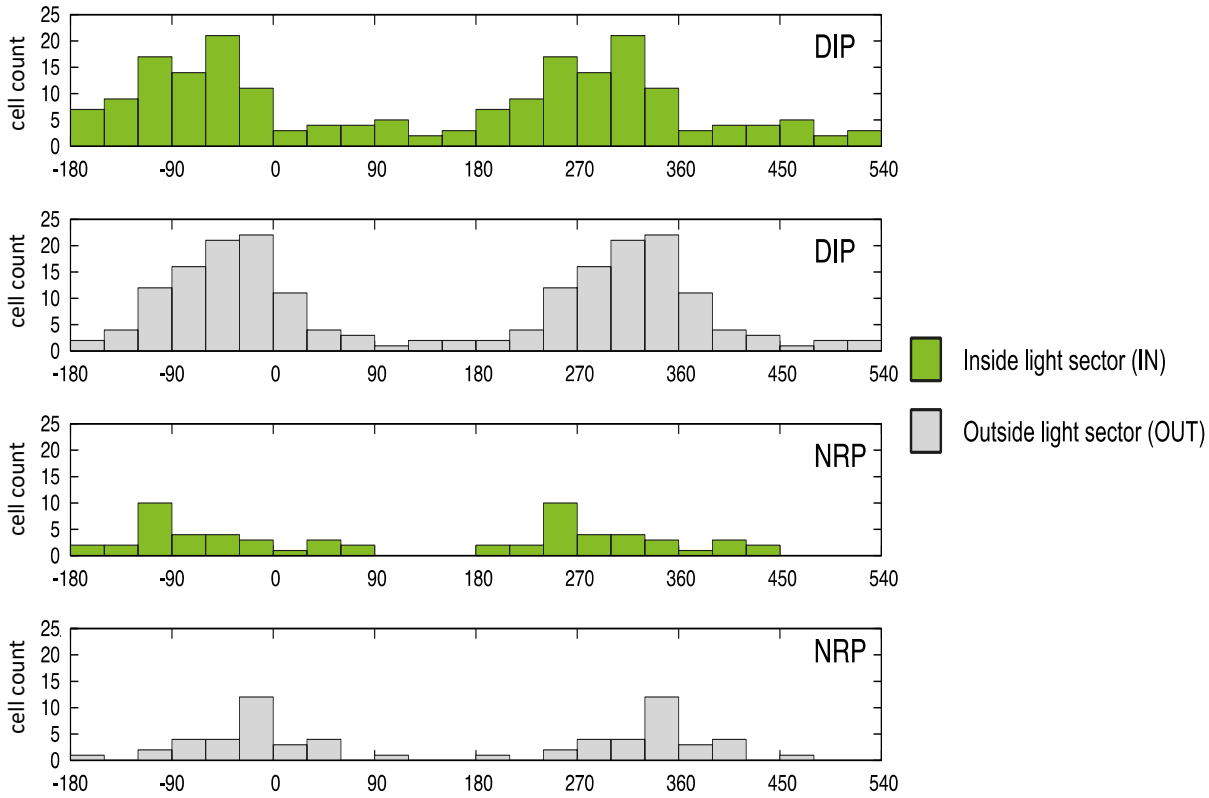

Fig. 16 *Theta phase histograms of preferred phases for DIP and NRP pyramidal cells at the IN or OUT sectors. Both significantly shifted their preferred theta phase (Wilcoxon Rank Test, DIP p = 0.02646; NRP 0.0221). For displaying periodicity the theta cycles were doubled.*

The second approach was to calculate the absolute shift between the phases identified at the IN and OUT sectors by applying a Wilcoxon test comparing how different from zero were the changes. That allowed us to compare if the shift was bigger for any of the subpopulations, e.g. whether there was a larger degree of change for those cells that were affected by light than those that were not. Regarding the pyramidal cells, their net shift was not different between DIP and NRP (Wilcoxon Rank Test p = 0.4764). When looking at the interneurons, we found differences between the DII and the NRI, but not when compared to the INI, while the NRI did not differ from the INI (Wilcoxon Rank Test, Bonferroni-Holm correction, DII vs NRI p = 0.03522; NRI vs INI p = 0.07296; INI vs DII p = 0.49910).

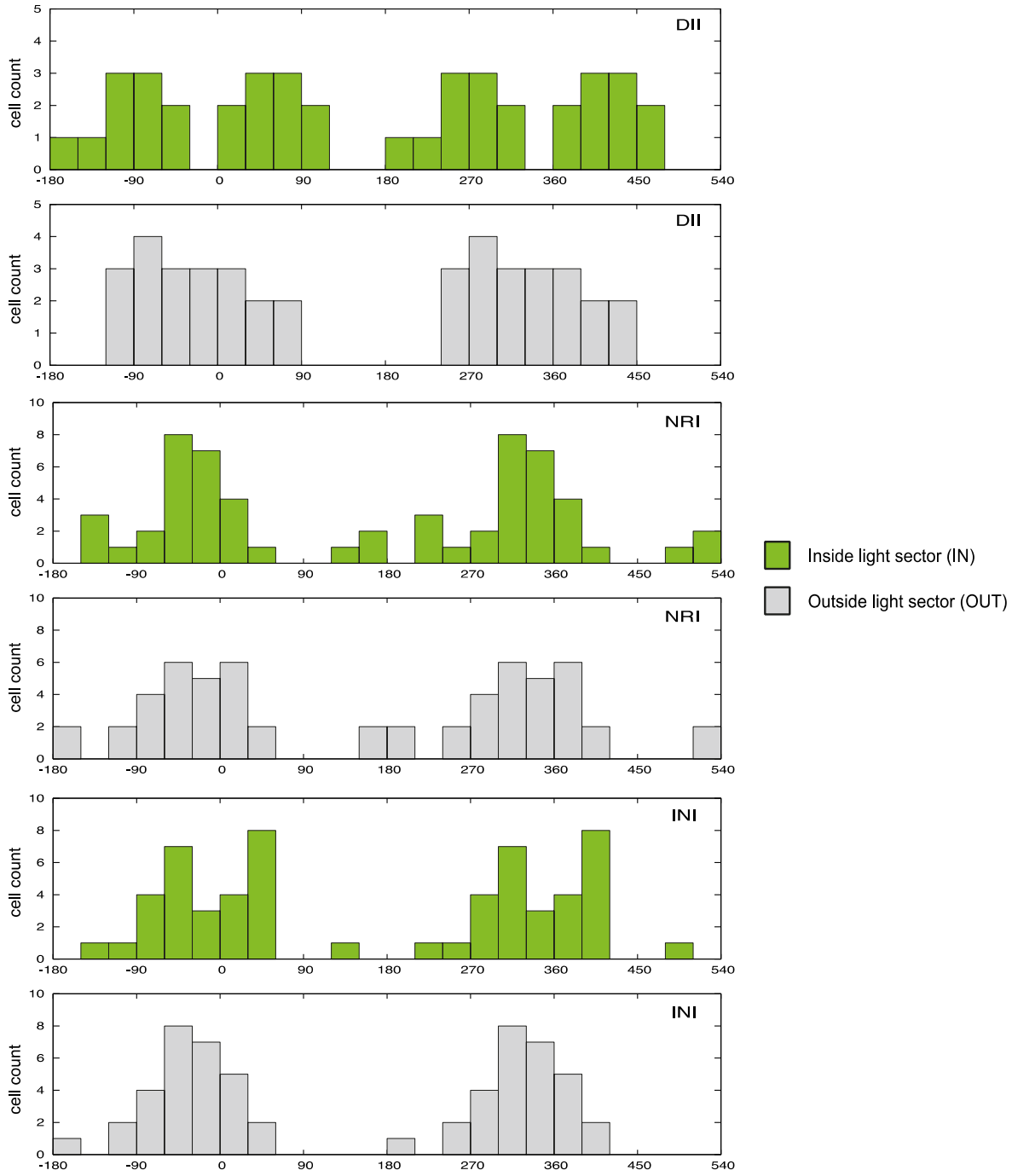

Fig. 17 *Theta phase histograms of preferred phases for the classes of interneurons (INI, DII and NRI) at the IN or OUT sectors. Only the INI significantly shifted their preferred theta phase (Wilcoxon Rank Test, DII p = 0.4749; NRI p = 0.2053; INI p = 0.03863). For displaying periodicity the theta cycles were doubled.*

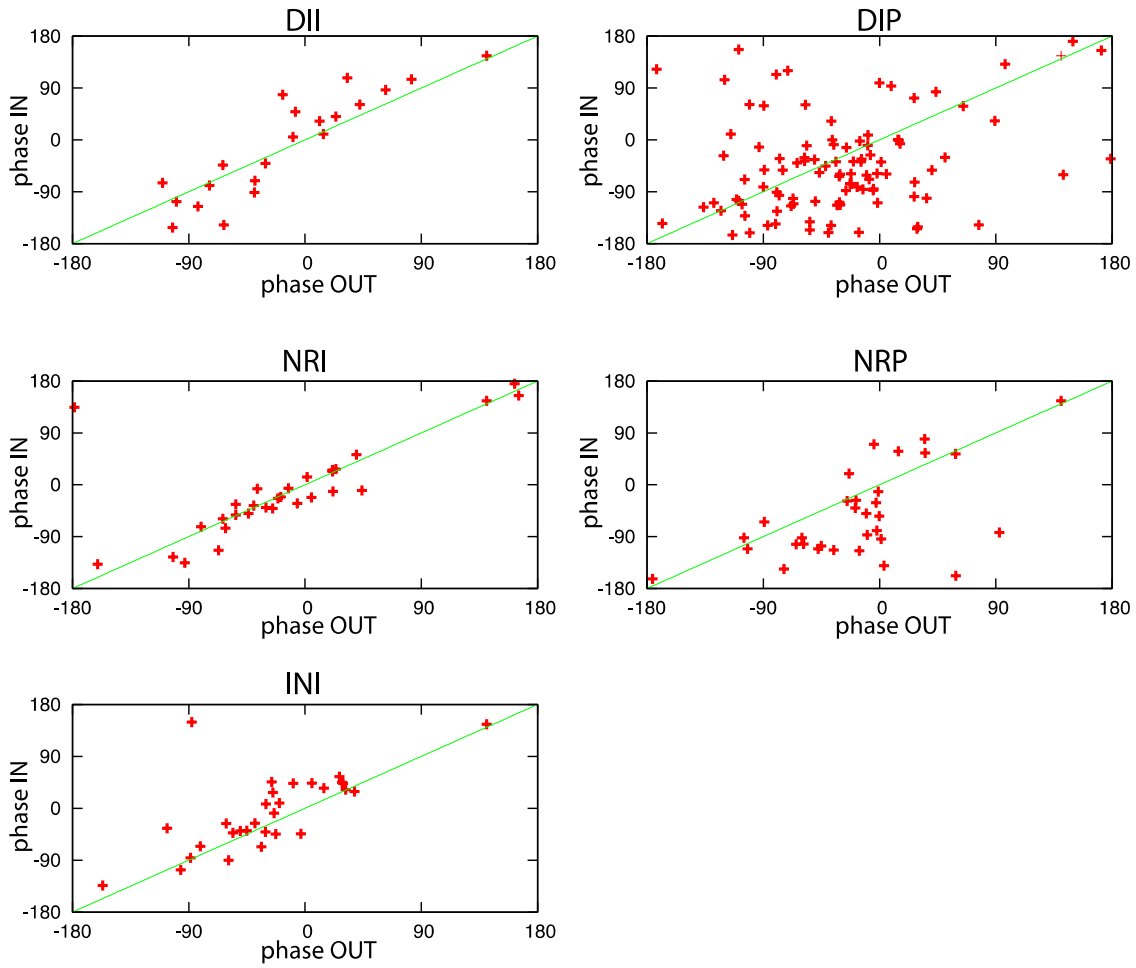

Fig. 18 *Scatterplots of the preferred theta phases for each class cells at the OUT (x-axis) versus the IN (y-axis) sectors. The diagonal line (green) indicates x=y.*

In summary, the two classes of pyramidal cells negatively shifted when the light was applied. While interneuron responses were less consistent. However the INI showed a positive shift in their preferred theta phase during the light application.

3.6.2 Evaluating preferred firing in gamma oscillations during the light session

We also studied the effects of our manipulation during gamma oscillations. Proceeding with the equivalent analysis as for the theta oscillations, we compared the preferred phase for each cell at the IN or OUT sectors during the light session (e2). The first approach was testing whether there was a consistent shift in the preferred phases as a population (Fig. 19), showing that the pyramidal cells (n = 35), but not the interneurons (n = 36), shifted (Wilcoxon Rank Test, pyramidal cells p = 0.03715; interneurons p = 0.6807).

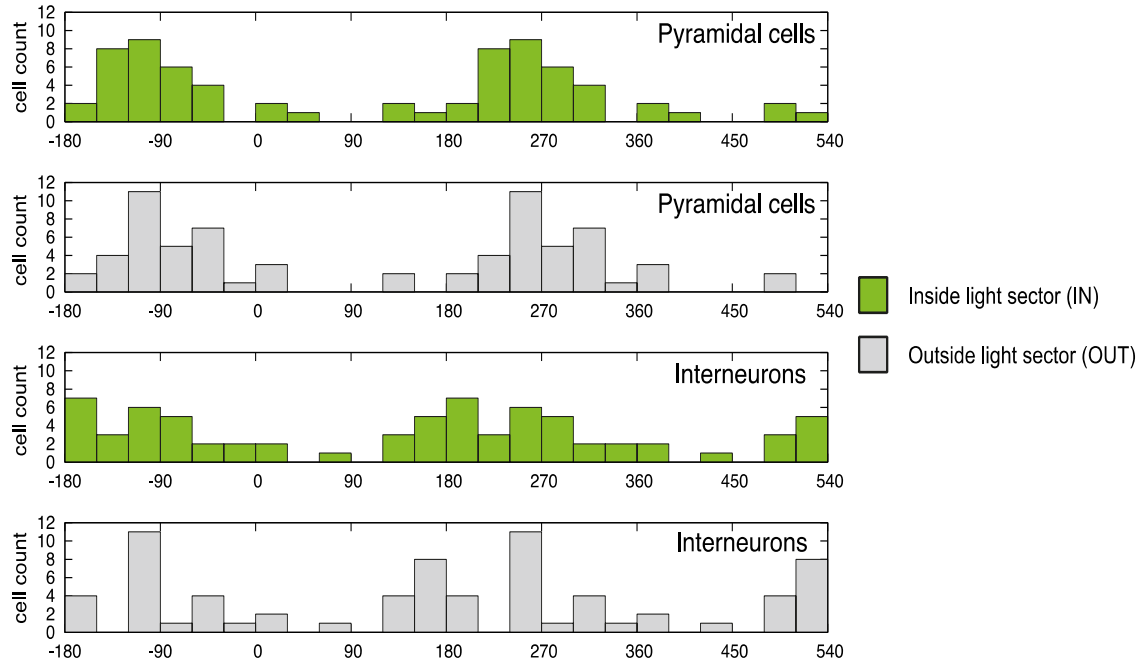

Fig. 19 *Gamma phase histograms of preferred phases for pyramidal cells and interneurons at the IN or OUT sectors. The pyramidal cells, but not the interneurons, shifted their preferred theta phase (Wilcoxon Rank Test, pyramidal cells p = 0.03715; interneurons p = 0.6807). For displaying periodicity the theta cycles were doubled.*

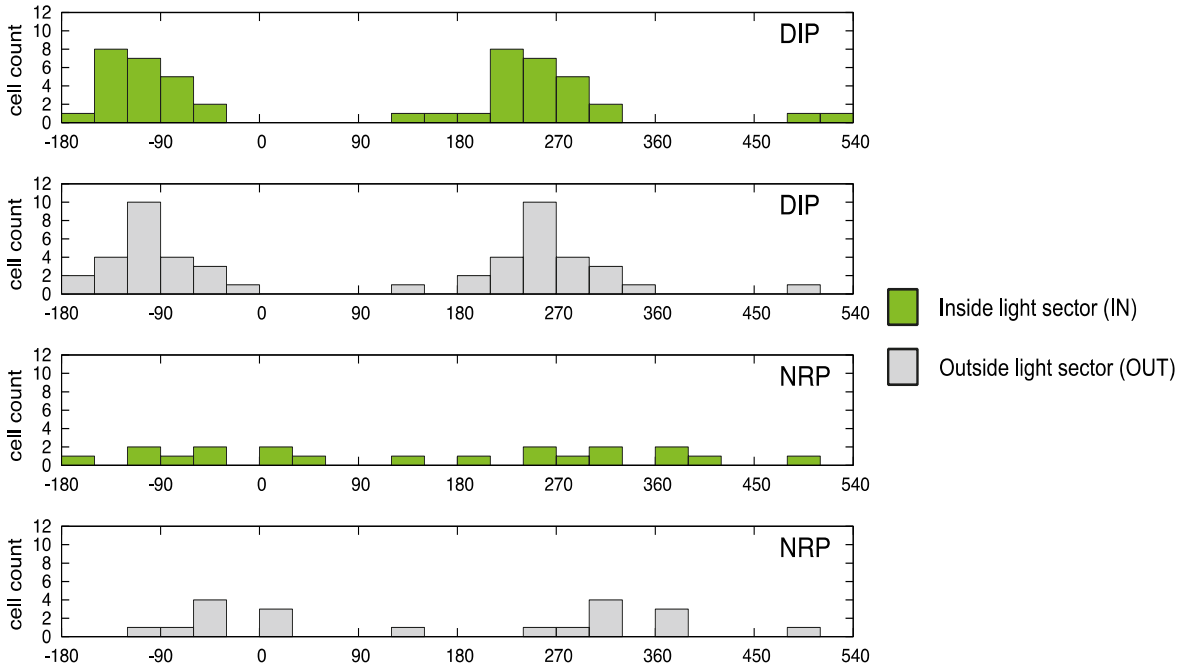

Fig. 20 *Gamma phase histograms of preferred phases for each class of pyramidal cells (DIP and NRP) at the IN or OUT sectors. None shifted their preferred phase (Wilcoxon Rank Test, DIP p = 0.1409; NRP 0.1055). For displaying periodicity the theta cycles were doubled.*

However, when looking at subpopulations (Fig. 20 and Fig. 21), we observed that neither the DIP (n = 25) nor the NRP (n = 10) had significantly shifted (Wilcoxon Rank Test,

DIP p = 0.1409; NRP 0.1055; DII p = 0.2524; NRI p = 0.4609; INI p = 0.2163) probably because not sufficient cells exhibited significant gamma phase locking in both the IN and OUT conditions.

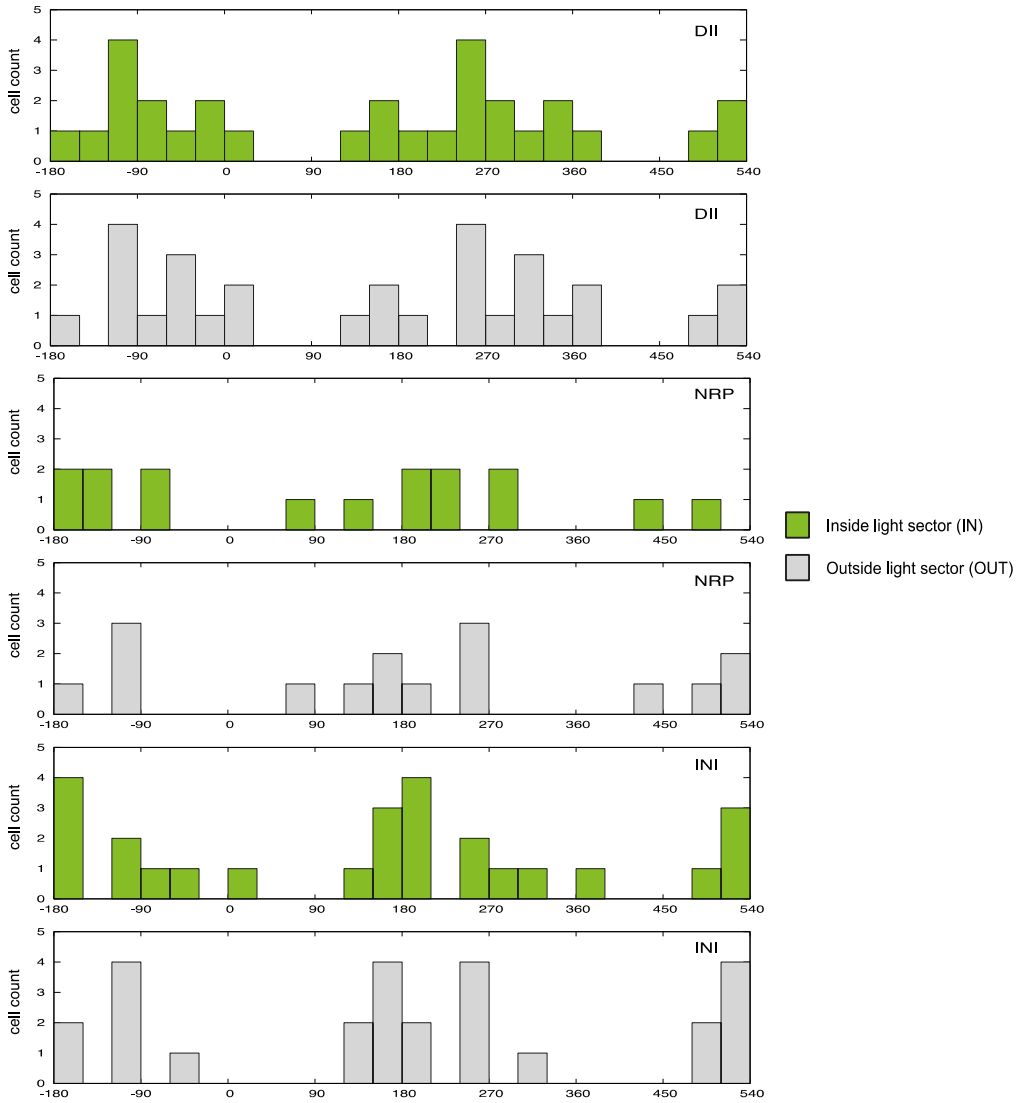

Fig. 21 *Gamma phase histograms of preferred phases for the classes of interneurons (INI, DII and NRI) at the IN or OUT sectors. None of them significantly shifted their preferred phase (Wilcoxon Rank Test, DII p = 0.2524; NRI p = 0.4609; INI p = 0.2163). For displaying periodicity the theta cycles were doubled.*

Congruently, the absolute shift between the phases identified at the IN and OUT sectors (Fig. 22) was also not different neither for pyramidal cells (Wilcoxon Rank Test p = 0.529) nor for the DII (n = 15), NRI (n = 8) or INI (n = 13) (Wilcoxon Rank Test, DII vs NRI p = 0.591; NRI vs INI p = 0.9718; INI vs DII p = 0.7856).

The fact that no significant change in the preferred phases was induced by the light for interneurons suggests that the CCK subpopulation has no role in their gamma modulation or alternatively these interneurons represent a diverse population in terms of their gamma role. Pyramidal cells were expected to have a modulatory role but after dividing them into the subgroups we no longer got sufficient number of cells to detect the change.

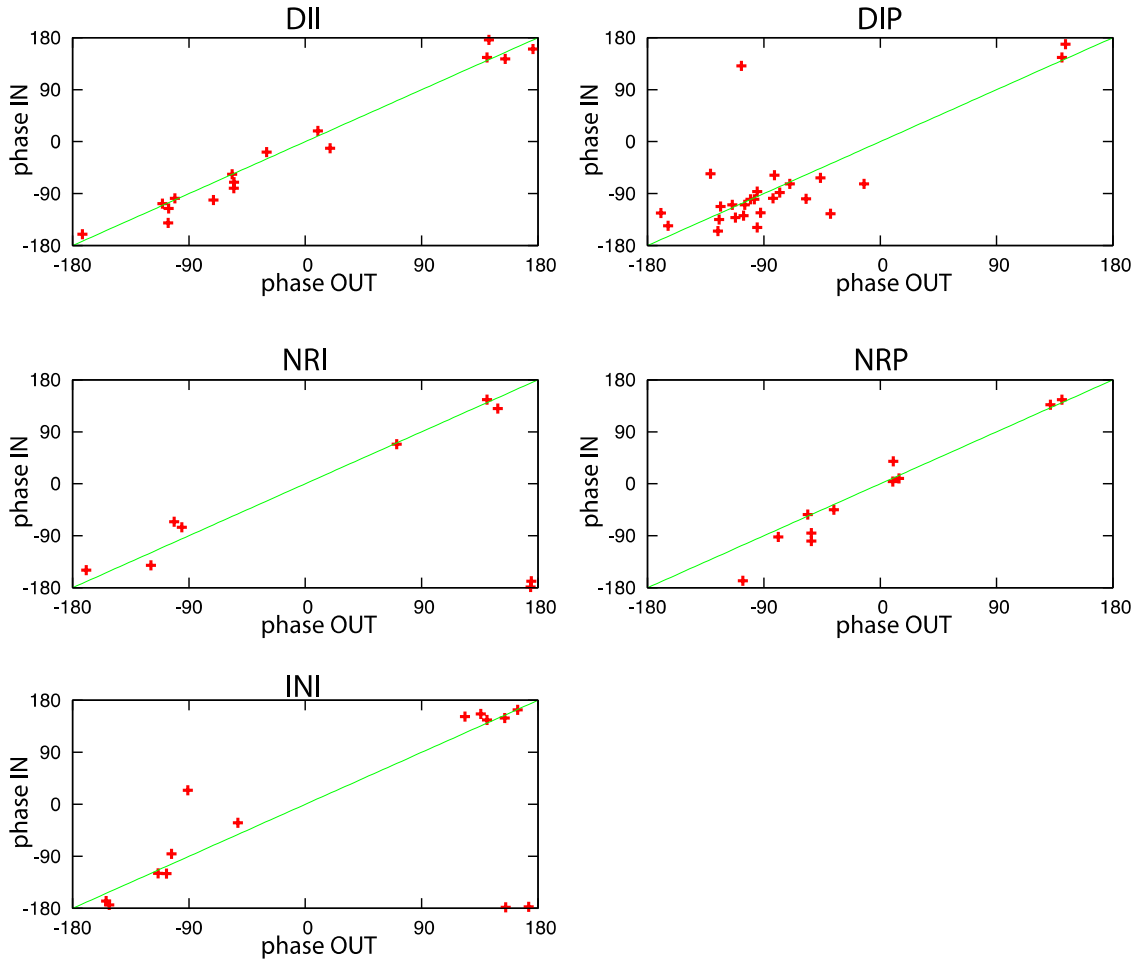

Fig. 22 *Scatterplots of the preferred gamma phases for each class cells at the OUT (x-axis) versus the IN (y-axis) sectors. The diagonal line (green) indicates x=y.*

3.6.3 Evaluating activity in SWR during the light session

3.6.3.1 Comparing SWR before and after the light session

The current theory of memory consolidation highlights the importance of the sharp-wave ripple (SWR) oscillations (Buzsáki, 2015). Considering that we had found changes in the bursting rate during sleep, we decided to assess whether there would be any change in SWR activity during the sleep following the light session. For evaluating the effect of the optogenetic manipulation upon the neuronal activity during the SWR events at sleep, we calculated the mean number of spikes per second (firing rate) around the SWR peaks (centred at zero) for all the cell classes defined in this work (DIP, n = 380; NRP, n = 95; DII, n = 39; NRI, n = 46; INI, n= 36).

In order to spot the evident changes, we plotted the activity of average firing modulation of different cell classes during sharp-wave ripples (SWR) in different sleep sessions. First, we compared the sleep sessions before (s1) and after (s2) the light triggering (Fig. 23). We observed no apparent differences for any cell class between both sleeps,

indicating that overall, the light application during exploration 2 did not have consequences on the subsequent sleep, at least at this level of analysis.

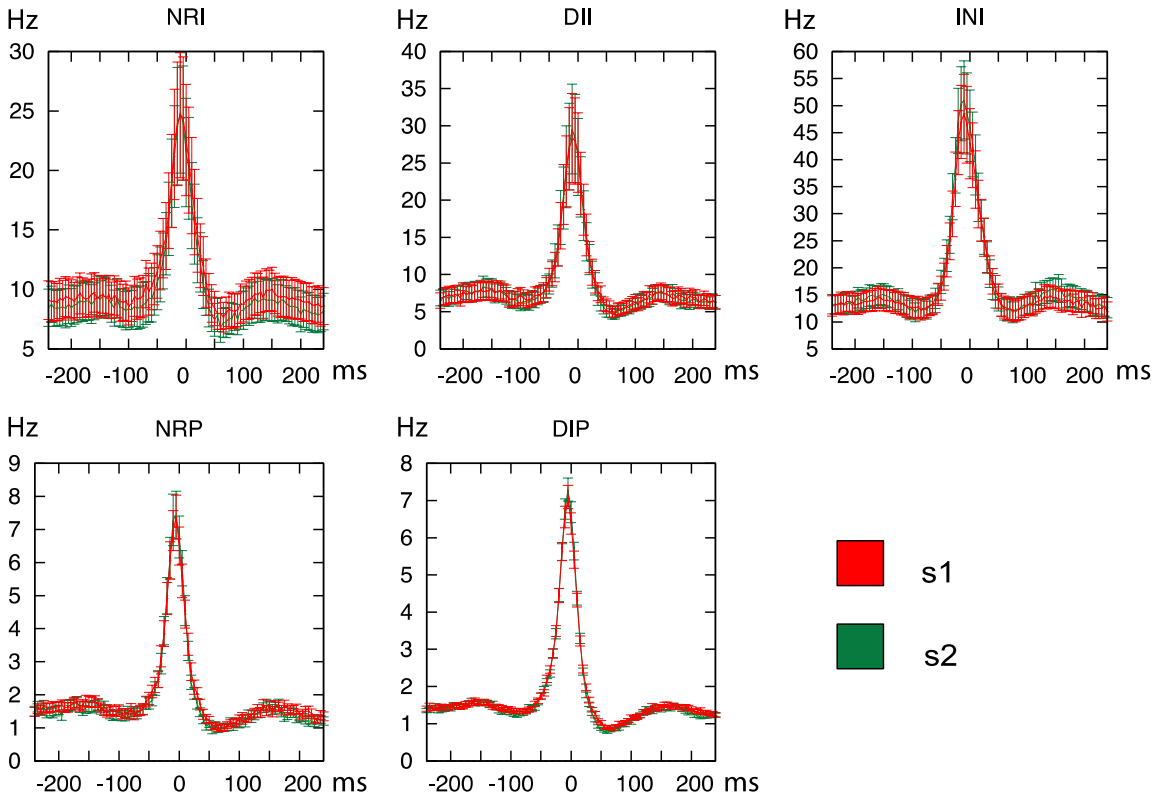

Fig. 23 *Average firing rate (±SEM) modulation for each of the cell classes during sharp-wave ripples in the sleep session before (s1) and after (s2) the light triggering. The firing rate histograms centre at the SWR peak. There were no apparent differences for any cell class between both sleeps.*

3.6.3.2 **Comparing SWR during the light session in sleep**

Whereas not having found an effect of the waking light application on the following sleep, it was relevant to ask if the light application itself during sleep would have any effect on SWR events. Therefore, we compared the average firing modulation of our recorded cells in the sleep following the last exploration of the linear track (s3), where regular 15 sec laser pulses (ON, OFF) were delivered, spanning the 25 minutes of the session. There were evident differences between the light ON and OFF periods, namely, the DII and DIP had higher firing during the ON events, whereas the INI showed a decrease (Fig. 24).

Aiming to quantify the apparent differences, we calculated the maximum mean firing rate (defined as the 'peak') of SWRs in each condition (ON or OFF) and the baseline rate before the SWR onset (Fig. 25 and Fig. 26). When comparing the peak SWR rate of the different cell groups (DIP, n = 209; NRP, n = 21; DII, n = 18; NRI, n = 14; INI, n= 14) we observed that all but the NRI class showed significant differences between the conditions: it increased during the light for the DIP and DII, while it decreased for the NRP and the INI (Wilcoxon Rank Test, DIP p = 0.004777; NRP p = 0.0001307; DII p = 0.0005341; NRI p =

0.104; INI p = 0.0002441). About the second measurement extracted from these firing rates, the mean baseline activity, we found a significant increase of baseline activity as a light effect for the DIP and the DII, while the INI class decreased (Wilcoxon Rank Test, DIP p < 2.2e-16; NRP p = 0.1907; DII p = 0.0001907; NRI p = 0.6257; INI p = 0.0006104).

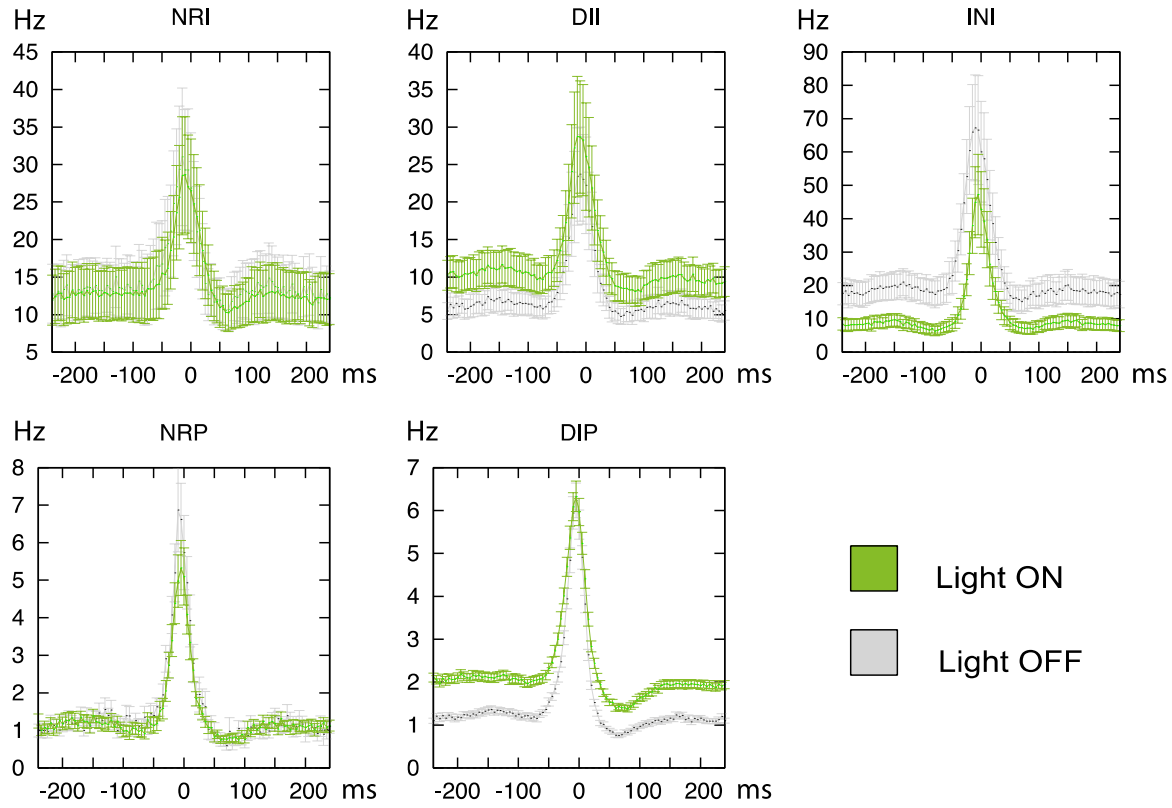

Fig. 24 *Average firing (±SEM) modulation of different cell classes during sharp-wave ripples (SWR) in the last sleep (s3) with laser pulses on and off (ON, OFF). The firing rate histograms center at peak of the SWR. During the laser ON condition, the disinhibited cells displayed a strong increase in the baseline firing rate compared to the OFF condition. The inhibited interneurons had the highest activity in the OFF condition. Whereas there is no apparent difference for the unresponsive cells among the conditions.*

In order to compare the relative change in firing from baseline to peak in the ON and OFF conditions, we calculated a baseline to peak ratio of firing. Both the DIP and the NRP displayed a clear decrease in the ratio during the light ON periods (Wilcoxon Rank Test, DIP p < 2.2e-16; NRP p = 0.0006075), suggesting that at the peak if SWRs activity saturated and disinhibition could not achieve a similar relative increase of peak rate in the ON condition (Fig. 25). Regarding to the interneurons (Fig. 26), the DII and NRI had a decrease in the ratio during the light pulses, while the INI increased (Wilcoxon Rank Test, DII p = 0.0001907; NRI p = 0.01343; INI p = 0.006714). This revealed that although having lower peak and baseline firing during the light periods (note that their firing was weaker but not totally suppressed), the INI actually increased their relative change in firing during the SWR events occurring inside of the light pulses, while the exact opposite trend applies for the DII.

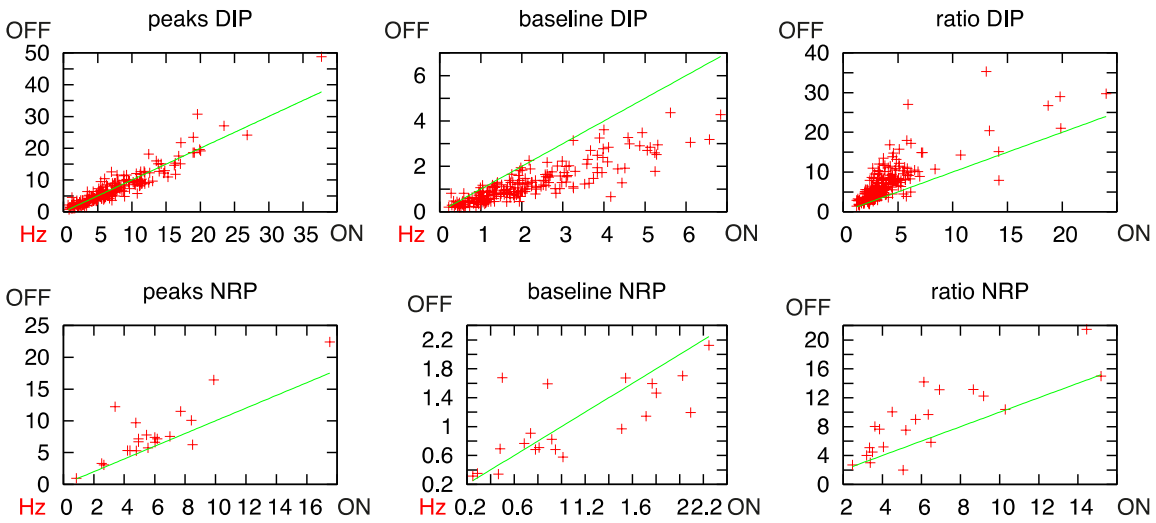

Fig. 25 *Mean firing rates around the SWR episodes detected on the sleep after the last exploration depicted for the disinhibited pyramidal cells (DIP, n = 209) and the non-responsive pyramidal cells (NRP, n = 21). The green line indicated the x=y line to compare light responses in the (ON, x axis) or outside the pulse (OFF, y axis) conditions.* ***Left****: The maximum mean firing rate is defined at the peak of SWRs in each condition (ON or OFF). The peak activity increased during the light for the DIP and decreased for the NRP (Wilcoxon Rank Test, DIP p = 0.004777; NRP p = 0.0001307).* ***Middle****: The baseline mean activity was calculated, showing that there is an increase of baseline activity as a light effect for the DIP, while the NRP showed no change (Wilcoxon Rank Test, DIP p < 2.2e-16; NRP p = 0.1907).* ***Right****: The baseline to peak ratio was calculated in order to determine the net change in each condition. Both cell classes showed a decrease during the light ON periods (Wilcoxon Rank Test, DIP p < 2.2e-16; NRP p = 0.0006075). P-values *p ≤ 0.05, **p ≤ 0.01, ***p ≤ 0.005, #p ≤ 0.0005, indicate significance level.*

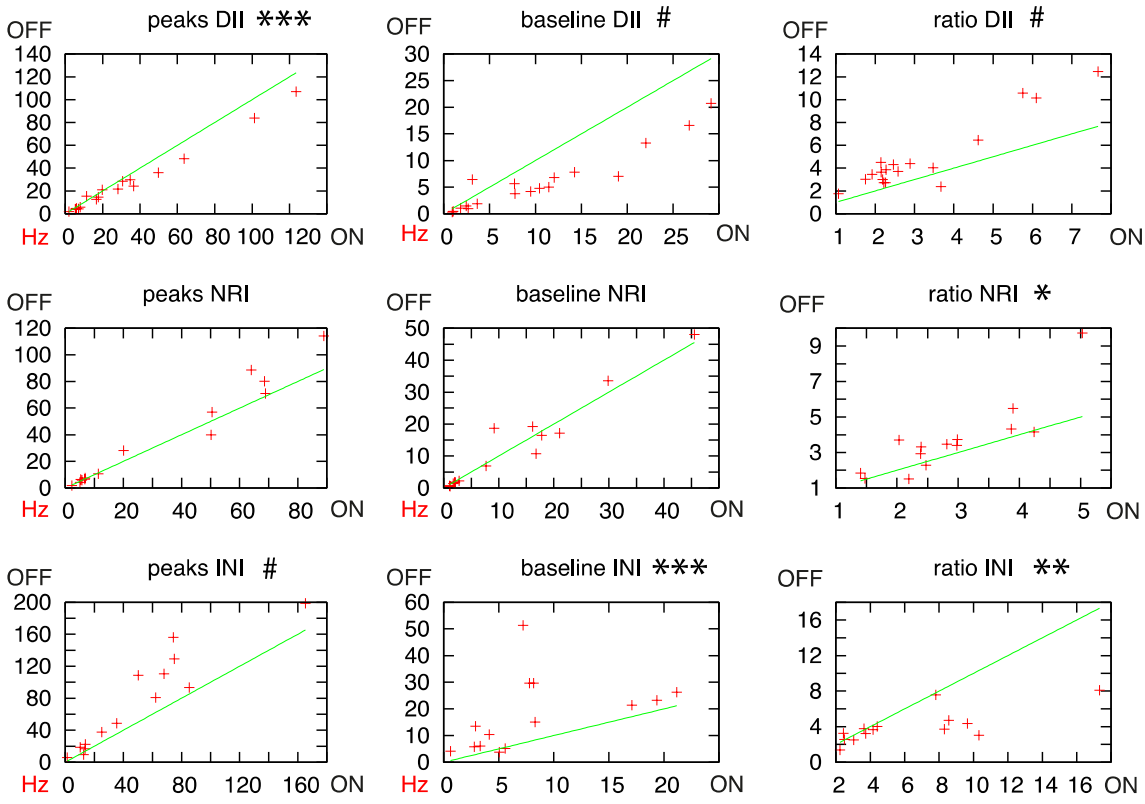

Fig. 26 *Mean firing rates around the SWR episodes detected on the sleep after the last exploration depicted for the disinhibited interneuron (DII, n = 18), the non-responsive interneuron (NRI, n = 14) and the inhibited interneuron (INI, n= 14) classes. The green line indicated the x=y line to compare light responses in the (ON, x axis) or outside of the pulse (OFF, y axis) conditions.* ***Left****: The maximum mean firing rate is defined at the peak of SWR in each condition (ON or OFF). The peak rates changed positively for the DII and negatively for the INI during the light (Wilcoxon Rank Test, DII p = 0.0005341; NRI p = 0.104; INI p = 0.0002441).* ***Middle****: The baseline analysis revealed an increase for the DII and a decrease for the INI during the light (Wilcoxon Rank Test, DII p = 0.0001907; NRI p = 0.6257; INI p = 0.0006104).* ***Right****: The peak to baseline ratio was calculated in order to determine the net change in each condition. In this case the DII and NRI decreased during the light ON periods, while the INI increased (Wilcoxon Rank Test, DII p = 0.0001907; NRI p = 0.01343; INI p = 0.006714). P-values *p ≤ 0.05, **p ≤ 0.01, ***p ≤ 0.005, #p ≤ 0.0005, indicate significance level.*

3.7 Effects in place cell activity

3.7.1 Evaluation of the light effects in place field similarity

Considering that the most relevant proposed function of the hippocampus is the characteristic property of the pyramidal cells to express place fields (O'Keefe, 1976), we evaluated if the place cell activity was affected by our manipulation (Fig. 27). First, we identified the place cells that satisfied the coherence and sparsity criteria (DIP n = 105; NRP n = 44). In order to study the wide-ranging network effect of the light-mediated silencing of the CCK-interneurons on the place coding of place cells, we compared the place-rate maps between two exploration sessions of the same familiar environment. For quantification of the place field changes, the place field similarity (PFS) of the cells rate maps was measured by the correlation coefficient measuring how similar (i.e. correlated) the rate maps were between the exploration sessions.

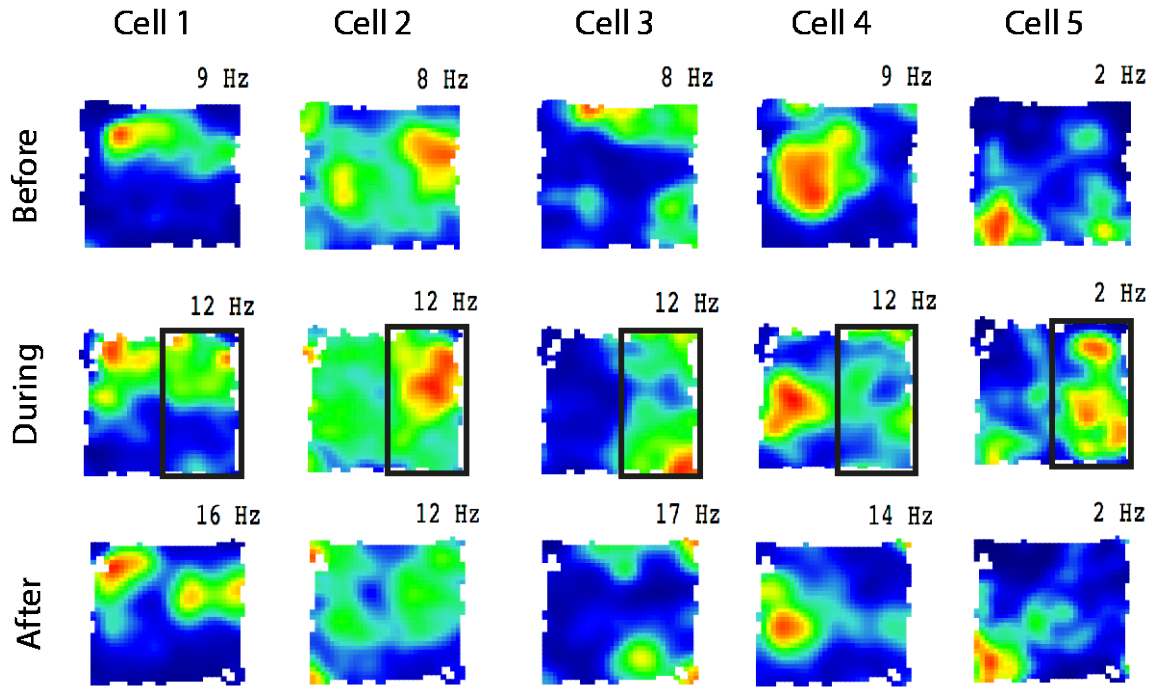

Fig. 27 *Examples of place fields from different identified place cells (belonging to the DIP class) during the three exploration sessions: before (top), during (middle) and after (bottom) the light application. The light sector is indicated by the black rectangle and the firing rates indicated on top of each map.*

We assessed whether the already existing place fields of the familiar environment in e1 were altered due to the light. For this we compared the exploration before the laser session (e1) and the laser session (e2) when the animal position during the exploration of the familiar environment conditioned the triggering of the light. Therefore, we separated the environment into two sectors: the half where the laser was triggered (IN) and the remaining part where the laser was turned off (OUT).

First we compared whether the PFS of individual cells significantly got reduced in the IN sector compared to the OUT sector (Fig. 28-A-B). Indeed the PFS values were different, and surprisingly not only for those place cells that were disinhibited by the light application but for the pyramidal cells classified as non-responsive as well (Wilcoxon Rank Test, DIP p = 0.004351; NRP p = 0.04088). The distribution of the differences between the IN and the OUT sector's PFS scores of individual cells (i.e. paired comparison) showed that place cells had place fields in the OUT sector that were more similar than the ones in the IN sector (Wilcoxon Rank Test, DIP p = 0.002175; NRP p = 0.02044).

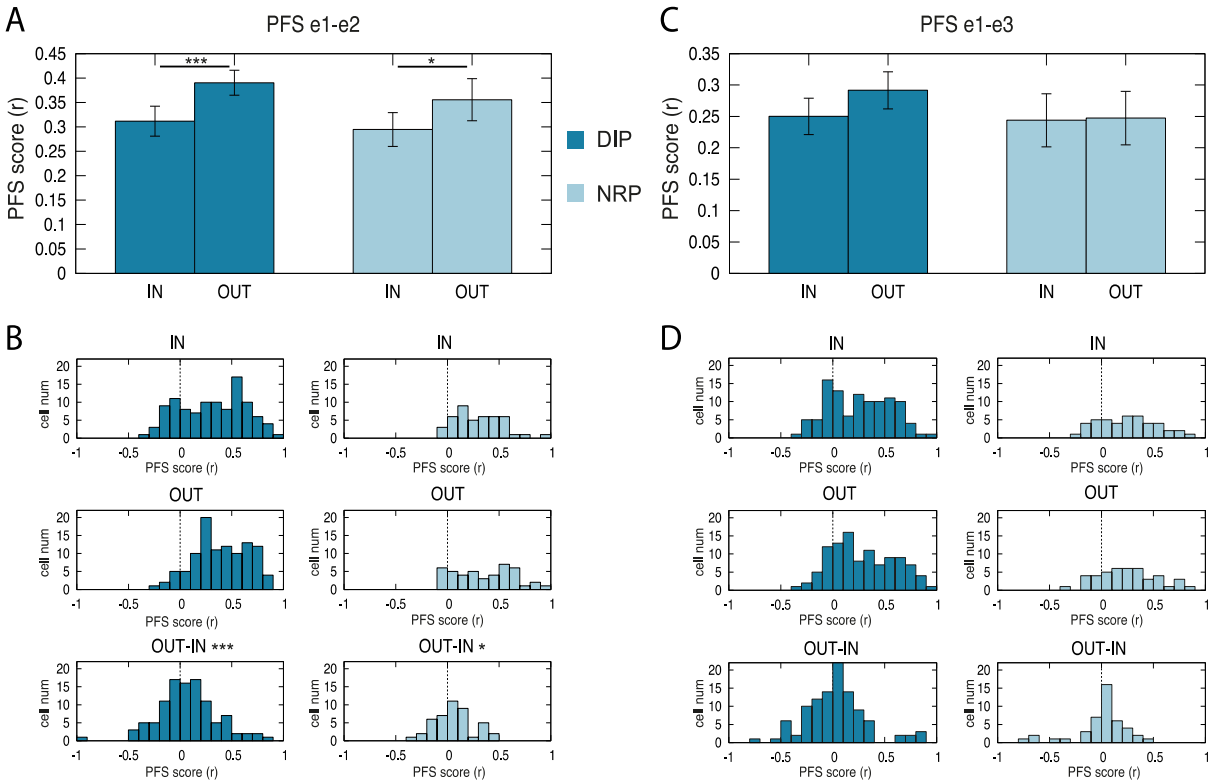

Fig. 28 *Comparisons of place field similarity (PFS) scores split into two sectors: the half where the laser was triggered (IN) and where it was not (OUT).* ***A****: Mean and SEM of the similarity scores between the exploration before the laser session (e1) and the laser session exploration (e2). Significantly higher PFS scores were found when comparing the IN and OUT sectors for any of the cell classes (Wilcoxon Rank Test, DIP p = 0.004351; NRP p = 0.04088).* ***B****: Histograms of the PFS scores distribution and the distribution of PFS differences between outside and the inside sectors for the same data as in A. The differences are asymmetric towards the positive values, meaning that more cells have higher PFS in the OUT than in the IN sector (Wilcoxon Rank Test, DIP p = 0.002175; NRP p = 0.02044).* ***C****: Mean and SEM of the similarity scores between e1 and the exploration after the laser session (e3). PFS did not significantly differ for any neuron class (Mann-Whitney U Test, DIP p = 0.3541; NRP p = 1).* ***D****: Histograms of the PFS scores distribution and the distribution of PFS differences between outside and the inside sectors for the same data as in C. The differences did not show a higher PFS in the OUT than in the IN sector (Wilcoxon Rank Test, DIP p = 0.14; NRP p = 0.0976). P-values *p ≤ 0.05, **p ≤ 0.01, ***p ≤ 0.005, #p ≤ 0.0005, indicate significance level.*

Secondly, in order to evaluate whether the light-induced place field modifications led to lasting remapping of place fields, we compared the PFS between the exploration before the light (e1) and the exploration after it (e3) without light (Fig. 28-C-D). The paired PFS scores did not differ significantly neither for the disinhibited nor for the non-responsive pyramidal cells when the IN and OUT sectors were compared (Wilcoxon Rank Test, DIP p = 0.2799; NRP p = 0.1952). This was in agreement with the distribution of the IN and OUT PFS score differences for these sessions: the differences did not show a significantly higher PFS in the OUT than in the IN sector (Wilcoxon Rank Test, DIP p = 0.14; NRP p = 0.0976). Therefore, both cell classes seem to preserve a certain degree of place field stability after the light session despite of the manipulation.

3.7.2 Assessment of the quality of place cell activity

As an estimate of firing pattern quality, we calculated the coherence: a first-order spatial autocorrelation (Muller and Kubie, 1989). During the second exploration session, when the position of the animal conditioned the light triggering, the coherence values of both pyramidal cell classes were higher in the OUT sector (Fig. 29-A) (Wilcoxon Rank Test, DIP p = 2.162e-06; NRP p = 0.0001696). On the other hand, when comparing the net spatial coherence of the three exploration sessions 1 to 3 (e1, e2, e3) we found no significant differences for none of the cell classes (Fig. 29-B) (Kruskal-Wallis Rank Test DIP p = 0.6656; NRP p = 0.1431). Therefore, we concluded that the coherence is reduced during the light session only in the IN sector.

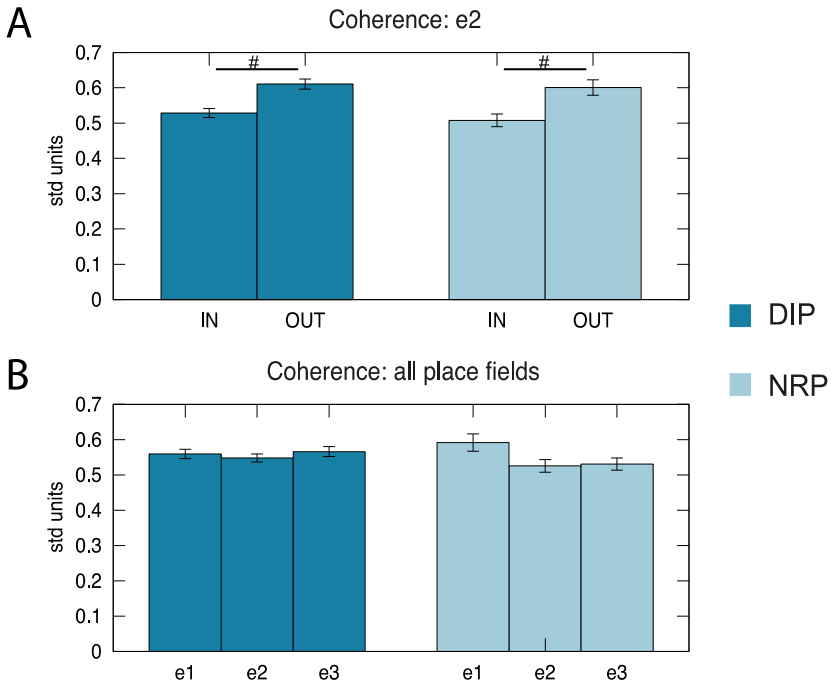

Fig. 29 A) *Comparisons between the coherence values of disinhibited (DIP, n = 105 cells) and non-responsive (NRP, n = 44) pyramidal neurons. When comparing the IN and OUT sectors during the second exploration session (e2), the OUT sector for both cell classes showed stronger coherence (Wilcoxon Rank Test, DIP p = 2.162e-06; NRP p = 0.0001696).* ***B)*** *Net spatial coherence values during each of the exploration sessions 1 to 3 (e1, e2, e3) show that no significant differences exist among the exploration sessions, neither for the DIP nor the NRP (Kruskal-Wallis Rank Test DIP p = 0.6656; NRP p = 0.1431). P-values *p ≤ 0.05, **p ≤ 0.01, ***p ≤ 0.005, #p ≤ 0.0005, indicate significance level.*

The spatial information is another measure of the spatial tuning of neurons. The spatial information content quantifies how well one can predict the location of the animal given that the firing information of a particular cell is known (Markus et al., 1994). We therefore measured the spatial information of disinhibited and non-responsive pyramidal cells during the e2 session split into the IN and OUT sectors (Fig. 30-A). There was significantly higher spatial information content in the OUT sector for DIP but not for NRP (Wilcoxon Rank Test, DIP p = 0.0001299; NRP p = 0.8308). On the other hand, when comparing all place fields against each other (Fig. 30-B), the net spatial information values during each of the exploration sessions 1 to 3 (e1, e2, e3) showed significant discrepancy among the rank sums only for the DIP (Kruskal-Wallis Rank Test DIP p = 0.01178; NRP p = 0.5528), while they showed higher spatial information content in e1 compared to e2 (post hoc Mann–Whitney U Test, Bonferroni-Holm correction, DIP: e1-e2 p = 0.01134539, e2-e3 p = 0.06226231, e1-e3 p = 0.59982451).

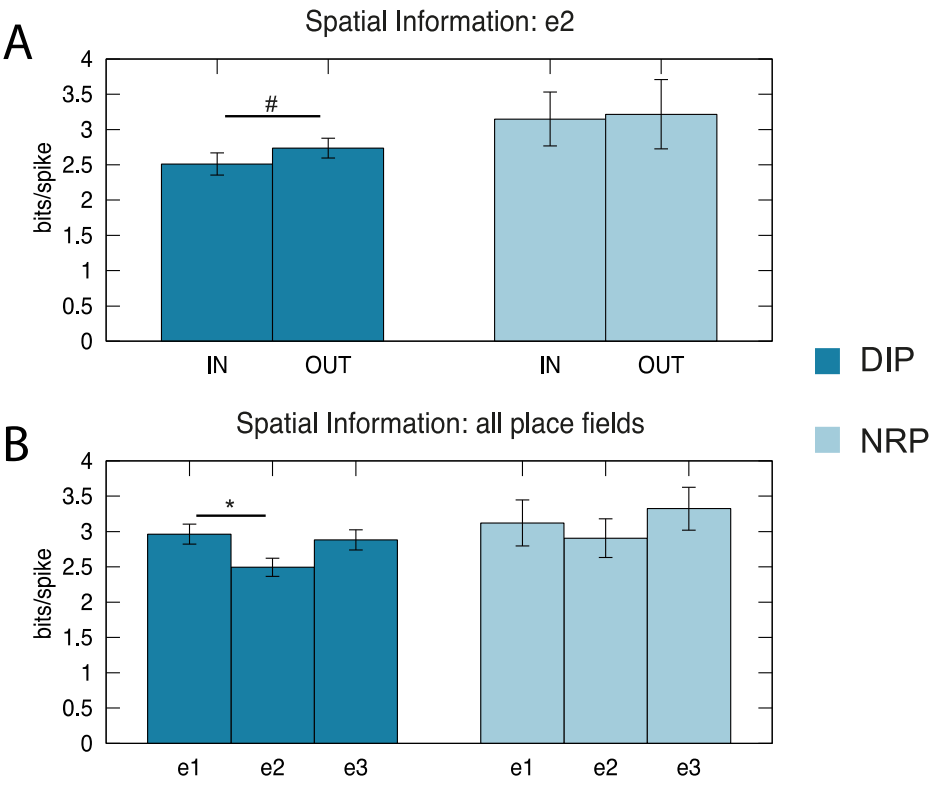

Fig. 30 A) *Measurement of the spatial information of disinhibited (DIP, n = 105 cells) and non-responsive (NRP, n = 44) pyramidal cells during the exploration 2 (e2) split into the IN and OUT sectors. There was higher spatial information content in the OUT sector for DIP (Wilcoxon Rank Test, DIP p = 0.0001299; NRP p = 0.8308).* ***B)*** *Net spatial information values during each of the exploration sessions 1 to 3 (e1, e2, e3) showed significant discrepancy among the rank sums only for the DIP (Kruskal-Wallis Rank Test DIP p = 0.01178; NRP p = 0.5528). DIP showed higher spatial information content in e1 compared to e2 (post hoc Mann–Whitney U Test, Bonferroni-Holm correction, DIP: e1-e2 p = 0.01134539, e2-e3 p = 0.06226231, e1-e3 p = 0.59982451). P-values *p ≤ 0.05, **p ≤ 0.01, ***p ≤ 0.005, #p ≤ 0.0005, indicate significance level.*

4 Discussion

4.1 The light triggered rate remapping in most of the cell classes

Besides the place-related firing of pyramidal cells, it is known that they can also encode information through changes in their firing rates, a phenomenon referred to as rate remapping (Muller, 1996). This phenomenon occurs in parallel to the location-specific activity of place cells, and is believed to allow the representation of non-spatial stimuli trough the changes in firing rate (Hampson et al., 1993; Leutgeb et al., 2005).

For studying the possible network effects of CCK-interneuron silencing in the CA1 hippocampal area, we quantified the firing rate of the recorded cells before, during and after the light session and calculated the rate remapping with respect to each other (Fig. 4). This revealed that the light application during exploration triggered rate remapping (an upregulation of DIP rate both inside and outside the light zone relative to the preceding exploration session). Furthermore, rate remapping was also seen with a firing rate increase in the third exploration session relative to the first one.

Therefore, the rate increase for the DIP case is seen not only during the light application but lasted even after the cessation of the light application in the following exploration session. In addition, in the case of the NRP, the rate remapping during the light session (relative to the previous exploration session without light) also showed rate remapping inside the light sector. Moreover, the DIP cells exhibited rate increase relative to the previous session even in the OUT sector, but this effect was not seen for NRP cells. This shows that the frequent suppression of CCK neuronal activity triggered an unspecific upregulation of the firing rate of the DIP but not the NRP cells. Note that previously Schoenenberger and collaborators (2016) observed similar lasting up-regulation of firing rates following disinhibition in which an unspecific group of interneurons were inhibited. In that case however only rates in the light zone were affected and non-disinhibited pyramidal cells did not show rate changes (Schoenenberger et al., 2016).

Altogether, the light-induced changes in pyramidal cell activity were not restricted neither in time nor space to the light delivery. Neither were they restricted to the DIP sub-population. This argues towards the theory that silencing the CCK-interneurons disinhibits pyramidal cells as a population, not only for the DIP but also in a secondary fashion through network interactions for the NRP, to an extent that persists after the manipulation is no longer present.

When we analysed the interneurons, we only found significant changes in the light session referenced to the first exploration (Fig. 5). We found a positive change in the rate remapping at the IN sector in the case of the DII, while the INI showed a significantly negative change. The positive remapping of the DII also matches with the classification based on its light response performed in the later sleep session: it was disinhibited by light even in the waking exploration session, and in this case, this change was significantly occurring only during the inhibition of CCK interneurons in e2 inside the light sector. The decrease in rate remapping was expected to a certain extent, reassuring that the classified INI are indeed CCK-interneurons reliably silenced by the viral expression of ArchT both during sleep and in the waking exploration. Furthermore, it was interesting to find a positive

change in the rate remapping at the OUT sector for the INI, which might reflect a rebound excitatory effect. It is important to mention that not observing remapping of the non-responsive interneurons suggests that the pyramidal responses are a consequence of the changes infringed on the cell types comprised by our DII and INI classes and yet it seems CCK (INI) cells have a stronger effect in regulating the disinhibited pyramidal cells than the DII population.

The fact that none of the interneurons exhibited lasting rate changes between e1 and e3 suggests that the lasting light-driven rate remapping of pyramidal cells did not alter sufficiently their network inputs to interneurons in the exploration of the same environment after the light session. The fact that only pyramidal cells exhibited rate remapping as a result of CCK inhibition is informative if we consider that rate remapping is believed to express changes of what the animal experiences. Such changes might be properties changing in certain segments of an exploration session, in subsequent sessions, or in differences between conditions (e.g. sensory or motivational inputs) even in the same session (Wood et al., 1999, 2000; Colgin et al., 2008). Therefore, the remapping observed in e1/e3 for the DIP might involve plastic changes that cause the re-emergence of such phenomenon even when the interneuron firing rate is not being affected anymore.

Finally, when comparing firing rates at the IN and OUT sectors during e2, all but the NRI exhibited significant differences (Fig. 6). Consistent with our previous observations, such changes were positive except for the INI, which had an expected negative direction of remapping. When comparing the difference in remapping across IN/OUT and ON/OFF periods between the e2 and in sleep laser pulse sessions, respectively, we found that the DIP, the NRI and the INI are recruited with the same efficiently by the light-mediated disinhibition in awake and in sleep periods. This indicates that the light-induced remapping and its direction are preserved regardless of the behavioural state of the animal and therefore, suggesting similar network mechanisms which are not affected by modulatory neurotransmitters such as acetylcholine, noradrenaline or serotonin whose levels are markedly reduced in slow wave sleep compared to waking periods.

On the other hand, the NRP were not recruited during sleep as much as in the waking condition, while the opposite case holds for the DII. The implication of these trends seems to be complex. One possible scenario is that the stronger recruitment of DII during the sleep light periods keeps the GABAergic tone for the NRP not to be indirectly disinhibited by the light.

4.2 The light induced changes in bursting and in single spike firing

The hippocampal pyramidal cells in CA1 have two modes of firing action potentials: individual spikes or high-frequency bursts (Ranck, 1973). These different firing modes tend to show different theta phase preference (Mizuseki et al., 2009) and to serve distinct functions (Graves et al., 2012). Bursting activity has been proposed to increase the reliability of synaptic communication by increasing the probability of evoking a postsynaptic spike (Lisman, 1997). By contrast, individual spikes are thought to serve temporal coding by allowing the precise place cell spike timing: the spike timing of place cells couples to the on-going theta oscillation before the increases in its firing rate (when the animal enters the place field) occur (Souza and Tort, 2017).

Given the relevance of the distinction between the pyramidal cell firing modes, we assessed whether the light manipulation led to any modification of such patterns. In our results, between e1 and e2, the DIP and NRP had an increase of burst and single spike events when the light was applied. Outside of the light sector, the DIP still increased single spike and burst frequency but the NRP had a non-significant change of bursts. However, the IN sector increases were in all cases significantly higher than the OUT sector ones (Fig. 7). This proves that we observed a general effect of the CCK-silencing during exploration on both, single spiking and bursting.

Despite the increase in both, the DIP bursting had higher relative rate change than the one of single spikes for both the IN and OUT sectors. Therefore, there was more change in the burst activity of pyramidal neurons than in the single spike firing as a consequence of disinhibition when the mouse was in the IN sector.

A strong increase in pyramidal cell bursting has also been obtained by silencing somatostatin-expressing interneurons targeting the dendrites but not by PV-interneurons preferentially targeting the soma (Royer et al., 2012). In this regard it is interesting that CCK-interneurons, which at least in part (CCK-basket cells) target the somatic region, can still effectively influence burst generation. This poses at least two possibilities: 1) CCK- and somatostatin-interneurons share mechanisms regulating pyramidal firing through controlling the dendritic generation of bursts via a small subpopulation of CCK interneurons targeting the dendrites, or 2) the common effect is rather a consequence of different mechanisms that converge on the pyramidal firing phenotype, for example, the strong somatic inhibition may prevent dendritic depolarization and spiking to propagate to the cell body and axon initial segments.

In general, complex spike bursts contribute more effectively to interneuron activation than single spikes (Csicsvari et al., 1998). But, at the same time, the firing of interneurons activates postsynaptic GABAa receptors and modulates bursts in pyramidal cells (Aradi and Maccaferri, 2004). This illustrates that altering interneuron activity may cause complex alterations in synaptic interactions and network activity and, therefore, the effects we observed may be due to complex effects. Burst has been shown to facilitate synaptic plasticity (Pike et al., 1999). Moreover, it is known that bursts are involved in the development of place fields and that the spatially-tuned bursts fired by place cells might induce plasticity and stabilize the hippocampal map (Epsztein et al., 2011). Therefore, our results suggest that CKK interneurons may be able to regulate place field formation through controlling burst activity.

Furthermore, for all pyramidal cells, we showed that there was an increase of the ON versus OFF change of burst and single spike rates both during e2 and during the last sleep when trains of light pulses were applied (Fig.8). The light-induced disinhibition caused changes during the sleep for both DIP and NRP. However, the cell classes showed different trends. While the DIP again showed stronger changes in burst than single spike rates during the wake and the sleep sessions, the NRP changes were not significantly different between burst and single spike firing during waking and sleep states. When comparing single spike and burst firing modalities between the exploration and sleep session, the DIP activity inside the light periods relative to the laser-off periods was higher in the bursting mode during exploration than the sleep session. However, for the NRP both bursting and single spiking were increased in a similar degree in the awake session in the IN than the OUT sector. In the

sleep, a weak increase in single spikes and a small decrease of bursts is seen during sleep light periods, albeit no significant differences could be seen here between single spike and burst firing.

The obtained burst propensity changes in DIP but not in NRP due to disinhibition might be an indication that our recorded pyramidal cells correspond to two previously proposed distinct cell types of pyramidal neurons in CA1, differentiated by the preference to fire bursts or single spikes (Graves et al., 2012). However, more detailed analysis of the two cell classes including the condition before the light application would be needed to explore that possibility.

4.3 The light correlated with changes in reactivation

In our experiments, there was a decrease in the reactivation of cofiring patterns corresponding to the light sector (Fig.9). It was interesting to note that the OUT sector of e2 was reactivated stronger in the subsequent sleep than the level of reactivation seen in e1 in the following sleep. This finding may be related to the upregulation of CCK-interneurons e2 firing rates in the OUT sector relative to e1 (Fig.6-B). Hence, upregulation of CCK-interneuron activity may paradoxically facilitate the reactivation of waking firing patterns, perhaps as a result of the network perturbation caused by the CCK-silencing in the light sector.

From our analysis we not only find that the firing activity patterns of exploratory periods in which CCK-interneurons were silenced were reactivated weaker than those in which CCK-interneuron activity was not affected. In addition we also found that, during sleep laser ON periods, there was also a decrease in the reactivation of cofiring patterns corresponding to the last exploration compared to sleep periods where CCK cells were not silenced. Therefore, the silencing of CCK interneurons during sleep disrupted the reactivation of recent waking patterns. This might have further consequences in respect to memory consolidation. For instance, it has been proposed that the reduced spike timing coordination and the associated impairment of physiological oscillations are responsible for cannabinoid-induced memory deficits (Robbe et al., 2006). Given that synaptic interactions between CCK interneurons and pyramidal cells are modulated by CB1 receptors, such interaction may be important in regulating reactivation.

4.4 CCK interneuron firing patterns during oscillations

It is known that interneurons synchronize network activity and time the occurrence of action potentials of pyramidal cell populations (Csicsvari et al., 1998; Allen and Monyer, 2015). Therefore, it is crucial to determine the activity patterns of each interneuron subtype during different brain states defined by oscillatory neuronal activity. For instance, despite the abundance of studies addressing this *in vivo*, to our knowledge there is only one report implying that it recorded in drug-free recordings of six putative CCK-interneurons (Klausberger et al., 2005). The hippocampal theta phase relationship of firing of these drug-free cells was related to the ones observed in the anesthetized preparation, but, the identity of the recorded interneurons could not be unequivocally determined due to the limitations of the tetrode-recording technique.

That work assumed that there are no major differences in the preferred theta phases between the anaesthetized and 'drug free' conditions (Klausberger et al., 2005). This is by no means unlikely, as exemplified by another study supporting this notion: Lapray and collaborators (2012) developed a technique to identify the identity of cells recorded in freely moving animals. They stated that the frequency of theta oscillations was twice as high in drug-free as in anesthetized animals. Despite that important difference, the spike timing of their recorded interneurons (PV-basket and ivy cells) had similar spike timing relative to the theta oscillations compared with those previously reported in urethane preparations (Lapray 2012).

However, as mentioned before, using the genetic tools to optogenetically label CCK interneurons enables us to study a big number of recorded CCK-interneurons in freely moving conditions. This has been an opportunity for us to verify the existing reports on the characteristics of this interneuron population. It also enabled us to study how these interneurons behave in the intact brain, and infer about their proposed involvement in the modulation of the hippocampal network and oscillations.

4.4.1 CCK-interneuron activity during theta oscillations

Thus, we tested how they participated during theta oscillations in our freely moving animals during the first exploration (e1) before performing the light-mediated silencing (Fig. 10). The presence of theta modulation was evident considering that all of our recoded CCK cells exhibited significant theta modulation. However, whereas in the previous report (Fig. 7 of Klausberger et al., 2005) putative CCK-interneurons had a mean theta phase grouping around 90° after the trough (at the beginning of the ascending phase), our results showed that CCK-interneuron preferred theta-phases group near the trough, actually skewed towards the descending portion.

Furthermore, our results contrast even more with the reported theta modulation of juxtacellularly labelled CCK cells in CA1 under urethane (Fig. 6-A of Klausberger et al., 2005). In this case, the preferred phase of CCK-interneurons clearly points to the ascending segment of the theta peak, somewhere in between 90° and 180°. However, our results are similar with the reported for the PPA CCK-interneuron type recorded in CA3 (Lasztóczi et al., 2011). Our CCK phases were almost antiphasic, similar to the pyramidal firing phases (Lasztóczi et al., 2011). As a conclusion, it seems that the activity of CA1 CCK-interneurons in the intact animal during exploration is not as previously assumed. Rather than firing in the ascending phase, we found that our light-inhibited neurons fired in the descending phase.

Therefore, our observations provide an evidence for the clear differences between the anaesthetized and drug free recording preparations. While for some other interneuron types both recording setups yielded similar results (Lapray et al., 2012), it is plausible that different populations, such as the CCK-interneurons subject of the current work, are differentially modulated in these conditions. For instance, there is the possibility that the CCK inhibitory cell population is more prone to be influenced by anaesthetics than other interneuron populations. This is because of the significant subcortical afferents received by CCK-interneurons (e.g. unique expression of serotonergic and nicotinic receptors). Such subcortical pathways are involved in behavioural states (e.g. attention, motivation and arousal), which would be interfered by the drug effects on the local excitation-inhibition ratio (Freund and Katona 2007).

4.4.2 CCK-interneuron activity during gamma oscillations

With regard to the optogenetically discerned CCK-interneurons activity during gamma oscillations recorded in the exploration before the light session (Fig. 11), we observed some degree of gamma modulation. We found that the average firing probability remained rather constant across the gamma cycle, aligned with the trough of the oscillation. As it could be expected, our results contrast with the reported average discharge probability reported for CA1 interneurons treated as a population: preferred phases align with the ascending phase of the gamma cycle as observed during gamma oscillations in freely moving rats (Csicsvari et al., 2003; Senior et al., 2008). But on the other hand, our observations agree with the reported activity during gamma oscillations occurring spontaneously in anaesthetized rats (Tukker et al., 2007). In this work, CCK-interneurons have been reported to fire at an early gamma phase also grouped around zero degrees (Tukker et al., 2007), which corresponds to a gamma phase just before the CA1 pyramidal cells fire in freely moving rats (Csicsvari et al., 2003).

It is therefore surprising to find that for the case of the gamma modulation, our results agree with the available equivalent information in the literature in anaesthesia, which contrasts with the previous results for the theta modulation. On the one hand, it is possible that the low depth of modulation is not providing enough resolution to see the consequences of the two brain states. On the other hand, this apparent incongruence can be explained by considering that the mechanisms behind the generation of these different oscillations differ. A likely explanation is that the mechanism behind the generation of gamma oscillations may be similar both under anaesthesia and the waking state – both possible involving reverberatory interactions between pyramidal cells and interneurons (Cobb et al., 1995). Moreover in the sleep and waking theta state, the population gamma phase of interneurons remain similar (Csicsvari et al., 1999; Senior et al., 2008).

4.4.3 CCK-interneuron activity during SWR

The last question we addressed about the endogenous patterns of the CCK-interneuron population was whether they were active during the SWR oscillations. For that we identified the SWR events during the sleep session 1 (s1) before the light session, therefore without any laser exposure. Our results showed that the average firing rate of the CCK-interneurons increased around the peak activity of the SWR events (Fig. 12-A). We observed that the distribution of the average firing rates was highly asymmetric around the SWR peak, meaning that the average firing of CCK-interneurons increased in a time window of -50 ms, reached its maximum before the SWR peak, and returned to the baseline activity within 50 ms. In addition, comparing the baseline to peak activity (Fig. 12-B) showed a widespread distribution of points, revealing that CCK-interneurons displayed a high variability in firing phenotypes during SWR. On the one hand, a group of cells that had a low firing rate (less than 10 Hz) in the baseline showed a minor increase in the peak rate. On the other hand, the majorly of cells had higher firing rates and showed higher increases during the peak times.

Our results contradict the common belief that the CCK-interneurons do not show a strong change of activity during SWR episodes (Klausberger et al., 2005). Therefore, our

results suggest that the urethane anaesthesia modifies the firing patterns of the CCK-interneurons also during SWR activity. And once more our recordings show the same trend as the recorded PPA cells in the CA3 during SWR events (Lasztóczi et al., 2011). This highlights the possibility that the referenced previous work had the only disadvantage of poor cell sampling.

In the light of our findings, it is also important to consider that there is functional connectivity between PV-basket and CCK-basket cells (Karson et al. 2009; Kohus et al., 2016). It is important to note that CCK-interneurons have not been considered so far in the proposed models for SWR generation (Cutsuridis and Taxidis, 2013; Allen and Monyer, 2015). The interneuron population that is thought to be determinant for the ripple events is the PV-interneuron class (Chiovini et al., 2014; Stark et al., 2014; Schlingloff et al., 2014). However, the CCK-interneuron population has been shown to preferentially innervate superficial pyramidal neurons (revealed by CB1 immunoreactivity), which are the pyramidal cell population that depolarizes during ripples (Valero et al., 2015). This actually places them in an important node of the SWR generating network, making our findings congruent with the expectations from such reports.

4.4.4 Identified cell types in freely moving mice

Given the particular correlates of the firing pattern of anatomically identified interneuron types during theta oscillations and other network patterns in anesthetized animals (Klausberger et al., 2003), the results from electrophysiological recordings in freely moving animals has presented us a preliminary panorama to speculate about the identity of our recorded non-inhibited interneurons.

In the CA1 region of the hippocampus, about 80% of the pyramidal cells and 90% of the interneurons are significantly phase-locked to theta oscillations (Csicsvari et al., 1999; Sirota et al., 2008). It is known that the positive phase of the local theta waves was associated with the least probability of discharge for both pyramidal cells and interneurons, with less than 5% of neurons in any cell group discharged preferentially on the positive portion of theta waves (Csicsvari et al., 1999). Specifically, the majority of pyramidal neurons fire at higher rates in the rise phase soon after the trough of the theta cycle, while interneurons as a population tend to fire in the descending phase prior to the trough and therefore before the pyramidal cell firing (Csicsvari et al., 1999).

In agreement with such reports, in our data, we observed that the preferred theta phase of the interneurons grouped around -30°, while the pyramidal cells as a population had a wide distribution of preferred phases, rising from -90° and abruptly dropped after 30° (Fig. 13). The further split of the pyramidal population into the light responsive (DIP) and the rest of the pyramidal cells (NRP) revealed that the gross population phases were dominated by the DIP class because their phase distributions matched the overall population pattern (Fig. 13). However, the NRP class had the preferred phases around the trough of the theta cycle, between -30° and 30°. This suggests that the classification based on the light-responsiveness corresponds to different pyramidal sub-populations independently of the light manipulation, because they were active at different times with respect to the theta oscillations.

In the recent times the CA1 pyramidal neurons have no longer been regarded as a homogeneous cell population. The updated view of hippocampal pyramidal cells as being divided into at least two sub-populations in rats: the pyramidal neurons residing in the deep and superficial CA1 sublayers (Baimbridge et al., 1991; Dong et al., 2009; Mizuseki et al., 2011). However, both the deep and superficial pyramidal cells have been reported to fire preferentially at the trough of theta oscillations during maze exploration (Fig.2-B from Mizuseki et al., 2011). Therefore, it is unlikely that our observed differences of theta-phase distributions between the light-response-derived classes of pyramidal cells correspond to the other classification of pyramidal subpopulations based on their anatomical location in the pyramidal layer. Besides, it shall be considered that both the DIP and NRP subpopulations increased their firing during SWRs.

Regarding to the assessment of the distribution of interneuron theta-phase modulation (Fig. 14), it was evident that there were indeed three different cell types. The DII preferred phases grouped between -60° and 60°. The NRI distribution on the other hand, began a sudden raise at -90°, peaked at -60° and decreased again at 30° from the trough of the theta cycle. The INI had preferred theta-phases grouped near the trough, beginning to rise at -120°, they slowly peaked at -30° and had a pronounced decrease up to 60° after the trough of the theta cycle.

It is useful to compare our results to the report of Csicsvari and collaborators (1999), where they observed that the interneurons recorded in the stratum pyramidale discharged 60° earlier than the population peak activity of the pyramidal neurons, while the ones in the stratum oriens had a 20° advance (Csicsvari et al., 1999). In this way, the NRI would fall into the category of interneurons in the stratum pyramidale, which is consistent with the placement of our recording tetrodes.

The INI class however, could still fall within these phases ranges, but shows a tendency towards later phases, therefore distinguishing from the two anatomically classified populations (i.e. from stratum oriens or from stratum pyramidale) that had been reported. It is not surprising though, since the preferential PV-basket cell activity during the descending theta phase (Klausberger et al., 2003) could mask the INI phenotype in general extracellular recordings.

4.5 Light-induced changes with respect to oscillations

4.5.1 CCK-interneuron theta modulation in the light session

It has been proposed that CCK-interneurons elicit slow, asynchronous inhibitory events in their targets and therefore they are thought to orchestrate the theta frequency network oscillations associated with cognitive processes (Curley and Lewis, 2012; Nagode et al., 2014). Given the importance of the link of theta oscillations to cognition and memory, we investigated how the theta phase distribution of our cell classes shifted due to the light-mediated silencing of the CCK-interneurons.

We found that the two classes of pyramidal cells (DIP and NRP) had similar shifts of their preferred phase: both negatively shifted when the light was applied (Fig. 16). However, the preferred phases of the interneuron population were less consistent (Fig. 17). As a population they did not show a significant phase shift. But when evaluating each class, we found that the absolute change of DII did not differ from the INI one, but it did from the NRI

net responses to light. Moreover INI group exhibited a significant positive shift. Looking more closely (Fig. 18), the DII subpopulation seems to behave in a bimodal fashion but further data would be needed to reach a statistically significant result here. This reminded us to consider that the DII classification very likely comprises more than one biological interneuron type.

In summary, the two classes of pyramidal cells negatively shifted when the light was applied. While interneuron responses were less consistent albeit INI showed a positive shift in their preferred theta phase during the light application. Therefore, there were major consequences of the light-driven CCK-interneuron silencing on the CA1 network activity. Given that phasic changes in synaptic transmission induced by theta oscillations have been proposed to regulate the gating of bidirectional synaptic plasticity at CA1 pyramidal neurons (Huerta and Lisman, 1995), the induced change could even alter neuronal plasticity. The shifts in the oscillatory properties of pyramidal neurons could induce perturbations of synaptic plasticity mechanisms that would ultimately lead to an alteration of learning and memory processes (Amilhon et al., 2010; Boyce et al., 2016).

In light of the literature reports, this phase shift might suggest that the CCK-interneurons have a role in cognitive processes. Considering that during theta oscillations CCK-interneurons are reported to fire at a phase when CA1 pyramidal cells start firing as the rat enters a spatial location, the place field of the cell (Tukker et al., 2007), the induced theta phase shift of pyramidal cells would be expected to alter their place fields. In addition, it is expected that altered pyramidal activity with respect to cortical oscillations would alter learning and memory processes. The direct involvement of CCK-interneurons has been suggested to modify memory and cognitive performance, but, their precise role in cortical oscillations has not been addressed yet (Whissell et al., 2019).

4.5.2 CCK-interneuron gamma modulation in the light session

Regarding to the effects of our manipulation during gamma oscillations, we observed that as populations, the pyramidal cells but not the interneurons, shifted their preferred gamma phase (Fig. 19). However, when looking at subpopulations neither the DIP nor the NRP showed significant shits (Fig. 20 and Fig. 21). This was probably due to not having sufficient cells exhibiting significant gamma phase locking in both the IN and OUT conditions to reach a significant effect when the shift of a smaller subgroup of cells were considered.

It was unexpected to observe no differences in the gamma modulation of the subclasses of pyramidal cells because the phase preference of CA1 pyramidal cells to gamma oscillations has been shown to follow a bimodal distribution (Senior et al., 2008). Furthermore, the lack of strong shifts might be related to the weak activity that CCK-interneurons are expected to have during the gamma rhythm. This is after considering that Zarnadze and collaborators (2016) stated that the effect of gamma oscillations on fast spiking PV-interneurons was an increase in their net excitation, while the effect in the regular spiking CCK-interneurons was a decrease in their activity (Zarnadze et al., 2016).

However, a role of CCK-interneurons during gamma oscillations was expected because of their specific expression of CB1 receptor and the evidence of its activation leading to memory disruption. In particular, it has been reported that cannabinoids disrupt the temporal coordination of hippocampal neurons and deteriorate, among other rhythms,

the gamma network patterns without substantial changes in pyramidal cell and interneuron average firing rates (Robbe et al., 2006). These negative results contrast once more with the ones observed during theta oscillations, and might be therefore explained by keeping in mind that the population gamma phase of interneurons remains similar during different network states (Csicsvari et al., 1999; Senior et al., 2008), which might be equivalent to the robustness of the network responses despite the light manipulation.

4.5.3 Changes in SWRs during the light periods in sleep

In the comparison of the average cell firing modulation between the light ON and OFF periods in the sleep following the last exploration, the DII and DIP had higher firing during the ON events, whereas the INI showed a decrease (Fig.24). Furthermore, when comparing the peak SWR rate of the different cell groups, we observed that it increased during the light for the DIP and DII, it did not change for the NRI class and it decreased for the NRP and the INI. About the mean baseline activity, we found a significant decrease for the INI class and an increase for the DIP and the DII (Fig.25 and Fig.26).

These light effects appear to be caused by a complex set of interactions. At this level of the analysis, we can mostly speculate about the relative change in firing from baseline to peak. In this sense, both the DIP and the NRP displayed a clear decrease in their firing increase at the peak of SWR as compared to that seen at SWR initiation.

For the DIP, we showed that although their peak activity increased during the light application, the baseline did so relatively more and, therefore, the actual change was less during the light. Such behaviour is indicative of saturation at the peak of SWR activity because the disinhibition could not achieve a similar relative increase of peak rate in the ON condition. It is likely that during natural conditions, the high pyramidal cell activity will lead to a depression of GABA release from the CCK-interneurons by the pyramidal release of eCBs activating the presynaptic CB1 receptors. This consideration would involve that the CCK-interneurons are normally not inhibiting pyramidal cells during the peak of a SWR event. This could explain why despite of the disinhibition during the light-mediated CCK-interneuron silencing, the pyramidal activity during SWR does not increase further.

4.6 The light effects in place fields

Our results showed that place fields in the OUT sector were more similar than the ones in the IN sector (Fig. 28). This reflected a locally defined light-effect and contrasts with other manipulation causing optogenetic disinhibition of pyramidal cells (Schoenenberger et al., 2016). Although relying on a less specific technique (light-mediated silencing of both pyramidal cells and interneurons), they observed that increasing the firing rate of place cells through disinhibition did not lead to place field remapping (Schoenenberger et al., 2016). Similarly, in a study by Royer and collaborators (2012), the inhibition of specific PV- and somatostatin interneurons and the resultant disinhibition of place cells did not seem to alter their please fields, it only upregulated the 'in-field' firing (Royer et al., 2012), albeit place field stability was not quantified in that work. However, when comparing the PFS between the exploration before the light and the exploration after it (without light), we observed no difference neither for the DIP nor for the NRP. In this manner, both cell classes seemed to

preserve their place field stability after the light session despite of the manipulation transiently altering their place fields in the previous exploration.

Regarding a place field quality metric, the spatial coherence between the IN and OUT sectors, we observed that the coherence is reduced during the light session only in the IN sector (Fig. 29). However, when comparing the net spatial coherence of the three exploration sessions 1 to 3 (e1, e2, e3) we found no significant differences for none of the cell classes (DIP and NRP). This argues in favour of a finely defined alteration of the place fields that is circumscribed to the light application in temporal and spatial manner. In addition to this, we quantified the spatial information of the pyramidal cells (Fig. 30). There was significantly higher spatial information content in the OUT sector than for the IN for DIP but not for NRP.

On the other hand, when comparing all place fields against each other, the net spatial information values during each of the exploration sessions showed significant discrepancy among the rank sums only for the DIP, while they showed higher spatial information content in e1 compared to e2. The reduction of place field quality is in agreement with a previous work of del Pino and collaborators (2017) in which a developmental disruption of the CCK-interneurons connectivity caused a decrease place cell coding during exploratory behaviour of adult mice (del Pino et al., 2018).

Given that place cell remapping is generated by activity-dependent plasticity (Isaac et al., 2009), it is straightforward to interpret these results in the light of the special plastic characteristics of the optogenetically-silenced CCK-interneurons. For instance, their expression of CB1 receptor implies that pyramidal cells can selectively reduce the inhibition from CCK-expressing cells via retrograde CB1 receptor activation. It has been suggested that CCK-interneurons contribute to setting dynamic and activity-dependent thresholds for pyramidal cells (Tukker et al., 2007). In addition, it has been proposed that CCK-interneurons are well suited to increase the contrast in the firing of strongly active (disinhibited via CB1 receptors) and weakly active or inactive (still inhibited by CCK interneurons) pyramidal cells, which is expected to aid in the implementation of sparse coding in cell assemblies (Klausberger and Somogyi, 2008).

In conclusion, by applying light in a specific part of the environment, we disinhibited a population of pyramidal cells. The DIP cells had reduced PFS, coherence and spatial information inside of the light sector during the light application. And importantly, such alterations were specific to the light session, meaning that the induced changes did not persist in the following exploration session. Such modifications are assumed to have been the consequence of the altered interplay between the pyramidal cells and the CCK-interneurons due to their light-mediated silencing. In particular, the increased pyramidal cell firing in the centre of their place fields might lead to presynaptic CCK-interneuron depression of GABA release, releasing the active place cells from inhibition while leaving the rest of the place cells (which are outside of their respective place fields) inhibited. In this fashion, it would follow that when the CCK-interneurons stopped being artificially inhibited by the light, as is the case of the exploration session after, the place field activity returned to normal.

5 Future direction

5.1 Evaluating spatial information of the recorded interneurons

It has been suggested that the role of interneurons may extend beyond a global damping of the network by participating in a finely-tuned local processing with the pyramidal cells. The properties of spatial selectivity and phase precession in CA1 may be a more general and may involve interaction between the different inputs from both excitatory and inhibitory cells in CA1 and influenced by differential intrinsic characteristics of those cells (Ego-Stengel and Wilson, 2010). Therefore, we propose future analysis to further examine the spatial properties of our recorded interneurons and assess if any of the optogenetically defined subclasses alters its spatial modulation due to the light administration.

5.2 Studying theta phase precession in the linear track running protocol

It is assumed that coordinated activity of hippocampal neurons in theta frequency range is implicated in the separation between encoding and retrieval of memory traces by means of oscillatory phase-locking with the entorhinal or CA3 inputs to pyramidal CA1 neurons (Huerta and Lisman, 1995). It has been suggested that an activity-dependent release of eCB from active place cells during late theta cycles can modulate the temporal profile of perisomatic GABA release by CCK-interneurons. This in turn may shape the pattern of theta related discharge of pyramidal cells (Losonczy et al. 2010). Moreover, our results showing that the two classes of pyramidal cells negatively shifted their preferred theta phase when the light was applied indeed suggests an involvement of CCK cells in theta phase precession.

5.3 Further dissection of the optogenetically identified CCK-interneuron population

The possibility of the existence of different functional states of the same interneuron type has been proposed (Parra, et al., 1998). This would be a way for adapting and responding to several different environmental stimuli, thus continuously redefining and reshaping its parameters according to the need of the network (Maccaferri and Lacaille, 2003). For instance, it has been reported that the PV-interneurons display a functional divergence of their subclasses during fast but not slow network oscillations, which is meant to increase the variety of GABA-release patterns and improve circuit operations (Varga et al., 2014). Recording from a larger group of CCK interneurons may enable a further characterization of their discharge patterns with respect to oscillations and other functions such as place coding. This might provide valuable information about their possible functional specialization in different network states.

5.4 Study of the CCK-activity and the possible effects of CCK-silencing in a spatial memory task

Several studies suggested a mnemonic role for CCK-interneurons (Basu et al., 2016; del Pino et al., 2017; Whissell et al., 2019), which transcends the previous notion limiting them to a 'mood' related fine tuning function (Freund and Katona, 2007).

With this in mind we have performed an object-location memory protocol to evaluate the effects of CCK-interneuron silencing in the memory performance of the subjects. In this case the light was administered during different phases of the task (i.e. learning, consolidation or retrieval) in order to test which, if any, of the manipulations yields behavioural effects. However, although these experiments involved a larger pool of animals (n = 7) the results of these experiments were inconclusive due to the large behavioural variability of different animals. Therefore, future experiments should try out a variety of hippocampal-dependent behavioural tests to probe the function of CCK interneurons.

References

1. Acsády L, Arabadzisz D, Freund TF. Correlated morphological and neurochemical features identify different subsets of vasoactive intestinal polypeptide-immunoreactive interneurons in rat hippocampus. Neuroscience. 1996; 73(2):299-315.
2. Allen K, Monyer H. Interneuron control of hippocampal oscillations. Current opinion in neurobiology. 2015; 31:81-7.
3. Amaral DG, Witter MP. The three-dimensional organization of the hippocampal formation: a review of anatomical data. Neuroscience. 1989; 31(3):571-91.
4. Amilhon B, Lepicard E, Renoir T, et al. VGLUT3 (vesicular glutamate transporter type 3) contribution to the regulation of serotonergic transmission and anxiety. Journal of Neuroscience. 2010;30(6):2198-210.
5. Andersen P, Holmqvist B, Voorhoeve P. Entorhinal activation of dentate granule cells. Acta Physiologica Scandinavica. 1966; 66(4):448-60.
6. Aradi I, Maccaferri G. Cell type-specific synaptic dynamics of synchronized bursting in the juvenile CA3 rat hippocampus. The Journal of neuroscience : the official journal of the Society for Neuroscience. 2004; 24(43):9681-92.
7. Arriaga M, Han EB. Dedicated Hippocampal Inhibitory Networks for Locomotion and Immobility. Journal of Neuroscience. 2017; 37(38):9222-9238.
8. Ascoli GA, Alonso-Nanclares L, et al. Petilla terminology: nomenclature of features of GABAergic interneurons of the cerebral cortex. Nature reviews. Neuroscience. 2008; 9(7):557-68.
9. Baimbridge KG, Peet MJ, McLennan H, Church J. Bursting response to current-evoked depolarization in rat CA1 pyramidal neurons is correlated with lucifer yellow dye coupling but not with the presence of calbindin-D28k. Synapse (New York, N.Y.). 1991; 7(4):269-77.
10. Bartesaghi R, Gessi T. Parallel activation of field CA2 and dentate gyrus by synaptically elicited perforant path volleys. Hippocampus. 2004; 14(8):948-63.
11. Bartos M, Elgueta C. Functional characteristics of parvalbumin- and cholecystokinin-expressing basket cells. Journal of Physiology. 2012; 590(4):669-81.
12. Basu J, Srinivas K, Cheung S, et al. A cortico-hippocampal learning rule shapes inhibitory microcircuit activity to enhance hippocampal information flow. Neuron. 2013;79:1208–1221.
13. Basu J, Zaremba JD, Cheung SK, Hitti FL, Zemelman BV, Losonczy A, Siegelbaum SA. Gating of hippocampal activity, plasticity, and memory by entorhinal cortex long-range inhibition. Science. 2016; 351:aaa5694.
14. Bezaire MJ, Soltesz I. Quantitative assessment of CA1 local circuits: knowledge base for interneuron-pyramidal cell connectivity. Hippocampus. 2013; 23(9):751-85.
15. Boyce R, Glasgow S, Williams S, Adamantidis A. Causal evidence for the role of REM sleep theta rhythm in contextual memory consolidation. Science. 2016; 352(6287):812-6.
16. Brown J, Horváth S, Garbett KA, et al. The role of cannabinoid 1 receptor expressing interneurons in behavior. Neurobiology of Disease. 2014;63:210-21.
17. Buzsáki G, Bickford RG, Ryan LJ, et al. Multisite recording of brain field potentials and unit activity in freely moving rats. Journal of neuroscience methods. 1989; 28(3):209-17.

18. Buzsáki G, Horváth Z, Urioste R, Hetke J, Wise K. High-frequency network oscillation in the hippocampus. Science (New York, N.Y.). 1992; 256(5059):1025-7.
19. Buzsáki G, Leung LW, Vanderwolf CH. Cellular bases of hippocampal EEG in the behaving rat. Brain research. 1983; 287(2):139-71.
20. Buzsáki G. Hippocampal sharp wave-ripple: A cognitive biomarker for episodic memory and planning. Hippocampus. 2015; 25(10):1073-188.
21. Buzsáki G. The hippocampo-neocortical dialogue. Cerebral Cortex. 1996; 6(2):81-92.
22. Buzsáki G. Theta oscillations in the hippocampus. Neuron. 2002; 33(3):325-40.
23. Carlson G, Wang Y, Alger B. Endocannabinoids facilitate the induction of LTP in the hippocampus. Nature Neuroscience. 2002; 5(8):723-4.
24. Castillo P, Younts T, Chávez A, Hashimotodani Y. Endocannabinoid signaling and synaptic function. Neuron. 2012;76(1):70-81.
25. Cenquizca LA, Swanson LW. Spatial organization of direct hippocampal field CA1 axonal projections to the rest of the cerebral cortex. Brain research reviews. 2007; 56(1):1-26.
26. Chamberland S, Topolnik L. Inhibitory control of hippocampal inhibitory neurons. Frontiers in neuroscience. 2012; 6:165.
27. Chevaleyre V, Siegelbaum SA. Strong CA2 pyramidal neuron synapses define a powerful disynaptic cortico-hippocampal loop. Neuron. 2010; 66(4):560-72.
28. Chevaleyre V, Takahashi KA, Castillo PE. Endocannabinoid-mediated synaptic plasticity in the CNS. Annual review of neuroscience. 2006; 29:37-76.
29. Chiovini B, Turi GF, Katona G, et al. Dendritic spikes induce ripples in parvalbumin interneurons during hippocampal sharp waves. Neuron. 2014; 82(4):908-24.
30. Chittajallu R, Craig MT, McFarland A, et al. Dual origins of functionally distinct O-LM interneurons revealed by differential 5-HT(3A)R expression. Nature neuroscience. 2013; 16(11):1598-607.
31. Chow B, Han X, Dobry A, et al. High-performance genetically targetable optical neural silencing by light-driven proton pumps. Nature. 2010; 463(7277): 98-102.
32. Chrobak JJ, Buzsáki G. High-frequency oscillations in the output networks of the hippocampal-entorhinal axis of the freely behaving rat. The Journal of neuroscience : the official journal of the Society for Neuroscience. 1996; 16(9):3056-66.
33. Cobb SR, Buhl EH, Halasy K, Paulsen O, Somogyi P. Synchronization of neuronal activity in hippocampus by individual GABAergic interneurons. Nature. 1995; 378(6552):75-8.
34. Colgin LL, Moser EI, Moser MB. Understanding memory through hippocampal remapping. Trends in neurosciences. 2008; 31(9):469-77.
35. Colgin LL, Moser EI. Gamma oscillations in the hippocampus. Physiology (Bethesda, Md.). 2010; 25(5):319-29.
36. Cope DW, Maccaferri G, Márton LF, Roberts JD, Cobden PM, Somogyi P. Cholecystokinin-immunopositive basket and Schaffer collateral-associated interneurones target different domains of pyramidal cells in the CA1 area of the rat hippocampus. Neuroscience. 2002; 109(1):63-80.
37. Csicsvari J, Hirase H, Czurko A, Buzsáki G. Reliability and state dependence of pyramidal cell-interneuron synapses in the hippocampus: an ensemble approach in the behaving rat. Neuron. 1998; 21(1):179-89.
38. Csicsvari J, Hirase H, Czurkó A, Mamiya A, Buzsáki G. Oscillatory coupling of hippocampal pyramidal cells and interneurons in the behaving Rat. The Journal of neuroscience : the official journal of the Society for Neuroscience. 1999; 19(1):274-87.

39. Csicsvari J, Hirase H, Mamiya A, Buzsáki G. Ensemble patterns of hippocampal CA3-CA1 neurons during sharp wave-associated population events. Neuron. 2000; 28(2):585-94.
40. Csicsvari J, Jamieson B, Wise KD, Buzsáki G. Mechanisms of gamma oscillations in the hippocampus of the behaving rat. Neuron. 2003; 37(2):311-22.
41. Curley A, Lewis D. Cortical basket cell dysfunction in schizophrenia.Journal of physiology. 2012; 590(4):715-24
42. Cutsuridis V, Taxidis J. Deciphering the role of CA1 inhibitory circuits in sharp wave-ripple complexes. Frontiers in systems neuroscience. 2013; 7:13.
43. Danielson NB, Zaremba JD, Kaifosh P, Bowler J, Ladow M, Losonczy A. Sublayer-Specific Coding Dynamics during Spatial Navigation and Learning in Hippocampal Area CA1. Neuron. 2016; 91(3):652-65.
44. Daumas S, Halley H, Francés B, Lassalle JM. Encoding, consolidation, and retrieval of contextual memory: differential involvement of dorsal CA3 and CA1 hippocampal subregions. Learning & memory (Cold Spring Harbor, N.Y.). 2005; 12(4):375-82.
45. Daw MI, Tricoire L, Erdelyi F, Szabo G, McBain CJ. Asynchronous transmitter release from cholecystokinin-containing inhibitory interneurons is widespread and target-cell independent. The Journal of neuroscience : the official journal of the Society for Neuroscience. 2009; 29(36):11112-22.
46. De-May C, Ali A. Cell type-specific regulation of inhibition via cannabinoid type 1 receptors in rat neocortex. Journal of neurophysiology. 2013; 109(1):216-24.
47. Del Pino I, Brotons-Mas J, Marques-Smith A, et al. Abnormal wiring of CCKbasket cells disrupts spatial information coding. Nature Neuroscience. 2017; 20:784–792.
48. Diba K, Buzsáki G. Forward and reverse hippocampal place-cell sequences during ripples. Nature neuroscience. 2007; 10(10):1241-2.
49. Dimidschstein J, Chen Q, Tremblay R, et al. Corrigendum: A viral strategy for targeting and manipulating interneurons across vertebrate species. Nature neuroscience. 2017; 20(7):1033.
50. Domínguez S, Fernández de Sevilla D, Buño W. Postsynaptic activity reverses the sign of the acetylcholine-induced long-term plasticity of GABAA inhibition. Proceedings of the National Academy of Sciences of the United States of America. 2014; 111(26):E2741-50.
51. Dong HW, Swanson LW, Chen L, Fanselow MS, Toga AW. Genomic-anatomic evidence for distinct functional domains in hippocampal field CA1. Proceedings of the National Academy of Sciences of the United States of America. 2009; 106(28):11794-9.
52. Dupret D, O'Neill J, Csicsvari J. Dynamic reconfiguration of hippocampal interneuron circuits during spatial learning. Neuron. 2013; 78(1):166-80.
53. Dupret D, O'Neill J, Pleydell-Bouverie B, Csicsvari J. The reorganization and reactivation of hippocampal maps predict spatial memory performance. Nature neuroscience. 2010; 13(8):995-1002.
54. Ego-Stengel V, Wilson MA. Disruption of ripple-associated hippocampal activity during rest impairs spatial learning in the rat. Hippocampus. 2010; 20(1):1-10.
55. El-Gaby M, Zhang Y, Wolf K, Schwiening CJ, Paulsen O, Shipton OA. Archaerhodopsin Selectively and Reversibly Silences Synaptic Transmission through Altered pH. Cell Reports. 2016; 16(8):2259-2268.
56. Elowitz MB, Levine AJ, Siggia ED, Swain PS. Stochastic gene expression in a single cell. Science (New York, N.Y.). 2002; 297(5584):1183-6.

57. Epsztein J, Brecht M, Lee AK. Intracellular determinants of hippocampal CA1 place and silent cell activity in a novel environment. Neuron. 2011; 70(1):109-20.
58. Fenno LE, Mattis J, Ramakrishnan C, et al. Targeting cells with single vectors using multiple-feature Boolean logic. Nature methods. 2014; 11(7):763-72.
59. Férézou I, Cauli B, Hill EL, Rossier J, Hamel E, Lambolez B. 5-HT3 receptors mediate serotonergic fast synaptic excitation of neocortical vasoactive intestinal peptide/cholecystokinin interneurons. The Journal of neuroscience : the official journal of the Society for Neuroscience. 2002; 22(17):7389-97.
60. Fox SE, Ranck JB. Electrophysiological characteristics of hippocampal complex-spike cells and theta cells. Experimental brain research. 1981; 41(3-4):399-410.
61. Freund TF, Buzsáki G. Interneurons of the hippocampus. Hippocampus. 1996; 6(4):347-470.
62. Freund TF, Katona I. Perisomatic inhibition. Neuron. 2007; 56(1):33-42.
63. Freund TF, Maglóczky Z, Soltész I, Somogyi P. Synaptic connections, axonal and dendritic patterns of neurons immunoreactive for cholecystokinin in the visual cortex of the cat. Neuroscience. 1986; 19(4):1133-59.
64. Freund TF. Interneuron Diversity series: Rhythm and mood in perisomatic inhibition. Trends Neuroscience. 2003; 26(9):489-95.
65. Galarreta M, Erdélyi F, Szabó G, Hestrin S.Electrical coupling among irregular-spiking GABAergic interneurons expressing cannabinoid receptors. The Journal of neuroscience : the official journal of the Society for Neuroscience. 2004; 24(44):9770-8.
66. Giacobini P, Wray S. Prenatal expression of cholecystokinin (CCK) in the central nervous system (CNS) of mouse. Neuroscience letters. 2008; 438(1):96-101.
67. Girardeau G, Benchenane K, Wiener S, et al. Selective suppression of hippocampal ripples impairs spatial memory. Nature Neuroscience. 2009; 12(10): 1222–1223.
68. Glickfeld LL, Scanziani M. Distinct timing in the activity of cannabinoid-sensitive and cannabinoid-insensitive basket cells. Nature neuroscience. 2006; 9(6):807-15.
69. Gloveli T. Hippocampal spatial navigation: interneurons take responsibility. The Journal of physiology. 2010; 588(Pt 23):4609-10.
70. Gong S, Doughty M, Harbaugh CR, et al. Targeting Cre recombinase to specific neuron populations with bacterial artificial chromosome constructs. The Journal of neuroscience : the official journal of the Society for Neuroscience. 2007; 27(37): 9817-9823.
71. Good M, Honey RC. Conditioning and contextual retrieval in hippocampal rats. Behavioral neuroscience. 1991; 105(4):499-509.
72. Graves AR, Moore SJ, Bloss EB, Mensh BD, Kath WL, Spruston N. Hippocampal pyramidal neurons comprise two distinct cell types that are countermodulated by metabotropic receptors. Neuron. 2012; 76(4):776-89.
73. Gulyás AI, Tóth K, Dános P, Freund TF. Subpopulations of GABAergic neurons containing parvalbumin, calbindin D28k, and cholecystokinin in the rat hippocampus. The Journal of comparative neurology. 1991; 312(3):371-8.
74. Gutiérrez-Rodríguez A,Puente N, Elezgarai I. Anatomical characterization of the cannabinoid CB1 receptor in cell-type-specific mutant mouse rescue models. Journal of Computational Neurology. 2017;525(2):302-318. doi: 10.1002/cne.24066. Epub 2016 Jul 8.

75. Hájos N, Mody I. Synaptic communication among hippocampal interneurons: properties of spontaneous IPSCs in morphologically identified cells. The Journal of neuroscience : the official journal of the Society for Neuroscience. 1997; 17(21):8427-42.
76. Hampson RE, Heyser CJ, Deadwyler SA. Hippocampal cell firing correlates of delayed-match-to-sample performance in the rat. Behavioral neuroscience. 1993; 107(5):715-39.
77. Han X, Chow BY, Zhou H, et al. A high-light sensitivity optical neural silencer: development and application to optogenetic control of non-human primate cortex.Frontiers in Systems Neuroscience. 2011; 5:18.
78. Harris KD, Hochgerner H, Skene NG, et al. Classes and continua of hippocampal CA1 inhibitory neurons revealed by single-cell transcriptomics. PLoS biology. 2018; 16(6):e2006387.
79. Harris KD, Henze DA, Csicsvari J, Hirase H, Buzsáki G. Accuracy of tetrode spike separation as determined by simultaneous intracellular and extracellular measurements. Journal of neurophysiology. 2000; 84(1):401-14.
80. Harris KM, Marshall PE, Landis DM. Ultrastructural study of cholecystokinin-immunoreactive cells and processes in area CA1 of the rat hippocampus. The Journal of comparative neurology. 1985; 233(2):147-58.
81. Hashimotodani Y, Ohno-Shosaku T, Kano M. Ca(2+)-assisted receptor-driven endocannabinoid release: mechanisms that associate presynaptic and postsynaptic activities. Current Opinion in Neurobiology. 2007;17:360–365.
82. Hasselmo M, Stern C. Theta rhythm and the encoding and retrieval of space and time. Neuroimage. 2014;85 Pt 2:656-66.
83. Hebb DO. The organization of behavior; a neuropsychological theory. Oxford, England: Wiley, 1949.
84. Hefft S, Jonas P. Asynchronous GABA release generates long-lasting inhibition at a hippocampal interneuron-principal neuron synapse. Nature neuroscience. 2005; 8(10):1319-28.
85. Heifets B, Castillo P. Endocannabinoid signaling and long-term synaptic plasticity.The Annual Review of Physiology. 2009;71:283-306.
86. Henze D, Borhegyi Z, Csicsvari J, et al. Intracellular features predicted by extracellular recordings in the hippocampus in vivo. Journal of Neurophysiology. 2000; 84(1):390-400.
87. Hippenmeyer S, Vrieseling E, Sigrist M, et al. A developmental switch in the response of DRG neurons to ETS transcription factor signaling. PLoS Biology. 2005. 3(5):e159.
88. Honda T, Wada E, Battey JF, Wank SA. Differential gene expression of CCK(A) and CCK(B) receptors in the rat brain. Molecular and Cellular Neuroscience. 1993; 4:143–154.
89. Hu H, Ma Y, Agmon A. Submillisecond firing synchrony between different subtypes of cortical interneurons connected chemically but not electrically. The Journal of neuroscience : the official journal of the Society for Neuroscience. 2011; 31:3351–3361.
90. Huerta P, Lisman J. Bidirectional synaptic plasticity induced by a single burst during cholinergic theta oscillation in CA1 in vitro. Neuron. 1995;15(5):1053-63.

91. Innis RB, Snyder SH. Distinct cholecystokinin receptors in brain and pancreas. Proceedings of the National Academy of Sciences of the United States of America. 1980; 77:6917–6921.
92. Isaac JT, Buchanan KA, Muller RU, Mellor JR. Hippocampal place cell firing patterns can induce long-term synaptic plasticity in vitro. The Journal of neuroscience : the official journal of the Society for Neuroscience. 2009; 29(21):6840-50.
93. Jadhav SP, Kemere C, German PW, Frank LM. Awake hippocampal sharp-wave ripples support spatial memory. Science. 2012; 336, 1454–1458.
94. Jappy D, Valiullina F, Draguhn A, Rozov A. GABABR-Dependent Long-Term Depression at Hippocampal Synapses between CB1-Positive Interneurons and CA1 Pyramidal Cells. Frontiers in cellular neuroscience. 2016; 10:4.
95. Ji J, Maren S. Differential roles for hippocampal areas CA1 and CA3 in the contextual encoding and retrieval of extinguished fear. Learning & memory (Cold Spring Harbor, N.Y.). 2008; 15(4):244-51.
96. Jinno S, Kosaka T. Patterns of expression of neuropeptides in GABAergic nonprincipal neurons in the mouse hippocampus: Quantitative analysis with optical disector. The Journal of comparative neurology. 2003; 461(3):333-49.
97. Johnson A, Redish A. Neural ensembles in CA3 transiently encode paths forward of the animal at a decision point. The Journal of neuroscience : the official journal of the Society for Neuroscience. 2007;27(45):12176-89.
98. Kamme F, Salunga R, Yu J, et al. Single-cell microarray analysis in hippocampus CA1: demonstration and validation of cellular heterogeneity. The Journal of neuroscience : the official journal of the Society for Neuroscience. 2003; 23(9):3607-15.
99. Kano M, Ohno-Shosaku T, Hashimotodani Y, Uchigashima M, Watanabe M. Endocannabinoid-mediated control of synaptic transmission. Physiological reviews. 2009; 89(1):309-80.
100. Karlsson MP, Frank LM. Awake replay of remote experiences in the hippocampus. Nature neuroscience. 2009; 12(7):913-8.
101. Karson MA, Tang AH, Milner TA, Alger BE. Synaptic cross talk between perisomatic-targeting interneuron classes expressing cholecystokinin and parvalbumin in hippocampus. The Journal of neuroscience : the official journal of the Society for Neuroscience. 2009; 29(13):4140-54.
102. Katona I, Sperlágh B, Sík A, et al. Presynaptically located CB1 cannabinoid receptors regulate GABA release from axon terminals of specific hippocampal interneurons. The Journal of neuroscience : the official journal of the Society for Neuroscience. 1999; 19(11):4544-58.
103. Katona I, Urbán G, Wallace M, et al. Molecular composition of the endocannabinoid system at glutamatergic synapses. The Journal of neuroscience : the official journal of the Society for Neuroscience. 2006; 26(21):5628-37.
104. Kawamura Y, Fukaya M, Maejima T, et al. The CB1 cannabinoid receptor is the major cannabinoid receptor at excitatory presynaptic sites in the hippocampus and cerebellum. The Journal of neuroscience : the official journal of the Society for Neuroscience. 2006; 26(11):2991-3001.
105. Kepecs A, Fishell G. Interneuron cell types are fit to function. Nature. 2014; 505(7483):318-26.
106. Kim J, Isokawa M, Ledent C, Alger BE. Activation of muscarinic acetylcholine receptors enhances the release of endogenous cannabinoids in the hippocampus. The Journal of

neuroscience : the official journal of the Society for Neuroscience. 2002; 22(23):10182-91.
107. Klausberger T, Magill PJ, Márton LF, et al. Brain-state- and cell-type-specific firing of hippocampal interneurons in vivo. Nature. 2003; 421(6925):844-8.
108. Klausberger T, Marton LF, O'Neill J, et al. Complementary roles of cholecystokinin- and parvalbumin-expressing GABAergic neurons in hippocampal network oscillations. The Journal of neuroscience : the official journal of the Society for Neuroscience. 2005; 25(42):9782-93.
109. Klausberger T, Somogyi P. Neuronal diversity and temporal dynamics: the unity of hippocampal circuit operations. Science (New York, N.Y.). 2008; 321(5885):53-7.
110. Klausberger T. GABAergic interneurons targeting dendrites of pyramidal cells in the CA1 area of the hippocampus. The European journal of neuroscience. 2009; 30(6):947-57.
111. Kohus Z, Káli S, Rovira-Esteban L, et al. Properties and dynamics of inhibitory synaptic communication within the CA3 microcircuits of pyramidal cells and interneurons expressing parvalbumin or cholecystokinin.The Journal of physiology. 2016; 594(13):3745-74.
112. Kosaka T, Kosaka K, Tateishi K, et al. GABAergic neurons containing CCK-8-like and/or VIP-like immunoreactivities in the rat hippocampus and dentate gyrus. The Journal of comparative neurology. 1985; 239(4):420-30.
113. Kreitzer AC, Regehr WG. Retrograde inhibition of presynaptic calcium influx by endogenous cannabinoids at excitatory synapses onto Purkinje cells. Neuron. 2001; 29(3):717-27.
114. Kubota Y, Kawaguchi Y. Two distinct subgroups of cholecystokinin-immunoreactive cortical interneurons. Brain Research. 1997;752(1-2):175-83.
115. Lapray D, Lasztoczi B, Lagler M, et al. Behavior-dependent specialization of identified hippocampal interneurons. Nature neuroscience. 2012; 15(9):1265-71.
116. Lasztóczi B, Tukker J, Somogyi P, Klausberger T. Terminal field and firing selectivity of cholecystokinin-expressing interneurons in the hippocampal CA3 area.The Journal of neuroscience : the official journal of the Society for Neuroscience. 2011; 31(49):18073-93.
117. Lee I, Kesner RP. Differential contributions of dorsal hippocampal subregions to memory acquisition and retrieval in contextual fear-conditioning. Hippocampus. 2004; 14(3):301-10.
118. Lee S, Földy C, Szabadics J, Soltesz I. Cell-type-specific CCK2 receptor signaling underlies the cholecystokinin-mediated selective excitation of hippocampal parvalbumin-positive fast-spiking basket cells. Journal of Neuroscience. 2011; 31(30):10993-1002.
119. Lee S, Hjerling-Leffler J, Zagha E, Fishell G, Rudy B. The largest group of superficial neocortical GABAergic interneurons expresses ionotropic serotonin receptors. The Journal of neuroscience : the official journal of the Society for Neuroscience. 2010; 30(50):16796-808.
120. Leutgeb S, Leutgeb JK, Barnes CA, Moser EI, McNaughton BL, Moser MB. Independent codes for spatial and episodic memory in hippocampal neuronal ensembles. Science (New York, N.Y.). 2005; 309(5734):619-23.

121. Li S, Xu J, Chen G, Lin L, Zhou D, Cai D. The characterization of hippocampal theta-driving neurons - a time-delayed mutual information approach. Scientific reports. 2017; 7(1):5637.
122. Lim L, Mi D, Llorca A, Marín O. Development and Functional Diversification of Cortical Interneurons. Neuron. 2018; 100(2):294-313.
123. Lisman J, Buzsáki G. A neural coding scheme formed by the combined function of gamma and theta oscillations. Schizophrenia Bulletin. 2008; 34(5):974-80.
124. Lisman J. Bursts as a unit of neural information: making unreliable synapses reliable. Trends in neurosciences. 1997; 20(1):38-43.
125. Lisman J, Jensen O. The q-g neural code. Neuron. 2013; 77: 1002–1016.
126. Lorente De Nó, R. Studies on the structure of the cerebral cortex. II. Continuation of the study of the ammonic system. Journal für Psychologie und Neurologie. 1934; 46: 113-177.
127. Losonczy A, Zemelman B, Vaziri A, Magee J. Network mechanisms of theta related neuronal activity in hippocampal CA1 pyramidal neurons. Nature Neuroscience. 2010; 13(8):967-72.
128. Luo L, Callaway E, Svoboda K. Genetic Dissection of Neural Circuits: A Decade of Progress. Neuron. 2018; 98(2):256-281.
129. Maccaferri G, Lacaille JC. Interneuron Diversity series: Hippocampal interneuron classifications--making things as simple as possible, not simpler. Trends in neurosciences. 2003; 26(10):564-71.
130. Madisen L, Mao T, Koch H, et al. A toolbox of Cre-dependent optogenetic transgenic mice for light-induced activation and silencing. Nature Neuroscience. 2012; 15(5): 793-802.
131. Madisen L, Zwingman T, Sunkin S, et al. A robust and high-throughput Cre reporting and characterization system for the whole mouse brain. Nature Neuroscience. 2010; 13(1): 133-140.
132. Maejima T, Hashimoto K, Yoshida T, Aiba A, Kano M. Presynaptic inhibition caused by retrograde signal from metabotropic glutamate to cannabinoid receptors. Neuron. 2001; 31(3):463-75.
133. Maejima T, Hashimoto K, Yoshida T, Aiba A, Kano M. Presynaptic inhibition caused by retrograde signal from metabotropic glutamate to cannabinoid receptors. Neuron. 2001; 31(3):463-75.
134. Markus EJ, Barnes CA, McNaughton BL, Gladden VL, Skaggs WE. Spatial information content and reliability of hippocampal CA1 neurons: effects of visual input. Hippocampus. 1994; 4(4):410-21.
135. Marsicano G, Lutz B. Expression of the cannabinoid receptor CB1 in distinct neuronal subpopulations in the adult mouse forebrain. The European journal of neuroscience. 1999; 11(12):4213-25.
136. McBain CJ, Fisahn A. Interneurons unbound. Nature reviews. Neuroscience. 2001; 2(1):11-23.
137. Mitra P, Pesaran B. Analysis of dynamic brain imaging data. The Biophysical Journal. 1999; 76(2):691-708.
138. Miyoshi G, Hjerling-Leffler J, Karayannis T, et al. Genetic fate mapping reveals that the caudal ganglionic eminence produces a large and diverse population of superficial cortical interneurons. The Journal of neuroscience : the official journal of the Society for Neuroscience. 2010; 30(5):1582-94.

139. Mizuseki K, Diba K, Pastalkova E, Buzsáki G. Hippocampal CA1 pyramidal cells form functionally distinct sublayers. Nature neuroscience. 2011; 14(9):1174-81.
140. Mizuseki K, Sirota A, Pastalkova E, Buzsáki G. Theta oscillations provide temporal windows for local circuit computation in the entorhinal-hippocampal loop. Neuron. 2009; 64(2):267-80.
141. Morales M, Bloom FE. The 5-HT3 receptor is present in different subpopulations of GABAergic neurons in the rat telencephalon. The Journal of neuroscience : the official journal of the Society for Neuroscience. 1997; 17(9):3157-67.
142. Morino P, Herrera-Marschitz M, Castel MN, et al. Cholecystokinin in cortico-striatal neurons in the rat: immunohistochemical studies at the light and electron microscopical level. The European journal of neuroscience. 1994; 6(5):681-92.
143. Morozov Y, Freund T. Postnatal development and migration of cholecystokinin-immunoreactive interneurons in rat hippocampus. Neuroscience. 2003;120(4):923-39.
144. Morris RG, Garrud P, Rawlins JN, O'Keefe J. Place navigation impaired in rats with hippocampal lesions. Nature. 1982; 297(5868):681-3.
145. Muller R. A quarter of a century of place cells. Neuron. 1996; 17(5):813-22.
146. Muller RU, Kubie JL. The firing of hippocampal place cells predicts the future position of freely moving rats. The Journal of neuroscience : the official journal of the Society for Neuroscience. 1989; 9(12):4101-10.
147. Murphey DK, Herman AM, Arenkiel BR. Dissecting inhibitory brain circuits with genetically-targeted technologies. Frontiers in neural circuits. 2014; 8:124.
148. Murray AJ, Sauer JF, Riedel G, et al. Parvalbumin-positive CA1 interneurons are required for spatial working but not for reference memory. Nature Neuroscience. 2011; 14(3):297-9.
149. Nagel G, Szellas T, Huhn W et al. Channelrhodopsin-2, a directly light-gated cation-selective membrane channel. Proceedings of the National Academy of Sciences of the United States of America. 2003;100(24):13940-5.
150. Nagode D, Tang A, Yang K, Alger B. Optogenetic identification of an intrinsic cholinergically driven inhibitory oscillator sensitive to cannabinoids and opioids in hippocampal CA1. The Journal of physiology. 2014; 592(1):103-23.
151. Nicolelis M, Ghazanfar A, Faggin B, Votaw S, Oliveira L. Reconstructing the engram: simultaneous, multisite, many single neuron recordings. Neuron. 1997; 18(4):529-37.
152. Nokia MS, Mikkonen JE, Penttonen M, Wikgren J. Disrupting neural activity related to awake-state sharp wave-ripple complexes prevents hippocampal learning. Frontiers in behavioral neuroscience. 2012; 6:84.
153. Nunzi M, Gorio A, Milan F. Cholecystokinin-immunoreactive cells form symmetrical synaptic contacts with pyramidal and nonpyramidal neurons in the hippocampus. Journal of comparative neurology. 1985;237(4):485-505.
154. O'Keefe J, Dostrovsky J. The hippocampus as a spatial map. Preliminary evidence from unit activity in the freely-moving rat. Brain research. 1971; 34(1):171-5.
155. O'Keefe J, Recce ML. Phase relationship between hippocampal place units and the EEG theta rhythm. Hippocampus. 1993; 3(3):317-30.
156. O'Keefe J. Place units in the hippocampus of the freely moving rat. Experimental neurology. 1976; 51(1):78-109.
157. O'Neill J, Senior T, Csicsvari J. Place-selective firing of CA1 pyramidal cells during sharp wave/ripple network patterns in exploratory behavior. Neuron. 2006; 49(1):143-55.

158. O'Neill J, Senior TJ, Allen K, Huxter JR, Csicsvari J. Reactivation of experience-dependent cell assembly patterns in the hippocampus. Nature neuroscience. 2008; 11(2):209-15.
159. Ohno-Shosaku T, Maejima T, Kano M. Endogenous cannabinoids mediate retrograde signals from depolarized postsynaptic neurons to presynaptic terminals. Neuron. 2001; 29(3):729-38.
160. Ohno-Shosaku T, Matsui M, Fukudome Y, et al. Postsynaptic M1 and M3 receptors are responsible for the muscarinic enhancement of retrograde endocannabinoid signalling in the hippocampus. The European journal of neuroscience. 2003; 18(1):109-16.
161. Ohno-Shosaku T, Tsubokawa H, Mizushima I, Yoneda N, Zimmer A, Kano M. Presynaptic cannabinoid sensitivity is a major determinant of depolarization-induced retrograde suppression at hippocampal synapses. The Journal of neuroscience : the official journal of the Society for Neuroscience. 2002; 22(10):3864-72.
162. Parra P, Gulyás AI, Miles R. How many subtypes of inhibitory cells in the hippocampus? Neuron. 1998; 20(5):983-93.
163. Pawelzik H, Hughes DI, Thomson AM. Physiological and morphological diversity of immunocytochemically defined parvalbumin- and cholecystokinin-positive interneurones in CA1 of the adult rat hippocampus. The Journal of comparative neurology. 2002; 443(4):346-67.
164. Pelkey KA, Chittajallu R, Craig MT, Tricoire L, Wester JC, McBain CJ. Hippocampal GABAergic Inhibitory Interneurons. Physiological reviews. 2017; 97(4):1619-1747.
165. Pike FG, Meredith RM, Olding AW, Paulsen O. Rapid report: postsynaptic bursting is essential for 'Hebbian' induction of associative long-term potentiation at excitatory synapses in rat hippocampus. The Journal of physiology. 1999; 518 (Pt 2):571-6.
166. Pinault, D. The Juxtacellular Recording-Labeling Technique. In Electrophysiological Recording Techniques (pp. 41–75). Humana Press. 2011
167. Que L, Winterer J, Földy C. Deep Survey of GABAergic Interneurons: Emerging Insights From Gene-Isoform Transcriptomics. Frontiers in molecular neuroscience. 2019; 12:115.
168. R Core Team (2014). R: A language and environment for statistical computing. R Foundation for Statistical Computing, Vienna, Austria. URL http://www.R-project.org/.
169. Ranck JB. Studies on single neurons in dorsal hippocampal formation and septum in unrestrained rats. I. Behavioral correlates and firing repertoires. Experimental neurology. 1973; 41(2):461-531.
170. Rangel Guerrero D, Donnett J, Csicsvari J, et al. Tetrode Recording from the Hippocampus of Behaving Mice Coupled with Four-Point-Irradiation Closed-Loop Optogenetics: A Technique to Study the Contribution of Hippocampal SWR Events to Learning. eNeuro. 2018; 5(4). pii: ENEURO.0087-18.2018.
171. Regehr WG, Carey MR, Best AR. Activity-dependent regulation of synapses by retrograde messengers. Neuron. 2009; 63(2):154-70.
172. Robbe D, Montgomery SM, Thome A, Rueda-Orozco PE, McNaughton BL, Buzsáki G. Cannabinoids reveal importance of spike timing coordination in hippocampal function. Nature neuroscience. 2006; 9(12):1526-33.
173. Roux L, Stark E, Sjulson L, Buzsáki G. In vivo optogenetic identification and manipulation of GABAergic interneuron subtypes. Current opinion in neurobiology. 2014; 26:88-95.

174. Royer S, Zemelman BV, Losonczy A, et al. Control of timing, rate and bursts of hippocampal place cells by dendritic and somatic inhibition. Nature neuroscience. 2012; 15(5):769-75.
175. Rudy B, Fishell G, Lee S, Hjerling-Leffler J. Three groups of interneurons account for nearly 100% of neocortical GABAergic neurons. Developmental neurobiology. 2011; 71(1):45-61.
176. Ruigt GS, Van Proosdij JN, Van Wezenbeek LA. A large scale, high resolution, automated system for rat sleep staging. II. Validation and application. Electroencephalography and clinical neurophysiology. 1989; 73(1):64-71.
177. Scharfman HE. The CA3 "backprojection" to the dentate gyrus. Progress in brain research. 2007; 163:627-37.
178. Schlingloff D, Káli S, Freund TF, Hájos N, Gulyás AI. Mechanisms of sharp wave initiation and ripple generation. The Journal of neuroscience : the official journal of the Society for Neuroscience. 2014; 34(34):11385-98.
179. Schmidt M, Horvath S, Ebert P, et al. Modulation of behavioral networks by selective interneuronal inactivation. Molecular Psychiatry. 2014; 19(5):580-7.
180. Schoenenberger P, O'Neill J, Csicsvari J. Activity-dependent plasticity of hippocampal place maps. Nature communications. 2016; 7:11824.
181. Scoville WB, Milner B. Loss of recent memory after bilateral hippocampal lesions. The Journal of Neurology, Neurosurgery and Psychiatry. 1957; 20:11–21.
182. Senior T, Huxter J, Allen K, et al. Gamma oscillatory firing reveals distinct populations of pyramidal cells in the CA1 region of the hippocampus. The Journal of neuroscience : the official journal of the Society for Neuroscience. 2008;28(9):2274-86.
183. Sirota A, Montgomery S, Fujisawa S, Isomura Y, Zugaro M, Buzsáki G. Entrainment of neocortical neurons and gamma oscillations by the hippocampal theta rhythm. Neuron. 2008; 60(4):683-97.
184. Skaggs W, McNaughton B, Wilson M, Barnes C. Theta phase precession in hippocampal neuronal populations and the compression of temporal sequences. Hippocampus. 1996;6(2):149-72.
185. Skaggs W, Wilson M, McNaughton B. Spatial specificity of hippocampal place cells changes with phase of the theta cycle. Society for Neuroscience Abstracts. 1993; 19:795 (324.16).
186. Slomianka L, Amrein I, Knuesel I, Sørensen JC, Wolfer DP. Hippocampal pyramidal cells: the reemergence of cortical lamination. Brain structure & function. 2011; 216(4):301-17.
187. Sloviter R, Nilaver G.Immunocytochemical localization of GABA-, cholecystokinin-, vasoactive intestinal polypeptide-, and somatostatin-like immunoreactivity in the area dentata and hippocampus of the rat. The Journal of Comparative Neurology. 1987;256(1):42-60.
188. Sloviter RS, Nilaver G. Immunocytochemical localization of GABA-, cholecystokinin-, vasoactive intestinal polypeptide-, and somatostatin-like immunoreactivity in the area dentata and hippocampus of the rat. The Journal of comparative neurology. 1987; 256(1):42-60.
189. Sohn J, Hioki H, Okamoto S, Kaneko T. Preprodynorphin-expressing neurons constitute a large subgroup of somatostatin-expressing GABAergic interneurons in the mouse neocortex. The Journal of comparative neurology. 2014; 522(7):1506-26.

190. Soltesz I, Losonczy A. CA1 pyramidal cell diversity enabling parallel information processing in the hippocampus. Nature neuroscience. 2018; 21(4):484-493.
191. Somogyi J, Baude A, Omori Y, et al. GABAergic basket cells expressing cholecystokinin contain vesicular glutamate transporter type 3 (VGLUT3) in their synaptic terminals in hippocampus and isocortex of the rat. The European journal of neuroscience. 2004; 19(3):552-69.
192. Somogyi P, Hodgson AJ, Smith AD, Nunzi MG, Gorio A, Wu JY. Different populations of GABAergic neurons in the visual cortex and hippocampus of cat contain somatostatin- or cholecystokinin-immunoreactive material. The Journal of neuroscience : the official journal of the Society for Neuroscience. 1984; 4(10):2590-603.
193. Somogyi P, Katona L, Klausberger T, Lasztóczi B, Viney TJ. Temporal redistribution of inhibition over neuronal subcellular domains underlies state-dependent rhythmic change of excitability in the hippocampus. Philosophical transactions of the Royal Society of London. Series B, Biological sciences. 2014; 369(1635):20120518.
194. Souza BC, Tort ABL. Asymmetry of the temporal code for space by hippocampal place cells. Scientific reports. 2017; 7(1):8507.
195. Stark E, Roux L, Eichler R, Senzai Y, Royer S, Buzsáki G. Pyramidal cell-interneuron interactions underlie hippocampal ripple oscillations. Neuron. 2014; 83(2):467-480.
196. Sutherland RJ, Kolb B, Whishaw IQ. Spatial mapping: definitive disruption by hippocampal or medial frontal cortical damage in the rat. Neuroscience letters. 1982; 31(3):271-6.
197. Suzuki SS, Smith GK. Spontaneous EEG spikes in the normal hippocampus. I. Behavioral correlates, laminar profiles and bilateral synchrony. Electroencephalography and clinical neurophysiology. 1987; 67(4):348-59.
198. Taniguchi H, He M, Wu P, et al. A resource of Cre driver lines for genetic targeting of GABAergic neurons in cerebral cortex. Neuron. 2011; 71(6):995-1013.
199. Taniguchi H. Genetic dissection of GABAergic neural circuits in mouse neocortex. Frontiers in cellular neuroscience. 2014; 8:8.
200. Tasic B, Menon V, Nguyen TN, et al. Adult mouse cortical cell taxonomy revealed by single cell transcriptomics. Nature neuroscience. 2016; 19(2):335-46.
201. Thomson D. Spectrum estimation and harmonic analysis. The Proceedings of the Institute of Electrical and Electronics Engineers. 1982; 70, 1055–1096.
202. Tricoire L, Pelkey KA, Erkkila BE, Jeffries BW, Yuan X, McBain CJ. A blueprint for the spatiotemporal origins of mouse hippocampal interneuron diversity. The Journal of neuroscience : the official journal of the Society for Neuroscience. 2011; 31(30):10948-70.
203. Tsou K, Mackie K, Sañudo-Peña MC, Walker JM. Cannabinoid CB1 receptors are localized primarily on cholecystokinin-containing GABAergic interneurons in the rat hippocampal formation. Neuroscience. 1999; 93(3):969-75.
204. Tukker JJ, Fuentealba P, Hartwich K, Somogyi P, Klausberger T. Cell type-specific tuning of hippocampal interneuron firing during gamma oscillations in vivo. The Journal of neuroscience : the official journal of the Society for Neuroscience. 2007; 27(31):8184-9.
205. Valero M, Cid E, Averkin R, et al. Determinants of different deep and superficial CA1 pyramidal cell dynamics during sharp-wave ripples. Nature Neuroscience. 2015;18(9):1281-1290.

206. van de Ven GM, Trouche S, McNamara CG, Allen K, Dupret D. Hippocampal Offline Reactivation Consolidates Recently Formed Cell Assembly Patterns during Sharp Wave-Ripples. Neuron. 2016; 92(5):968-974.
207. Vanderwolf CH. Hippocampal electrical activity and voluntary movement in the rat. Electroencephalography and clinical neurophysiology. 1969; 26(4):407-18.
208. Varga C, Oijala M, Lish J, et al. Functional fission of parvalbumin interneuron classes during fast network events. eLife. 2014; 3:.
209. Vida I, Halasy K, Szinyei C, Somogyi P, Buhl EH. Unitary IPSPs evoked by interneurons at the stratum radiatum-stratum lacunosum-moleculare border in the CA1 area of the rat hippocampus in vitro. The Journal of physiology. 1998; 506 (Pt 3):755-73.
210. Vucurovic K, Gallopin T, Ferezou I, et al. Serotonin 3A receptor subtype as an early and protracted marker of cortical interneuron subpopulations. Cerebral cortex (New York, N.Y. : 1991). 2010; 20(10):2333-47.
211. Whissell PD, Bang JY, Khan I, et al. Selective Activation of Cholecystokinin-Expressing GABA (CCK-GABA) Neurons Enhances Memory and Cognition. eNeuro. 2019; 6(1).
212. Whissell PD, Cajanding JD, Fogel N, Kim JC. Comparative density of CCK- and PV-GABA cells within the cortex and hippocampus. Frontiers in neuroanatomy. 2015; 9:124.
213. Whissell PD, Rosenzweig S, Lecker I, Wang DS, Wojtowicz JM, Orser BA. γ-aminobutyric acid type A receptors that contain the δ subunit promote memory and neurogenesis in the dentate gyrus. Annals of neurology. 2013; 74(4):611-21.
214. Wilson MA, McNaughton BL. Reactivation of hippocampal ensemble memories during sleep. Science (New York, N.Y.). 1994; 265(5172):676-9.
215. Wilson RI, Nicoll RA. Endogenous cannabinoids mediate retrograde signalling at hippocampal synapses. Nature. 2001; 410(6828):588-92.
216. Wood ER, Dudchenko PA, Eichenbaum H. The global record of memory in hippocampal neuronal activity. Nature. 1999; 397(6720):613-6.
217. Wood ER, Dudchenko PA, Robitsek RJ, Eichenbaum H. Hippocampal neurons encode information about different types of memory episodes occurring in the same location. Neuron. 2000; 27(3):623-33.
218. Xu X, Roby KD, Callaway EM. Immunochemical characterization of inhibitory mouse cortical neurons: three chemically distinct classes of inhibitory cells. Journal of Computational Neurology. 2010; 518(3):389-404.
219. Younts TJ, Chevaleyre V, Castillo PE. CA1 pyramidal cell theta-burst firing triggers endocannabinoid-mediated long-term depression at both somatic and dendritic inhibitory synapses. The Journal of neuroscience : the official journal of the Society for Neuroscience. 2013; 33(34):13743-57.
220. Zarnadze S, Bäuerle P, Santos-torres J, et al. Cell-specific synaptic plasticity induced by network oscillations. Elife. 2016;5.